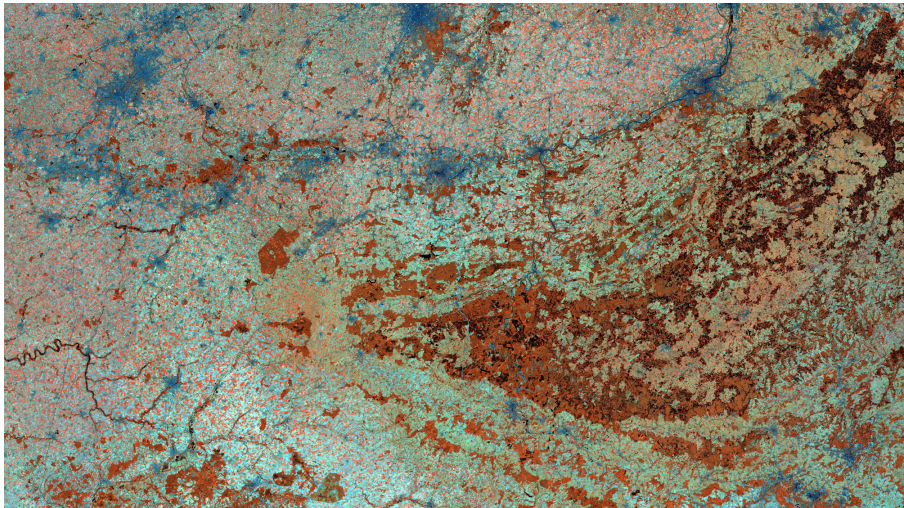# Mapping trees inside and outside of the forest using remote sensing

Application to temperate European landscapes

Corentin BOLYN

COMMUNAUTÉ FRANÇAISE DE BELGIQUE

UNIVERSITÉ DE LIÈGE - GEMBLOUX AGRO-BIO TECH

Mapping trees inside and outside of the forest using remote sensing

Application to temperate European landscapes

Corentin BOLYN

Dissertation originale présentée en vue de l'obtention du grade de docteur en sciences agronomiques et ingénierie biologique

Promoteur: Pr. Philippe LEJEUNE

Année civile: 2023

Abstract

Forest ecosystems provide ecological and socio-economic services and values that are vital to human societies around the world. Trees outside the forest (TOF), which are receiving increasing attention, also provide these services. Adequate management and decision-making regarding the tree resource depends on a good understanding of its status and trends, even more so in a context of uncertainties and crises caused by climate change and biodiversity loss. In addition to the exhaustiveness of field measurements, the use of remote sensing technology allows for widespread and rapid data collection campaigns with high potential for tree monitoring. One of the key elements in the characterisation of forest areas is the tree species composition. Despite the increasing number of remote sensing studies on tree species mapping, the prediction of reliable maps at large scales is still a research challenge. We explored the opportunity presented by the Copernicus Sentinel-2 (S2) mission, which began acquiring multispectral satellite imagery in 2015. Our first objective was to develop a method for mapping tree species in European temperate forests using S2 imagery. The second objective of this work was to develop a method for mapping TOF using remote sensing. Existing studies that have mapped TOF have not characterised them further than a simple classification into linear elements and patches. Commonly used definitions of TOF are more complex and refer to their use, form and spatial pattern structuring the landscape. We developed an algorithm for TOF classification with a typology closer to that used by managers and administrations in Europe.

First, we explored the potential of S2 for tree species classification per pixel in pure forest stands. We used two S2 scenes covering the Belgian Ardennes ecoregion. We trained two random forest classifier models: the first to predict forest areas, and the second to classify 11 classes in the forest: Fagus sylvatica L., Betula sp., Quercus sp., other broad-leaved stands, Pseudotsuga menziesii (Mirb.) Franco, Larix sp., Pinus sylvestris L., Picea abies (L.) H.Karst, young needle-leaved stands, other needle-leaved stands and recent clear-cuts. A second version of these two models was trained after adding 3D variables generated from LiDAR and photogrammetry datasets. Using S2 data only, the overall accuracy (OA) of the forest map model was 0.92, the OA of the tree species classification was 0.89, with a mean user's accuracy (UA) also of 0.89. Inclusion of 3D variables improved model accuracy only slightly. Although a simplified approach, the results of the study demonstrated the ability of S2 to separate common Belgian tree species based on their spectral signature.

Second, we developed a method using satellite imagery to map tree species in pure and mixed forest stands with a pixel size too coarse to resolve individual trees. We used a deep learning model (convolutional neural network) to predict per pixel a vector of tree species proportions (sum equal to 1), taking into account the surrounding environment. The model was trained using a map of forest parcel polygons extracted from the geodatabase of the Public Forest Administration of Wallonia. Nine species

or groups of species were considered: Spruce genus, Oak genus, Beech, Douglas fir, Pine genus, Poplar genus, Larch genus, Birch genus and the remaining species. We produced a map of tree species proportions for the Walloon region (southern Belgium) and evaluated its quality using the regional forest inventory of Wallonia. We proposed a method to evaluate proportions maps in three parts: (1) majority species, (2) species composition (presence or absence) and (3) species proportions (proportion values). The R^2_{adj} of the predicted proportions was 0.50. High values obtained for the indicators overall accuracy of majority class assessment (OA_{maj}, 0.73) and mean score (MS, 0.89) demonstrated the ability of the method to predict the majority tree species and species composition in mixed and pure forest stands of the study area. The proposed tree species mapping method is suitable for forest characterisation over extended areas as it uses public satellite imagery and the most common reference data on tree species composition.

Third, we developed a tool to map TOF and classify them into groups defined on the basis of European agri-environmental measures. In the first step of the process, TOF were separated from trees inside the forest (TIF) on the basis of a vegetation mask. Then, an algorithm classified TOF features into 7 classes: Isolated tree, Aligned trees, Agglomerated trees, Hedge, Grove, Shrub and Other. This algorithm was developed in two steps: (1) the geometrical classification of each TOF feature, and (2) the spatial neighbouring analysis of the features and their final classification according to possible spatial combinations. The OA of the TOF classification was 0.78, demonstrating the potential of the approach for TOF monitoring in rural landscapes.

In perspective, for tree species proportions mapping, further research should explore the added value of a time dimension to the current version of our deep learning model, which only exploits the spectral and spatial dimensions of S2 images. For TOF mapping, we will go beyond the prototype by optimising the classification tool. Taking advantage of the new generation of LiDAR acquisitions, it will be possible to go further in automated TOF characterisation. We encourage future remote sensing research related to concrete applications, as this stimulates innovation where it is needed in a field that is by nature applied.

Résumé

Les écosystèmes forestiers fournissent des services et des ressources écologiques et socio-économiques qui sont vitaux pour les sociétés humaines du monde entier. Ces services sont également fournis par les arbres hors forêt (AHF), qui font l'objet d'une attention croissante. La gestion adéquate et la prise de décision concernant la ressource arborée dépendent d'une bonne compréhension de son statut et de son évolution, d'autant plus dans un contexte d'incertitudes et de crises causées par le changement climatique et l'appauvrissement de la biodiversité. En complément de l'exhaustivité des mesures de terrain, l'utilisation de la technologie de télédétection permet des campagnes de collecte de données étendues et rapides présentant un fort potentiel pour la gestion de la ressource arborée. L'un des éléments clés de la caractérisation des massifs forestiers est leur composition en essences d'arbres. Malgré le nombre croissant d'études de télédétection sur la cartographie des espèces d'arbres, la prédiction de cartes fiables à grande échelle reste un défi pour la recherche. Nous avons exploré l'opportunité offerte par la mission Copernicus Sentinel-2 (S2), qui a commencé à acquérir des images satellites multispectrales en 2015. Notre premier objectif était de développer une méthode pour cartographier les espèces d'arbres dans les forêts tempérées européennes en utilisant l'imagerie S2. Le second objectif de ce travail était de développer une méthode pour cartographier les AHF à l'aide de la télédétection. Les études existantes qui ont cartographié les AHF ne les ont pas caractérisés au-delà d'une simple classification en éléments linéaires et en parcelles. Les définitions communément utilisées des AHF sont plus complexes et se réfèrent à leur utilisation, à leur forme et à leur configuration spatiale structurant le paysage. Nous avons développé un algorithme de classification des AHF avec une typologie plus proche de celle utilisée par les gestionnaires et les administrations en Europe.

Tout d'abord, nous avons exploré le potentiel de S2 pour la classification des espèces d'arbres par pixel dans les peuplements forestiers purs. Nous avons utilisé deux scènes S2 couvrant l'écorégion des Ardennes belges. Nous avons entraîné deux modèles classifieur forêt aléatoire: le premier pour prédire les zones forestières, et le second pour classifier 11 classes dans la forêt : Fagus sylvatica L., Betula sp., Quercus sp., autres peuplements feuillus, Pseudotsuga menziesii (Mirb.) Franco, Larix sp., Pinus sylvestris L., Picea abies (L.) H.Karst, jeunes peuplements résineux, autres peuplements résineux et coupes à blanc récentes. Une deuxième version de ces deux modèles a été entraînée après l'ajout de variables 3D générées à partir de jeux de données LiDAR et photogrammétriques. En utilisant uniquement les données S2, la précision globale (OA) du modèle de carte forestière était de 0,92, l'OA de la classification des espèces d'arbres était de 0,89, avec une précision moyenne de l'utilisateur (UA) également de 0,89. L'inclusion de variables 3D n'a que légèrement amélioré la précision du modèle. Bien qu'il s'agisse d'une approche simplifiée, les résultats de l'étude ont démontré la capacité de S2 à séparer les espèces d'arbres belges communes sur la base

de leur signature spectrale.

Deuxièmement, nous avons développé une méthode utilisant l'imagerie satellite pour cartographier les espèces d'arbres dans les peuplements forestiers purs et mixtes avec une taille de pixel trop grossière pour résoudre individuellement des arbres. Nous avons utilisé un modèle d'apprentissage profond (réseau neuronal convolutionnel) pour prédire par pixel un vecteur de proportions d'espèces d'arbres (somme égale à 1), en tenant compte de la zone environnante. Le modèle a été entraîné à l'aide d'une carte de polygones de parcelles forestières extraite de la géodatabase de l'Administration publique des forêts de Wallonie. Neuf espèces ou groupes d'espèces ont été considérés : Le genre épicéa, le genre chêne, le hêtre, le douglas, le genre pin, le genre peuplier, le genre mélèze, le genre bouleau et les autres espèces. Nous avons produit une carte des proportions d'espèces d'arbres pour la région wallonne (sud de la Belgique) et évalué sa qualité à l'aide de l'inventaire forestier régional de Wallonie. Nous avons proposé une méthode pour évaluer les cartes de proportions en trois parties : (1) l'espèce majoritaire, (2) la composition spécifique (présence ou absence) et (3) les proportions d'espèces (valeurs de proportion). Le R^2_{adj} des proportions prédites était de 0,50. Les valeurs élevées obtenues pour les indicateurs overall accuracy of majority class assessment (OA_{maj}, 0.73) et mean score (MS, 0.89) ont démontré la capacité de la méthode à prédire l'espèce d'arbre majoritaire et la composition spécifique dans les peuplements forestiers mixtes et purs de la zone d'étude. La méthode de cartographie des espèces d'arbres proposée est adaptée à la caractérisation des forêts sur des zones étendues car elle utilise des images satellites publiques et les données de référence les plus courantes en matière de composition spécifique des arbres.

Troisièmement, nous avons développé un outil permettant de cartographier les AHF et de les classer dans des groupes établis sur la base des mesures agro-environnementales européennes. Dans la première étape du processus, les AHF ont été séparés des arbres en forêt sur la base d'un masque de végétation. Ensuite, un algorithme a classé les éléments AHF en 7 classes : Arbres isolés, Arbres alignés, Arbres agglomérés, Haies, Bosquets, Arbustes et Autres. Cet algorithme a été développé en deux étapes : (1) la classification géométrique de chaque élément AHF et (2) l'analyse du voisinage spatial des éléments et leur classification finale en fonction des combinaisons spatiales possibles. L'OA de la classification des AHF était de 0,78, démontrant le potentiel de l'approche pour la surveillance des AHF dans les paysages ruraux.

En perspective, pour la cartographie des proportions des espèces d'arbres, des recherches ultérieures devraient explorer la valeur ajoutée d'une dimension temporelle à la version actuelle de notre modèle d'apprentissage profond, qui n'exploite que les dimensions spectrales et spatiales des images S2. Pour la cartographie AHF, nous irons au-delà du prototype en optimisant l'outil de classification. En tirant parti de la nouvelle génération d'acquisitions LiDAR, il sera possible d'aller plus loin dans la caractérisation automatisée des AHF. Nous encourageons les futures recherches en télédétection liées

à des applications concrètes, car cela stimule l'innovation là où elle est nécessaire dans un domaine qui est par nature appliqué.

Acknowledgments

pause quotidienne du couloir. C'est clairement dans ce bureau que j'ai appris le métier (les fléchettes bien sûr!). Merci Stéphanie Bonnet pour ton soutien, ta gentillesse et ton franc-parler au début de ma thèse. Merci Adrien Michez et Peter Gaucher pour ces innombrables parties (de statistiques bien sûr!). Merci Peter pour ta folie. Merci Blandine Georges (blanblan!) pour avoir amené un peu de bon sens dans ce bureau! Merci aussi à tous ceux que j'ai pu cotoyer dans ce bon vieux couloir de Forêt: Chloé Dupuis, Alain Monseur, Cédric Geerts, Gauthier Ligot, Jérôme Perin, Jonathan Lisein, Mikhail Pitchugin, Nicolas Latte, Romain Candaele, Samuel Quevauvillers, Sébastien Bauwens et tous les autres! Le cadre de travail de l'unité est optimal grâce à vous tous! Plus largement, j'en profite pour remercier l'infrasctructure de Gembloux Agro-Bio Tech et l'ensemble de la communauté gembloutoise. Mes pas à Gembloux resteront gravés dans ma mémoire.

Merci Nicolas! Collaborer avec toi fut un réel plaisir. Merci pour nos interminables discussions lors de la conception de cette carte des espèces. Nous aurons partagé un goût poussé pour la réflexion! Sans toi, cette carte et l'article associé n'auraient pas vu le jour. Merci pour ta passion.

Romain, nous avons partagé l'angoisse d'une thèse qui n'en finit pas. En tant que compagnon de galère avant mon départ pour l'Italie, merci pour le soutien! Merci pour nos conversations passionnées, merci pour ton amitié.

Je remercie également mes amis et ma famille, au sens large, pour leur soutien. Je pense notamment à mon grand-père, Jacques Bolyn, qui est probablement très heureux que cette thèse se finalise.

Murielle, merci pour ton amour, merci de me faire rire, merci de me rendre fou, merci d'être là, toujours. C'est aussi toi qui a permis ce travail en me rattachant à ma vie. Merci mille fois d'avoir été présente lorsque je me suis isolé dans le travail.

Enfin, je suis heureux d'avoir trouvé la force de terminer ce travail par delà ces vieux murs de Gembloux. En cela, je remercie le Joint Research Centre et l'équipe de Pieter Beck de me permettre de continuer ma carrière de chercheur. L'environnement stimulant et passionnant que j'y ai trouvé m'a apporté un nouveau regard, contribuant à la finalisation de mon manuscrit. Merci à la communauté scientifique et à tous ceux qui contribuent à faire du métier de chercheur une aventure incroyable d'enrichissement.

Contents

List of Figures

Acronyms

ALS aerial laser scanning. 15, 51, 83, 84

CHM canopy height model. 7, 51, 69, 70, 78, 79, 83, 84

CNN convolutional neural network. iii, 35, 71, 72, 75–77

ERTS Earth Resources Technology Satellite. 7

ESA European Space Agency. 7, 8

FAO Food and Agriculture Organization of the United Nations. iii, 3–5

LiDAR light detection and ranging. 7, 9, 10, 78, 79, 83, 84

MPS mean producer's score. 71

MS mean score. 71

MSI MultiSpectral Instrument. 8

MUS mean user's score. 71

NFI national forest inventories. 5, 6

OA overall accuracy. 70, 73, 74

OA$_{maj}$ overall accuracy of majority class assessment. 72

OB broadleaved stands. 69

ON other needle-leaved stands. 69

PA producer's accuracy. 71, 73, 74

PA$_{maj}$ producer's accuracy of majority class assessment. 72

RCC recent clear-cuts. 69, 70

S2 Sentinel-2. iii, 8–11, 15, 35, 69–72, 74, 75, 78–80, 84

SAR Synthetic Aperture Radar. 7

TIF trees inside the forest. 3, 4, 10, 69, 73, 84

TOF trees outside of the forest. 3–6, 9–11, 51, 69, 73, 74, 79, 83–85, 89

UA user's accuracy. 70, 71, 74

UA$_{maj}$ user's accuracy of majority class assessment. 72

YN young needle-leaved stands. 69

1

Introduction

1. Trees inside and outside of the forest

Forest ecosystems provide ecological and socio-economic services and values that are vital to human societies around the world. The urgent need to address the crises of climate change and biodiversity highlights the crucial role that forests play in the balance of our systems. Forests provide primary habitat for a wide range of species. They are themselves essential for the conservation of biodiversity. They are a key element in regulating the global carbon cycle, thereby helping to mitigate climate change. By conserving soil and stabilising water flows and run-off, healthy forest ecosystems prevent land degradation and desertification and reduce the risk of natural disasters such as floods and droughts. They are a source of food, timber and other forest products that play an important role in the security and economic development of human societies. In addition, forests are a place of recreational, aesthetic and spiritual value for many social contexts (Jenkins & Schaap, 2018).

In recent decades it has been recognised that the services provided by trees are not only concentrated in the forest, leading to the consideration of trees outside of the forest (TOF) (Bellefontaine et al., 2002; Rawat et al., 2003). The functions of TOF have been increasingly taken into account. TOF are a potential source of wood, for example for wood energy production. In addition to forests, the Food and Agriculture Organization of the United Nations (FAO) considers TOF as essential for global food security and nutrition (FAO, 2013). They have a significant impact on national biomass and carbon stocks (Schnell, Altrell, et al., 2015; Zomer et al., 2016). Locally, they host biodiversity and at the landscape scale they are elements of connectivity corridors for many species (McCollin et al., 2000; Rossi et al., 2016). They also protect soils from erosion, maintain water quality and provide protection from flooding and wind. Taking advantage of these benefits, agroforestry systems combine tree plantations with agricultural crops in a mutually beneficial way. In cities, their presence is crucial to mitigate the urban heat island effect (Hulley, 2012).

Understanding the state of a resource at a regional or national level is a prerequisite for implementing a well-designed policy. There is no management without monitoring the present, and no decision without modelling the future. A recent study illustrates how ecosystem services and biodiversity indicators are highly dependent on forest management and site characteristics (Schwaiger et al., 2019). In contrast, (Jandl et al., 2019) concluded that only a few forest types are either not strongly affected by climate change or do not have an immediate need for adaptation in forest management. For forest ecosystems, these findings illustrate how a crisis increases the need for information, forecasting and thus research. The bark beetle outbreak crisis in Europe is one such example, for which Hlásny et al. (2021) established a state of knowledge and proposed ways forward for management.

Both trees inside the forest (TIF) and TOF form essential ecosystems. However, their characteristics, location and distribution in the landscape mosaic are different.

Therefore, these two contexts require a separate approach in order to be properly studied. This requires that the two classes of trees are clearly defined. There is no universal definition of forest, as it takes different forms from one region to another, depending on climatic and environmental conditions. Furthermore, its management and human representation can also vary, affecting definitions. As an example, the definition of the Cambridge dictionary illustrates how the common representation of forest is relative and does not allow the distinction of an exclusive class in the landscape:

Forest

A large area of land covered with trees and plants, usually larger than a wood, or the trees and plants themselves. ("Cambridge Dictionary", 2023)

National forest inventories define forest clearly (Tomppo et al., 2010), but each country administration has its own definition related to local forest characteristics. In this thesis we have preferred to use an international definition. We have chosen the FAO classification ("Food and agriculture organisation of the united nations", 2020), which defines two classes of wooded land: forest and other wooded land:

Forest

Land spanning more than 0.5 hectares with trees higher than 5 meters and a canopy cover of more than 10 percent, or trees able to reach these thresholds in situ. It does not include land that is predominantly under agricultural or urban land use.

To complement this definition, the FAO provides a number of explanatory notes, two of which are most relevant to this research:

1. *Includes areas with young trees that have not yet reached but which are expected to reach a canopy cover of 10 percent and tree height of 5 meters. It also includes areas that are temporarily unstocked due to clear-cutting as part of a forest management practice or natural disasters, and which are expected to be regenerated within 5 years. Local conditions may, in exceptional cases, justify that a longer time frame is used.*

2. *Includes windbreaks, shelterbelts and corridors of trees with an area of more than 0.5 hectares and width of more than 20 meters.*

Other wooded land

Land not classified as "Forest", spanning more than 0.5 hectares; with trees higher than 5 meters and a canopy cover of 5-10 percent, or trees able to reach these thresholds in situ ; or with a combined cover of shrubs, bushes and trees above 10 percent. It does not include land that is predominantly under agricultural or urban land use.

Essentially, the key criteria for this land cover classification are the area, the canopy cover and the tree height (Figure 1.1).

In this document, the use of the the term TIF refers to trees located in forest and other wooded land. In opposition, TOF denotes all trees that do not fit the definition
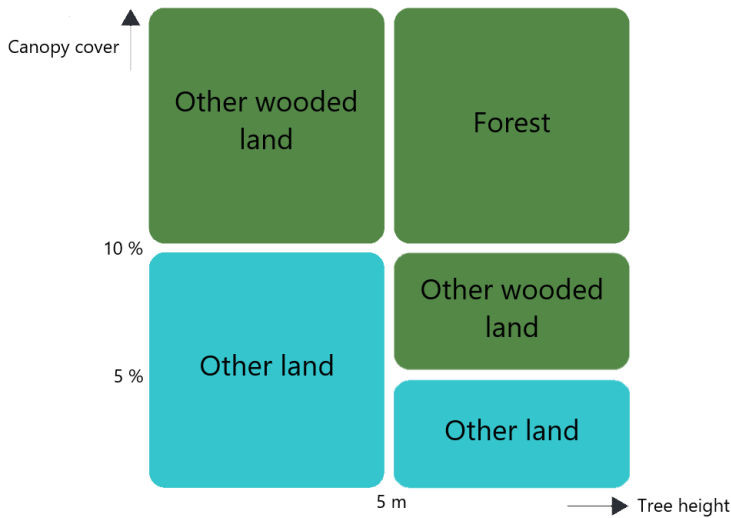
Figure 1.1: Definition of forest, other wooded land and other land as a function of the canopy cover and the tree height, according to the FAO ("Food and agriculture organisation of the united nations", 2020). Wooded areas less than 0.5 ha or less than 20 m wide are included in other land.

of either of these two classes (Figure 1.1). In other words, all trees less than 5 m in height that are not part of a wooded patch with a canopy cover higher than 10 %, an area higher than 0.5 ha and a width higher than 20 m are TOF. For trees taller than 5 m, the minimum canopy cover to be considered as wooded area is reduced to 5 %.

2. Remote sensing as a tool for monitoring trees

For decades, Knowledge about forests has been obtained through extended forest inventories carried out by sampling. National forest inventories (NFI) are implemented in many countries and have evolved with users' needs (Tomppo et al., 2010). Although NFIs provide information of high value, they are time-consuming, quite expensive and have to be sample-based (not wall to wall) for obvious reasons. Futhermore, NFI present three important limitations. First, the sampling design is often not adapted to provide relevant results for small areas. Second, the monitoring of forest dynamics is limited by the long cycle of regional and national inventories, which can exceed 10 years. Finally, restricting the inventory to the administrative boundary is limiting for international studies, which then rely on the methodological and temporal compatibility of the different inventories.

Compared to forests, TOF are less monitored and studied. However, TOF are becoming central to regional policies on climate change mitigation and biodiversity pro-

tection and restoration. For example, the Walloon government (southern Belgium) supports some agroforestry practices like the planting of hedges and trees to achieve the ambitious goal of planting 4000 km of hedges and/or 1 million trees (Wallonie, 2019). Monitoring of TOF is not often included in NFIs. Where it is implemented, inventory design is not adapted to TOF monitoring and results in low accuracy. Schnell, Kleinn, and Ståhl (2015) conducted a review of TOF monitoring. They highlighted the lack of monitoring, which could be addressed by implementing remote sensing methods in addition to field acquisition. The dispersed nature of TOF makes it difficult to design a sampling design with an acceptable cost of implementation. This is where technological innovation becomes very relevant.

"Remote sensing is the acquiring of information from a distance" (NASA, 2019). Passive or active remote sensors on aircraft and satellites measure the intensity of electromagnetic radiation emitted or reflected by an area. The use of these data, directly or through remote sensing models, is a great opportunity for the study and management of ecosystems (Girard & Girard, 2010). For trees, spectral imagery can only be used to estimate canopy metrics. Eventually, under-canopy metrics can be derived from canopy metrics, whereas field inventories measure them directly. However, remote sensing has several advantages. First, it reduces the cost of data acquisition while increasing the coverage of the acquisition campaign without the need for a sampling design. Second, spatially explicit remote sensing acquisitions allow the production of a wall-to-wall forest attribute map, providing information on the location and distribution of a given attribute. Third, acquisition units are related to a precise time period. Successive acquisitions, such as those from satellite sensors, can even allow time series analysis. Forest and tree attributes derived from remote sensing data are then of high value as they are complementary to those derived from NFIs. The latter have a higher degree of certainty, but can only summarise information regionally over a long period of time (Tomppo et al., 2010).

Sustainable forest management requires accurate information on forest structure and monitoring of spatial and temporal changes. In this sense, remote sensing is a relevant method to monitor forest degradation, deforestation and to measure forest variables. Improvements in remote sensing technology, machine learning and geographic information systems have had a profound impact on forest research in recent years. Indeed, the availability of open source data, the development of open source and free software, and the emergence of cloud-based platforms now provide incredible opportunities to develop effective and efficient methods (Nandasena et al., 2022).

3. Motivation and problem statement

3.1. *Trees inside the forest (TIF)*

The use of remote sensing in forest resource assessment began in the first half of the 20th century with the use of aerial photography for local level mapping. In recent decades, the main satellite platforms relevant to forest applications have carried two broad types of sensor systems: optical (passive sensor) and Synthetic Aperture Radar (SAR) (active sensor). According to Boyd and Danson (2005), the information collected in forests using remote sensing can be divided into three levels: first, the spatial extent of the forest cover and its dynamics; second, the forest type; third, the biophysical and biochemical properties of forests.

The first, tree cover mapping, is a prerequisite for characterising the forest of an area of interest in more detail. Remote sensing models have been continuously improved and are now operational and used to produce accurate layers on a global scale. For example, (Hansen et al., 2013) used time series analysis of Landsat imagery to characterise and map forest extent and change at a global scale with a spatial resolution of 30 m. They extended the time period of their analysis (Global Forest Change) from 2012 to 2021 ("Global Forest Change", 2023). At country or regional levels where aerial surveys are feasible, light detection and ranging (LiDAR) datasets or photogrammetric canopy height model (CHM)s (Michez et al., 2020) allow the production of forest maps with better spatial resolution and very high accuracy.

The forest type level of information, and in particular the subdivision of the forest into tree species classes, is more complicated. However, tree species are a key feature in the description of forest ecosystems. The use of remote sensing for tree species classification has been an increasing research topic in recent decades. However, in their review, Fassnacht et al. (2016) highlighted the lack of studies over large geographical areas and noted a preponderance of purely data-driven studies aimed at improving classification accuracy without a targeted application.

Optical sensors provide valuable information to distinguish tree species based on their spectral signature. In 1972, NASA launched the first satellite to monitor Earth resources: Earth Resources Technology Satellite (ERTS), later known as Landsat 1. Among existing satellite sensors, the Landsat mission ("Landsat Science", 2023) had the benefit of providing free access to multispectral imagery covering the globe. With a lifespan of 50 years, the Landsat programme has created an Earth observation archive that is highly valuable for understanding natural resources. Landsat 8 and 9 provide height spectral bands at 30 m spatial resolution and a panchromatic band at 15 m for an 8-day repeat coverage. These characteristics make Landsat data a relevant choice to realise interesting studies in tree species classification, as in Konrad Turlej et al. (2022).

The European Space Agency (ESA) launched a new Earth observation mission called
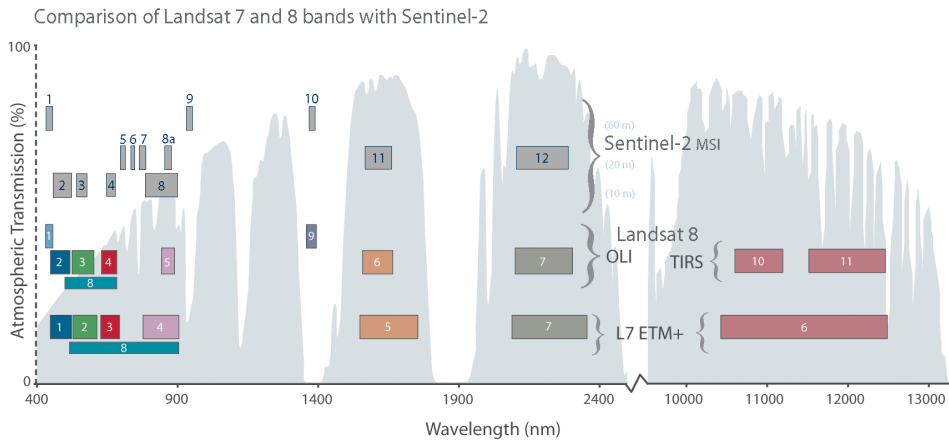
Figure 1.2: Comparison of Landsat 7 and 8 bands with S2 ("USGS EROS Archive", 2023).

Sentinel-2 (S2) in 2015. Its main purpose and characteristics are described on the ESA website as follows:

"The Copernicus SENTINEL-2 mission comprises a constellation of two polar-orbiting satellites placed in the same sun-synchronous orbit, phased at 180° to each other. It aims at monitoring variability in land surface conditions, and its wide swath width (290 km) and high revisit time (10 days at the equator with one satellite, and 5 days with 2 satellites under cloud-free conditions which results in 2-3 days at mid-latitudes) will support monitoring of Earth's surface changes."

The sensor on board S2 is the MultiSpectral Instrument (MSI), which measures the Earth's reflected radiation in 13 spectral bands from VNIR to SWIR. The S2 mission has greatly increased the availability of free imagery with properties relevant to land cover and land use mapping in recent years (Phiri et al., 2020). S2 provides images with spectral bands at 20 m spatial resolution, which are very valuable for vegetation discrimination (1.2). In particular, "red-edge" bands not covered by Landsat sensors. The availability of such free, high quality data at this spatial and temporal resolution was unprecedented and has great potential for tree species mapping. In a study comparing Landsat and S2 imagery, Astola et al. (2019) concluded that S2 outperformed Landsat 8 in predicting forest variables. They highlighted that the S2 red-edge bands and the better spatial resolution of S2 were explaining factors.

The potential of machine learning and deep learning algorithms combined with satellite imagery is high in environmental remote sensing research (Maxwell et al., 2018; Yuan et al., 2020). The high spatial, spectral and temporal resolution of S2 imagery, combined with free access to the data, provides the opportunity to advance research in tree species mapping. However, the use of S2 imagery in the context of mixed forest

stands can be challenging. There are two main limitations. First, the spatial resolution of S2 is too coarse to delineate tree crowns: 20 m for the most discriminating spectral bands for vegetation. Pixel-based classification assumes that elements can be resolved individually, i.e. that target objects are larger than the resolution cells of the image. (Strahler et al., 1986). The use of images with a spatial resolution coarser than tree crowns implies theoretical accuracy limits. Furthermore, the availability of reference data is very limited in mixed forest stands. Tree level observations over large areas with a sufficiently accurate location are typically not available. Together, these two constraints lead to practical limits for image classification methods. Classification model training (e.g. using machine learning) would be limited to pure or near pure forest stands to label pixels with tree species classes. A number of recent studies on tree species classification have generated their reference database in this way (Axelsson et al., 2021; Bjerreskov et al., 2021; Grabska et al., 2019, 2020; Hoscilo & Lewandowska, 2019; Immitzer et al., 2019; Persson et al., 2018; Wessel et al., 2018; Xi et al., 2021; Zagajewski et al., 2021), including the first study of this thesis (Bolyn et al., 2018). Evaluating the behaviour of such a model in a mixed forest context is then as necessary as it is difficult to realise due to the lack of reference data. As a consequence, most studies only assess the performance of the predictive model, but do not perform a validation of the generated map for the study area. This performance assessment is usually achieved by randomly selecting a proportion of pure reference pixels for validation.

In the context of the availability of S2 images since 2015, the first aim of this thesis was to explore its potential for tree species classification. The second purpose of the thesis (related to forest mapping) was to address the issues of tree species mapping in mixed forest stands using satellite imagery with a spatial resolution coarser than tree crowns. The overall objective was to develop a wall-to-wall tree species mapping method for both pure and mixed forest contexts in temperate forests.

3.2. Trees outside of the forest (TOF)

Recent studies have highlighted the value of remote sensing in monitoring TOF through visual interpretation or automated detection (Brandt et al., 2020; Kumar et al., 2021; Li et al., 2023). In particular, deep learning is increasingly being used to develop automated monitoring of TOF. Remote sensing research on TOF is often aimed at estimating biomass or carbon storage. A recent study by Liu et al. (2023) used LiDAR datasets across Europe to train a deep learning model and predict height and tree cover from PlanetScope imagery at the European scale. They were able to distinguish between forest and TOF thanks to their high-resolution dataset. They then derived country-scale estimates of above-ground biomass with a systematic bias of only 7.6% (overestimation; Pearson correlation of 0.98) when compared to 24 national inventories from 30 countries. This achievement illustrates how the large increase in available satellite data over the last decade, combined with improvements in artificial intelli-

gence methods, will lead to impressive automated applications.

Studies using TOF mapping have either mapped TOF as a single overall category, distinct from forest, or divided TOF into simple classes that structure the landscape, such as linear elements and patches. For example, the European layer "Small Woody Features" ("Small Woody Features — Copernicus Land Monitoring Service", 2015) for the reference year 2015 distinguishes between linear and patchy structures. Although this type of dataset is very relevant for studying the distribution of TOF and estimating biomass at a regional scale, its classification is too simple compared to existing TOF definitions, which refer to the use, form and location of TOF in the landscape. Hedges, aligned trees and orchards are examples of commonly described TOF elements whose definition is based on parameters such as length, width and height, as well as the spatial pattern of tree groups. In this sense, a tool dedicated to the automatic classification of TOF types was missing. Indeed, the production of a TOF map with a typology close to that used by managers and administrations has the potential to improve the monitoring and management of TOF. Therefore, the aim of this thesis was to develop an algorithm for TOF mapping and classification. Since such a classification would exploit the shape of the TOF elements and their spatial organisation, we needed to generate an initial TOF map with a very high spatial resolution. For this reason, we based our method on aerial LiDAR data, which model the landscape as 3D point clouds with very high spatial accuracy.

4. Objectives and structure of the thesis

4.1. Objectives

The purpose of this thesis was to contribute to the research in tree monitoring using remote sensing. Two objectives were defined for TIF and TOF respectively, in order to meet the current needs according to the state of the art in the field of remote sensing and the characteristics of these two resources.

Objective 1

The first objective was to develop a method for mapping tree species in pure and mixed stands in European temperate forests using S2 imagery.

We divided the research related to Objective 1 into two steps. First, we set up a study to explore the potential of S2 imagery for tree species classification. Second, we developed a method to map tree species in pure and mixed forest stands with a pixel size too coarse to resolve individual trees.

Objective 2

The second objective was to develop a tool dedicated to the automated classification of TOF types, with a typology close to that used by managers and administrations.

4.2. Structure of the thesis

The thesis is structured around the above two objectives. Three scientific articles have been published in peer-reviewed journals. Two for the two steps of objective 1, the third for objective 2.

Research related to Objective 1 is presented in chapters 2 and 3. Chapter 2 presents a peer-reviewed paper exploring the potential of S2 imagery for mapping tree species composition using per-pixel classification. This publication is the result of the first step of Objective 1. Chapter 3 presents the research related to the second step with a peer-reviewed paper on the use of deep learning and S2 images for mapping tree species proportions in forests.

Chapter 4 presents the publication resulting from Objective 2. This peer-reviewed paper dealt with the design of a tool for the mapping and characterisation of TOF.

Chapter 5 begins with a synthesis of the main findings of the thesis. We then discuss in more detail the results achieved for Objectives 1 and 2 and present the perspectives of this research.

Appendices A.1 and A.2 present two popularised articles published in the context of this thesis. Appendix B.1 provides additional illustrations for the work presented in chapter 3.

2

Exploring the potential of Sentinel-2 imagery for tree species classification

1. Preamble

This section presents the first step of the developments related to Objective 1. We selected two cloud-free S2 images of the Ardenne ecoregion (Southern Belgium) for a first test of tree species classification in temperate forests. In comparison to using only S2 spectral bands, we also evaluated the added value of 3D information from aerial laser scanning (ALS) and photogrammetry. This research has been published in the peer-reviewed journal *Biotechnology, Agronomy, Society and Environment (BASE)*.

2. Peer reviewed article

Bolyn, C., Michez, A., Gaucher, P., Lejeune, P., & Bonnet, S. (2018). Forest mapping and species composition using supervised per pixel classification of sentinel-2 imagery. *Biotechnol. Agron. Soc. Environ.*, 16.

Forest mapping and species composition using supervised per pixel classification of Sentinel-2 imagery

Corentin Bolyn, Adrien Michez, Peter Gaucher, Philippe Lejeune, Stéphanie Bonnet

Université de Liège - Gembloux Agro-Bio Tech. TERRA Forest is life. Passage des Déportés, 2. BE-5030 Gembloux (Belgium). E-mail: p.lejeune@uliege.be

Description of the subject. Understanding the current situation and evolution of forests is essential for a sustainable management plan that maintains forests' ecological and socio-economic functions. Remote sensing is a helpful tool in developing this knowledge.

Objectives. This paper investigates the new opportunities offered by using Sentinel-2 (S2) imagery for forest mapping in Belgian Ardenne ecoregion. The first classification objective was to create a forest map at the regional scale. The second objective was the discrimination of 11 forest classes (*Fagus sylvatica* L., *Betula* sp., *Quercus* sp., other broad-leaved stands, *Pseudotsuga menziesii* (Mirb.) Franco, *Larix* sp., *Pinus sylvestris* L., *Picea abies* (L.) H.Karst., young needle-leaved stands, other needle-leaved stands, and recent clear-cuts).

Method. Two S2 scenes were used and a series of spectral indices were computed for each. We applied supervised pixel-based classifications with a Random Forest classifier. The classification models were processed with a pure S2 dataset and with additional 3D data to compare obtained precisions.

Results. 3D data slightly improved the precision of each objective, but the overall improvement in accuracy was only significant for objective 1. The produced forest map had an overall accuracy of 93.3%. However, the model testing tree species discrimination was also encouraging, with an overall accuracy of 88.9%.

Conclusions. Because of the simple analyses done in this study, results need to be interpreted with caution. However, this paper confirms the great potential of S2 imagery, particularly SWIR and red-edge bands, which are the most important S2 bands in our study.

Keywords. Belgian Ardenne ecoregion, tree species, remote sensing, satellites, per-pixel classification, random forest.

Cartographie forestière et composition spécifique par classification supervisée par pixel d'imagerie Sentinel-2

Description du sujet. Étudier l'état et l'évolution des forêts est essentiel pour assurer une gestion durable maintenant leurs fonctions écologiques et socio-économiques. La télédétection est un outil précieux pour le développement de ces connaissances.

Objectifs. Cette étude analyse l'opportunité offerte par l'imagerie Sentinel-2 (S2) pour cartographier les forêts de l'écorégion de l'Ardenne belge. Le premier objectif de classification était la création d'une carte forestière à l'échelle régionale. Le second objectif était la discrimination de 11 classes forestières (*Fagus sylvatica* L., *Betula* sp., *Quercus* sp., other broad-leaved stands, *Pseudotsuga menziesii* (Mirb.) Franco, *Larix* sp., *Pinus sylvestris* L., *Picea abies* (L.) H.Karst., young needle-leaved stands, other needle-leaved stands, and recent clear-cuts).

Méthode. Deux scènes S2 ont été utilisées et une série d'indices spectraux ont été générés pour chacune d'entre elles. Nous avons réalisé une classification supervisée par pixel avec l'algorithme de classification *Random Forest*. Les modèles de classification ont été générés avec un jeu de données S2 pur et avec des données 3D supplémentaires pour comparer les précisions obtenues.

Résultats. Les données 3D ont légèrement amélioré la précision de chaque objectif, mais l'amélioration globale de précision fut uniquement significative pour l'objectif 1. La carte forestière produite avait une précision globale de 93,3 %. Le modèle testant la discrimination des espèces d'arbre fut encourageant également, avec une précision globale de 88,9 %.

Conclusions. Tenant compte des simples analyses réalisées dans cette étude, les résultats doivent être interprétés avec prudence. Cependant, ce travail confirme le grand potentiel de l'imagerie S2, particulièrement les bandes SWIR et *red-edge,* qui jouèrent un rôle essentiel dans ce travail.

Mots-clés. Écorégion de l'Ardenne belge, espèces d'arbre, télédétection, satellite, classification par pixel, forêt aléatoire.

1. INTRODUCTION

Forest ecosystems provide important services to society, and sustainable management and adapted policies are essential to maintain their ecological and socio-economic functions. Forest managers and policy makers must consider the relationships between forest function and ecosystem characteristics and the evolution of forests in order to manage forests and make regional decisions (Führer, 2000; Lindenmayer et al., 2000). Given the globalization of today's society, this need has become even more important, as understanding forests is important for international agreements and reporting requirements (*e.g.* the Kyoto Protocol).

For decades, field inventories have been used to better characterize forest. National inventories exist in countries around the world and have evolved over time to adapt to users' needs (Tomppo et al., 2010). Field inventories provide timely and accurate estimates of forest resources and their evolution at a large scale. Nevertheless, this method is time-consuming and quite expensive. Furthermore, an inventory of an entire area is, for obvious reasons, impossible and sample-based procedures are necessary. Therefore, technological innovation is becoming crucial to improve the efficiency of measurements and estimations while making the production of inventory data simpler (McRoberts & Tomppo, 2007).

Remote sensing is one of the technological tools at our disposal: it decreases the cost of data acquisition, increases the area it is possible to cover without sampling, and enables the production of high-resolution forest attribute maps. Remote sensing enables the production of map layers that give precious information about the distribution of forest resources. These complement sample-based procedures in the field and today are commonly used by researchers and managers (McDermid et al., 2009).

Today advances in technology such as satellite remote sensing and digital photogrammetry have increased the possible applications of remote sensing and image classification. Light detection and ranging (LiDAR) data and photogrammetry technologies have made it possible to use 3D data, such as Canopy Height Models (CHM) when investigating forests. These technologies improve the classification accuracy of forest classes (Waser et al., 2011). However, 3D data is still rare at the large scale and the technology remains expensive.

This may be different for satellite imagery. On 28 February 2008, the European Union (EU) and European Space Agency (ESA) signed an agreement over the creation of the COPERNICUS program. The aim of this program is to provide earth surface monitoring services (European Commission, 2015) (Land, Atmosphere & Marine Monitoring, Climate Change, Security & Emergency Management Services). The launch of the two Sentinel-2 (S2) satellites is an opportunity to enhance forest characterization on a large scale. The satellites multispectral 13-band sensors produce high-quality images at a 5-day equatorial temporal resolution (Suhet & Hoersch, 2015). Such an availability of free data is unprecedented and will substantially promote research in this topic.

In preparation for the arrival of the new S2 imagery, Inglada et al. (2017) present a methodology to automatize the production of a land cover map at the country scale using high-resolution optical image time series. Using this methodology, the study constructs a map of metropolitan France with a coefficient of kappa 0.86 describing 17 land cover classes, including broad-leaved forest and coniferous forest. In the first study to use pre-operational S2 data, Immitzer et al. (2016) test both a pixel-and object-based classification of tree species in Germany for 7 classes, getting an overall accuracy (OA) of 0.64 and 0.66, respectively. These studies demonstrate the powerful potential of satellite imagery for forest mapping, and research is necessary to exploit the potential of these new S2 data. In their review of tree species classification studies, Fassnacht et al. (2016) observe the increasing number of works on this topic over the last 40 years. However, they note that most investigations are oriented toward optimizing classification accuracy over a relatively small test site and it is therefore often difficult to draw general conclusions from these studies. The authors recommend using well-defined applications in future research in order to avoid purely data-driven studies of limited values and increase understanding of broader factors affecting tree species classification.

In this context, we use S2 imagery to investigate image classification in European temperate forests at the regional scale. Our study has three goals:
– to create a highly accurate regional forest map using S2 imagery;
– to evaluate the potential of S2 imagery in identifying the main tree species encountered in the study area;
– to assess the benefits of incorporating 3D data into our study of the previous two goals and therefore determining how precise S2 data is in these approaches.

For these purposes, we implemented supervised classification per pixel using a random forest (RF) algorithm. We used two S2 images acquired at different dates to take account for species seasonality. Then, we computed a range of spectral indices. After a step of variables selection, we trained random forest classifiers for two datasets: the first contains only S2 bands and spectral indices, while the second also contains 3D data. The quality of the results was assessed and

compared in terms of a confusion matrix with a strong reference dataset.

2. MATERIALS

2.1. Study site

The study was conducted for the entire Belgian Ardenne ecoregion. This region constitutes a plateau whose altitude increases gradually from the South-West to the North-East, culminating at nearly 700 m. The annual mean temperature is smaller than 9 °C and annual precipitations are nearly 1,200 mm. With an afforestation rate of 58%, the Ardenne represents 333,850 ha of forest and is the largest forest area in Wallonia. This forest is mainly coniferous (64%), according to Wallonia's Regional Forest Inventory (RFI) (Alderweireld et al., 2015), and the most frequently found tree species are (in order of quantity): spruce (*Picea abies* [L.] H.Karst.), oak (*Quercus* sp.), beech (*Fagus sylvatica* L.), Douglas fir (*Pseudotsuga menziesii* (Mirb.) Franco), pine (*Pinus* sp.), and larch (*Larix* sp.). These six species represent 85.8 % of the forest. Most of the time, coniferous stands are pure species plantations. Deciduous stands are most of the

time naturally regenerated and thus present an uneven-aged structure and a composition dominated by beech and oak, the level of mixture being driven mainly by soil depth and topography. **Figure 1** provides an overview of the study site.

2.2. Remotely sensed data

Sentinel-2. The onboard S2 sensor is a passive multi-spectral instrument (MSI). It provides 13 spectral bands (**Table 1**). In order to simplify pre-processing, the only two available S2 images with less than 10% cloud cover over the entire Ardenne ecoregion were selected. Their sensing times were 2 August 2015 and 8 May 2016 (further referred as D1 and D2). These dates have a potential interest as they could help to difference some broad-leaved species between themselves or from resinous species. Indeed in this region, in May, *Fagus sylvatica* and *Betula* sp. have begun foliation period since more than a month while *Quercus* sp. have just started (https://fichierecologique. be). It is widely acknowledged that reflectance from the Earth's surface, called top-of-atmosphere (TOA), is significantly modified by the atmosphere (Jensen, 2005; Lillesand et al., 2008; Richards, 2013). There are many remote sensing studies that have investigated how to
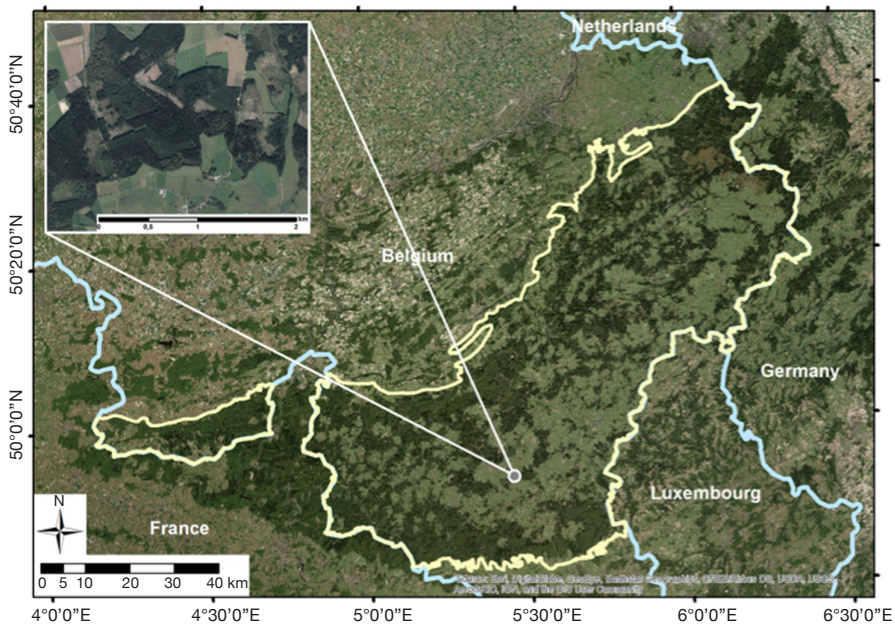
Figure 1. The study area, the Belgian Ardenne ecoregion, is shown in yellow. A more detailed view is presented in the top left corner (orthophoto 2016, Public Service of Wallonia) — *La zone d'étude, l'écorégion de l'Ardenne belge, est en jaune. Une vue plus détaillée est présentée dans le coin supérieur gauche (orthophoto 2016, Service Public de Wallonie).*

Table 1. Sentinel-2 bands properties, band number, band name in this study, central wavelength (nm), bandwidth (nm), spatial resolution (m) and purpose. Only band numbers marked with asterisks were used in this study. Data compilation and purpose from the European Space Agency (2015) — *Propriétés des bandes S2, numéro de la bande, nom de la bande dans cette étude, longueur d'onde centrale (nm), largeur de la bande (nm), résolution spatiale (m) et objectif. Seuls les numéros de bandes annotés avec une astérisque ont été utilisés dans cette étude. Données et objectifs provenant de European Space Agency (2015).*

Band number	Band name	Central wavelength (nm)	Bandwidth (nm)	Spatial resolution (m)	Purpose
2 *	Blue	490	65	10	Blue
3 *	Green	560	35	10	Green
4 *	Red	665	30	10	Red
8 *	NIRwide	842	115	10	Sensitive to chlorophyll, biomass and protein
5 *	Rededge 1	705	15	20	Vegetation Classification
6 *	Rededge 2	740	15	20	Vegetation Classification
7 *	Rededge 3	786	20	20	Vegetation Classification
8a *	NIRnarrow	865	20	20	Vegetation Classification
11 *	SWIR 1	1,610	90	20	Sensitive to lignin, starch and forest above ground biomass
12 *	SWIR 2	2,190	180	20	Distinction of live biomass, dead biomass and soil
1	-	443	20	60	Aerosol scattering
9	-	945	20	60	Water vapor absorption
10	-	1,375	20	60	Detection of thin cirrus

reduce the effects of the atmosphere on the signal (Kaufman et al., 1997; Song et al., 2001; Guanter et al., 2008). This is even more important in case of multi-temporal date analyses (Agapiou et al., 2011; Hagolle et al., 2015), therefore we used the atmospheric correction proposed by the Sen2Cor processor (version 2.2.) (Müller-Wilm, 2016). Hence, Level-1C data were processed into Level-2A (bottom-of-atmosphere corrected reflectance images). S2 bands at 20 m of spatial resolution were resampled at 10 m during this step (nearest neighbor method). Then we compiled a layer stack of 20 spectral bands with D1 and D2.

3D data. Three Canopy Height Models (CHM) and one slope layer, based on LiDAR and photogrammetric point clouds, were used covering the entire study area at a resolution of 1 m.

A CHM was made using LiDAR (LiDAR DSM - LiDAR DTM) and referred to as CHM3 in this paper. The average point density of small footprint discrete airborne Lidar data was 0.8 points·m^{-1}. Survey flights were realized by the Public Service of Wallonia from 12 December 2012 to 21 April 2013 and from 20 December 2013 to 9 March 2014. The survey covered Wallonia with a regional digital terrain model (1 m ground sampling distance [GSD]). A digital surface model (DSM) at the same resolution was also computed and a slope layer was generated based on the Lidar digital terrain model (DTM).

For two other CHMs, raw images from two regional orthophoto datasets (acquired by the Public Service of Wallonia) were used to generate two high-density photogrammetric point clouds. Both survey flights took place between April and September, the first in 2006 and 2007 (0.50 m GSD), the second in 2009 and 2010 (0.25 m GSD). Considering that the regional topography did not change significantly, hybrid CHMs were computed using photogrammetric DSM and LiDAR DTM, as described above, following the approach of Michez et al. (2017) (photogrammetric DSM-LiDAR DTM). Their spatial resolution is 1 m. The precision of this approach has been evaluated in Michez et al. (2017) using field tree height measurements (root mean square error smaller than 3 m). These hybrids CHM are called CHM1 and CHM2 in this paper. They were used in this study to improve the detection of recent clear cuts and young stands, adding height information in the past.

These four layers (CHM1, CHM2, CHM3, and SLOPE) were aggregated at 10 m of spatial resolution using median value.

3. METHODS

3.1. Image classification models

To accomplish our first two goals, we defined two models of classification. The model called Objective 1 created a forest map, and was trained to identify four classes: broad-leaved stands, coniferous stands, recent clear-cuts, and non-forest areas. The non-forest class dataset contained an equal proportion of observations for agricultural lands, urban landscapes, and water bodies. In order to create our forest map, we applied the obtained classifier to the entire study area. We then generated a forest land use map by merging the three forest classes into one. By first growing a model with four classes, clear cuts are integrated into the produced forest map, as it forms an integral part of the forest estate covered by management plans.

Second model called Objective 2 aims at classifying the tree species present in the study site to evaluate the discrimination potential of S2 data using a pixel-based approach. Based on the RFI, we defined 11 classes that corresponds to the main species or types of stands: beech, birch (*Betula* sp.), oak, other broad-leaved stands (OB), Douglas fir, larch, Scots pine (*Pinus sylvestris* L.), spruce, young needle-leaved stands (YN), other needle-leaved stands (ON), and recent clear-cuts (RCC). Young stands correspond to plantations between 4 and 12 years old, and recent clear-cuts are stands that have been harvested in the last four years. For each class, pixels contain at least 80% of the species or group of species.

The global workflow of the study is synthesized in **figure 2**.

3.2. Dataset preparation

In order to determine the most pertinent classification variables in each model, we added a large selection of spectral indices to the original S2 dataset. Each indice was generated for D1 and D2. The list is presented in **table 2**.

We then created another dataset that include 3D data and compared results of the two datasets for each classification objective. In other words, for each objective we tested the following datasets: the S2 bottom-of-atmosphere data D1 and D2 with spectral indices (S2) and the S2 bottom-of-atmosphere data D1 and D2 with spectral indices and 3D data (S2-3D).

All together, there were 10 S2 Bands, 34 indices by sensing time, 3 CHM dates, and 1 slope layer. So, depending on whether we included 3D data, we had 89 or 93 variables by dataset.

Reference pixels were produced from delineated management forest units (DFU) extracted from the regional forest administration geodatabase and from four bands (RGB and IR) 0.25 m resolution orthophotos covering the entire region. These image layers are available for the years 2006, 2009, 2012, and 2015 (http://geoportail.wallonie.be).

DFU were used for both Objectives 1 and 2 to extract reference data for forest classes. Before that, DFU polygons were visually interpreted to verify eventual errors or modifications since the last update. For each class, the chosen forest stands were supposed to be "pure stands" according to the DFU database (percentage > 80%). **Table 3** shows by class the number of polygons and the number of extracted pixels. Reference polygons were delineated for non-forest classes by visual interpretation of orthophotos.

3.3. Variable selection and classification

The following steps were executed in the same way for Objectives 1 and 2 using Dataset 1 or 2 (**Figure 2**). Before building classification models, we rationally reduced the number of variables by selecting the most important using *VSurf* (Genuer et al., 2016) in R software (R Core Team, 2016). The *VSurf* package allows variable selection based on the estimation of RF's variable importance (Genuer et al., 2015). As a result, the process provides two variables subsets. The first, called "variable interpretation", is intended to show variables highly related to the response variable. It does not matter if there is some, or even much, redundancy in this subset. The second, called "prediction", is a smaller subset with low redundancy intended to assure a good prediction of the response variable.

The following parameters were set to allow the maximum performance in a reasonable time with the used computer:
– each RF was built using *ntree* = 1,000 trees, the number of variables randomly sampled as candidates at each split (*mtry*) was set by default (sqrt[p], where p is the number of variables);
– the number of random forests grown was 20 for the three main steps of the *Vsurf* process: "thresholding step", "interpretation step", and "prediction step" (*nfor.thres* = 20, *nfor.interp* = 20 and *nfor.pred* = 20);
– the mean jump is the threshold of decreasing mean OOB error used in the *Vsurf*'s prediction step to add variables to the model in a stepwise manner. It was multiplied 4 times (*nmj* = 4) in order to make this step more selective, considering the large number of variables.

For the two objectives, we realized supervised classifications per pixel with a RF classifier (Breiman, 2001), using the randomForest package (Liaw & Wiener, 2002) in R software (R Core Team, 2016). Only the variables selected during the prediction step
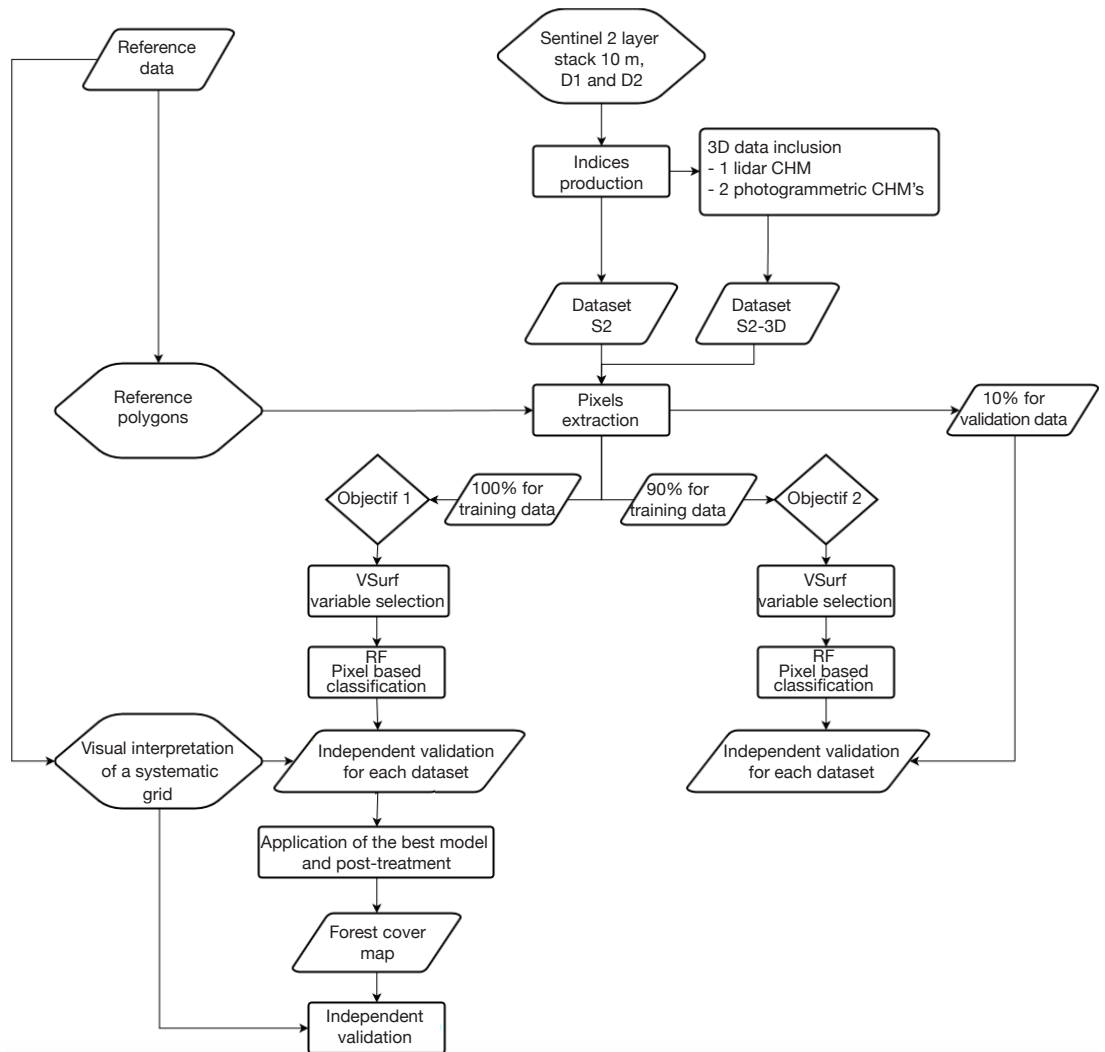
Figure 2. Global workflow of the study divided in two goals of classification. The first classification model called Objective 1 created a forest map, and was trained to identify four classes: broad-leaved stands, coniferous stands, recent clear-cuts, and non-forest areas. Second model called Objective 2 aimed at classifying the tree species present in the study site to evaluate the discrimination potential of S2 data using a pixel-based approach. After a step of variables selection, random forest classifiers were trained for two datasets: the first contained only S2 bands and spectral indices (Dataset S2), while the second also contained 3D data (Dataset S2-3D) — Workflow *global de l'étude divisé en deux objectifs de classification. Le premier modèle de classification nommé Objectif 1 a généré une carte forestière et a été entraîné à identifier quatre classes : les peuplements feuillus, les peuplements résineux, les coupes rases récentes et les surfaces non forestières. Le second modèle nommé Objectif 2 visait à classifier les espèces d'arbre présentes sur le site d'étude afin d'évaluer le potentiel discriminant des données S2 via une approche par pixel. Après une étape de sélection de variables, des forêts aléatoires ont été entraînées pour deux jeux de données : le premier contenant uniquement les bandes S2 et des indices spectraux (Dataset S2), le second incluant aussi des données 3D (Dataset S2-3D).*

Table 2. List of spectral indices generated for D1 (2 August 2015) and D2 (8 May 2016) S2 images — *Liste des indices spectraux générés pour les images S2 D1 (2 aout 2015) et D2 (8 mai 2016).*

Indice	Name	Formula	References
BAI	Built-up Area Index	$\dfrac{Blue - NIRnarrow}{Blue + NIRnarrow}$	Shahi et al., 2015
Chlogreen	Chlorophyll Green index	$\dfrac{NIRnarrow}{Green + Rededge1}$	Datt, 1999
GEMI	Global Environment Monitoring Vegetation Index	$n \times (1 - 0.25n) \dfrac{Red - 0.125}{1 - Red}$ $n = \dfrac{2 \times (NIRnarrow^2 - Red^2) + 1.5 \times NIRnarrow + 0.5 \times Red}{NIRnarrow + Red + 0.5}$	Pinty & Verstraete, 1992
GI	Greenness Index	$\dfrac{Green}{Red}$	le Maire et al., 2004
gNDVI	Green normalized difference vegetation index	$\dfrac{NIRnarrow - Green}{NIRnarrow + Green}$	Gitelson et al., 1996
LAnthoC	Leaf Anthocyanid Content	$\dfrac{Rededge3}{Green - Rededge1}$	Wulf & Stuhler, n.d.
LCaroC	Leaf Carotenoid Content	$\dfrac{Rededge3}{Blue - Rededge1}$	Wulf & Stuhler, n.d.
LChloC	Leaf Chlorophyll Content	$\dfrac{Rededge3}{Rededge1}$	Wulf & Stuhler, n.d.
MSI	Moisture stress index	$\dfrac{SWIR1}{NIRnarrow}$	Vogelmann & Rock, 1985
NDrededgeSWIR	Normalized Difference of Red-edge and SWIR2	$\dfrac{Rededge2 - SWIR2}{Rededge2 + SWIR2}$	Radoux et al., 2016
NDTI	Normalized Difference Tillage Index	$\dfrac{SWIR1 - SWIR2}{SWIR1 + SWIR2}$	Van Deventer et al., 1997
NDVI	Normalized difference vegetation index	$\dfrac{NIRnarrow - Red}{NIRnarrow + Red}$	Tucker; 1979
NDVIre	Red-edge normalized difference vegetation index	$\dfrac{NIRnarrow - Rededge1}{NIRnarrow + Rededge1}$	Gitelson et al., 1996
NDWI1	Normalized Difference Water Index 1	$\dfrac{NIRnarrow - SWIR1}{NIRnarrow + SWIR1}$	Gao, 1996
NDWI2	Normalized Difference Water Index 2	$\dfrac{Green - NIRnarrow}{Green + NIRnarrow}$	Gitelson et al., 1996
NHI	Normalized Humidity Index	$\dfrac{SWIR1 - Green}{SWIR1 + Green}$	Lacaux et al., 2007

Table 2 (continued). List of spectral indices generated for D1 (2 August 2015) and D2 (8 May 2016) S2 images — *Liste des indices spectraux générés pour les images S2 D1 (2 août 2015) et D2 (8 mai 2016).*

Indice	Name	Formula	References
Norm-G	Normalized Green	$\dfrac{Green}{NIRwide + Red + Green}$	Sripada et al., 2006
Norm-NIR	Normalized Near Infra-red	$\dfrac{NIRwide}{NIRwide + Red + Green}$	Sripada et al., 2006
Norm-R	Normalized red	$\dfrac{Red}{NIRwide + Red + Green}$	Sripada et al., 2006
RededgePeakArea	Red-edge peak area	$Red + Rededge1 + Rededge2 + Rededge3 + NIRnarrow$	Filella & Penuelas, 1994; Radoux et al., 2016
RedSWIR1	Bands difference	$Red - SWIR1$	Jacques et al., 2014
RTVIcore	Red-edge Triangular Vegetation Index	$100 \times (NIRnarrow - Rededge1) - 10 \times (NIRnarrow - Green)$	Chen et al., 2010
SAVI	Soil Adjusted Vegetation Index	$\dfrac{NIRnarrow - Red}{NIRnarrow + Red + 0.5} \times 1.5$	Huete, 1988
SR-BlueRededge1	Simple Blue and Red-edge 1 Ratio	$\dfrac{Blue}{Rededge1}$	le Maire et al., 2004
SR-BlueRededge2	Simple Blue and Red-edge 2 Ratio	$\dfrac{Blue}{Rededge2}$	Lichtenthaler et al., 1996
SR-BlueRededge3	Simple Blue and Red-edge 3 Ratio	$\dfrac{Blue}{Rededge3}$	Radoux et al., 2016
SR-NIRnarrowBlue	Simple ratio NIR narrow and Blue	$\dfrac{NIRnarrow}{Blue}$	Blackburn, 1998
SR-NIRnarrowGreen	Simple ratio NIR narrow and Green	$\dfrac{NIRnarrow}{Green}$	le Maire et al., 2004
SR-NIRnarrowRed	Simple ratio NIR narrow and Red	$\dfrac{NIRnarrow}{Red}$	Blackburn, 1998
SR-NIRnarrowRededge1	Simple NIR and Red-edge 1 Ratio	$\dfrac{NIRnarrow}{Rededge1}$	Datt, 1999
SR-NIRnarrowRededge2	Simple NIR and Red-edge 2 Ratio	$\dfrac{NIRnarrow}{Rededge2}$	Radoux et al., 2016
SR-NIRnarrowRededge3	Simple NIR and Red-edge 3 Ratio	$\dfrac{NIRnarrow}{Rededge3}$	Radoux et al., 2016
STI	Soil Tillage Index	$\dfrac{SWIR1}{SWIR2}$	Van Deventer et al., 1997
WBI	Water Body Index	$\dfrac{Blue - Red}{Blue + Red}$	Domenech & Mallet, 2014

Table 3. The number of DFU polygons and extracted pixels by forest class: recent clear cuts (RCC), beech, birch, oak, other broad-leaved stands (OB), Douglas fir, larch, other needle-leaved stands (ON), Scots pine, spruce, young needle-leaved stands (YN) — *Nombre de polygones DFU et nombre de pixels extraits par classe forestière : coupes récentes (RCC), hêtre (beech), bouleau (birch), chêne (oak), autres peuplements feuillus (OB), Douglas (Douglas fir), mélèze (larch), autres peuplements résineux (ON), pin sylvestre (Scots pine), épicéa (spruce), jeunes peuplements résineux (YN).*

	RCC	Beech	Birch	Oak	OB	Douglas fir	Larch	ON	Scots pine	Spruce	YN
Number of polygons	51	64	57	37	34	46	44	45	33	31	47
Number of pixels	7,068	6,327	2,589	4,572	3,623	5,929	5,799	3,251	4,180	4,028	3,858

of *VSurf* were considered for this classification. The process was executed with 2,000 trees to grow and *mtry* set by default. A series of parameters combinations were tested to find the most relevant parameters for this study. Before training the models, the number of observations by class was randomly downsampled to balance classes.

3.4. Accuracy assessment

All the reference data extracted from DFU polygons were used to train Objective 1. The accuracy assessment was carried out with a set of points systematically distributed over the study area (1 km x 1 km, n = 5,744 points) and photo-interpreted on the orthophotos. Confusion matrices were built comparing attributed classes for these points.

Concerning Objective 2, 10% of the reference data extracted from DFU polygons was randomly selected to create a validation dataset. The number of observations by class was randomly downsampled to balance classes for the validation. Confusion matrices were built using these validation data. For Objectives 1 and 2, we computed the OA (overall accuracy) as well as producer (PA) and user accuracy (UA) for each class.

4. RESULTS

4.1. Objective 1: forest map

Comparing the performance of both datasets. **Table 4** shows the accuracy of the forest maps generated using the S2 and S2-3D datasets. These results were computed before post treatments and are presented to compare dataset performances. The presentation of the final forest map is described in Section 4.1.3. S2-3D gave the best results, with an overall accuracy difference of 0.9% between the two approaches. This difference is significant (*p-value* = 0.002421, McNemar's chi-squared test realized on the contingency table of correctly classified and incorrectly classified points). The PA of the non-forest class had the highest difference in accuracy (1.7%) between S2 and

Table 4. Accuracy comparison of the RF classifiers built with the S2 and S2-3D datasets for classification Objective 1. A visual interpretation of a systematic point grid (1 km x 1 km, n = 5,744 points) was used to compute accuracy indices: overall accuracy (OA), production accuracy (PA) and user accuracy (UA) by class — *Comparaison des précisions atteintes résultant de l'utilisation des jeux de données S2 et S2-3D pour la classification Objectif 1. Une photointerprétation d'une grille de points systématique (1 km x 1 km, n = 5 744 points) a été utilisée pour calculer les indices de précision :* overall accuracy *(OA),* production accuracy *(PA) and* user accuracy *(UA) par classe.*

	S2	S2-3D
OA (%)	91,7	92,6
PA forest (%)	91,9	92,3
UA forest (%)	94,5	95,5
PA non-forest (%)	91,3	93,0
UA non-forest (%)	87,5	88,2

S2-3D. The lowest difference in accuracy (0.4%) was for the PA of the forest class.

Selected variables. The results presented in this section are based on the classifier trained with the S2-3D dataset, which obtained the best precisions. **Figure 3** illustrates which S2 bands were mostly identified as relevant regarding our classification goals. A band was counted if it was selected at the *VSurf* interpretation step and each time it was used in a variable selected during the interpretation step. For Model 1, the three bands used the most were B8A, B11 and B12, all of which have a 20 m GSD.

In **table 5**, variables were sorted according to their sensing date and native spatial resolution. The term "mixed" means that S2 bands of both spatial resolutions were used to generate the index.

Fourteen variables were selected during the *VSurf* prediction step. The list is presented in descending order of occurrence: CHM2, CHM3, B11-D2, CHM1, B7-D2, B12-D1, SLOPE, STI-D1, NDTI-D1, RTVIcore-D2, B5-D2, MSI-D2, NDrededgeSWIR-D1, and B5-D1.

Objective 1

Objective 2
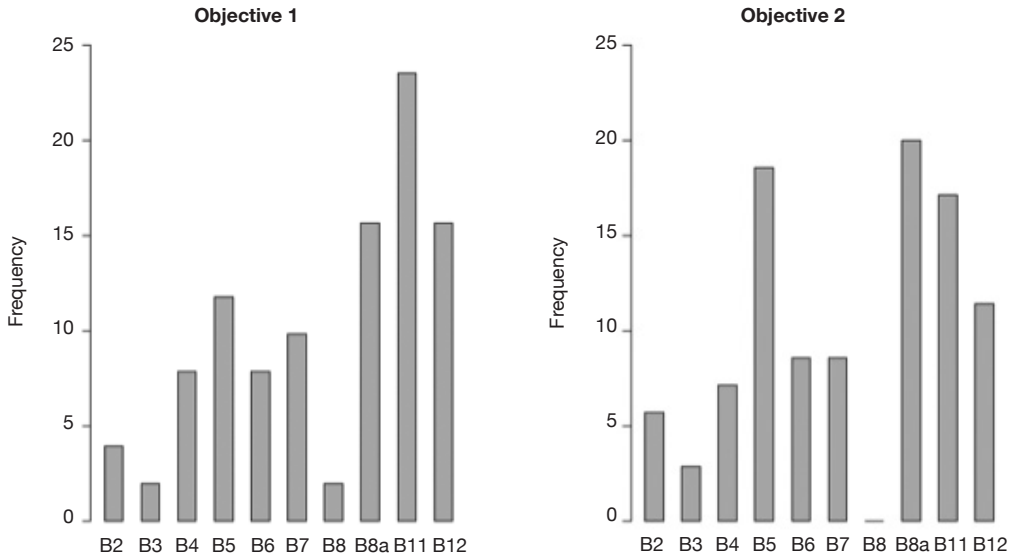
Figure 3. Frequency of selection for each S2 band (**Table 1**) by the *VSurf* selection process (Genuer et al., 2016) during the interpretation step. A band is counted if selected itself or inside a spectral indice variable — *Fréquence de sélection de chaque bande S2 (**Tableau 1**) par le processus de sélection* VSurf *(Genuer et al., 2016) durant la phase d'interprétation. Une bande est comptabilisée si elle est sélectionnée elle-même ou au sein d'une variable d'indice spectral.*

Table 5. Percentage of selected S2 variables by spatial resolution and acquisition date of S2 image. The class "mixed" lists the variables computed with 10 m S2 bands and 20 m S2 bands — *Pourcentage des variables S2 sélectionnées par résolution spatiale et par date d'acquisition de l'image S2. La classe « mixed » concerne les variables générées avec des bandes S2 à 10 m et des bandes S2 à 20 m.*

	By date (%)		By spatial resolution (%)		
	8/2/2015	5/8/2016	10 m	mixed	20 m
Objective 1	32.1	67.9	7.1	21.4	71.4
Objective 2	47.4	52.6	5.3	34.2	60.5

Production of a forest map. The RF classifier generated with previous variables was used to compute a final forest map. This map was then filtered using the Majority Filter tool of ArcMap® (Number of neighbors to use: 8, Replacement threshold: MAJORITY). **Figure 4** presents the result. A validation was carried out for the produced map. The OA value of the confusion matrix was 93.3%. PA and UA were 93.2% and 95.8% for the forest class while it was 93.3% and 89.5% for the non-forest class.

4.2. Objective 2: tree species classification

Comparing the performance of both datasets. In order to compare the accuracies of achieved results for both the S2 and S2-3D dataset, user accuracies of all classes have been summarized by mean to make the comparison easier. For dataset S2, OA and the user accuracy mean (UA mean) were 88.5% and 88.6% while for dataset S2-3D, it was 88.9% and 89%. As with Model 1, the 3D dataset gave the best results but the differences in precision can be considered as negligible: in all cases the value was less than 0.5%.

Selected variables. The results presented in this section concern the classifier trained with the S2-3D dataset that obtained the best precision values. They are summarized in **figure 3** and **table 5**. The three most-selected bands at the *VSurf* interpretation step were B8A (NIR narrow), B5 (Red Edge 1), and B11 (SWIR 1), all of which have a 20 m GSD.

Eighteen variables were selected during *VSurf* prediction step. The list is presented in descending number of appearances: SLOPE, CHM1, CHM2, CHM3, RedSWIR1-D2, B8A-D2, B7-D2, B11-D2, NDrededgeSWIR-D1, B5D2, MSI-D2, NDWI1-D2, B12-D2, B6-D2, B11-D1, STI-D1, B5-D1, and LChloC-D1.
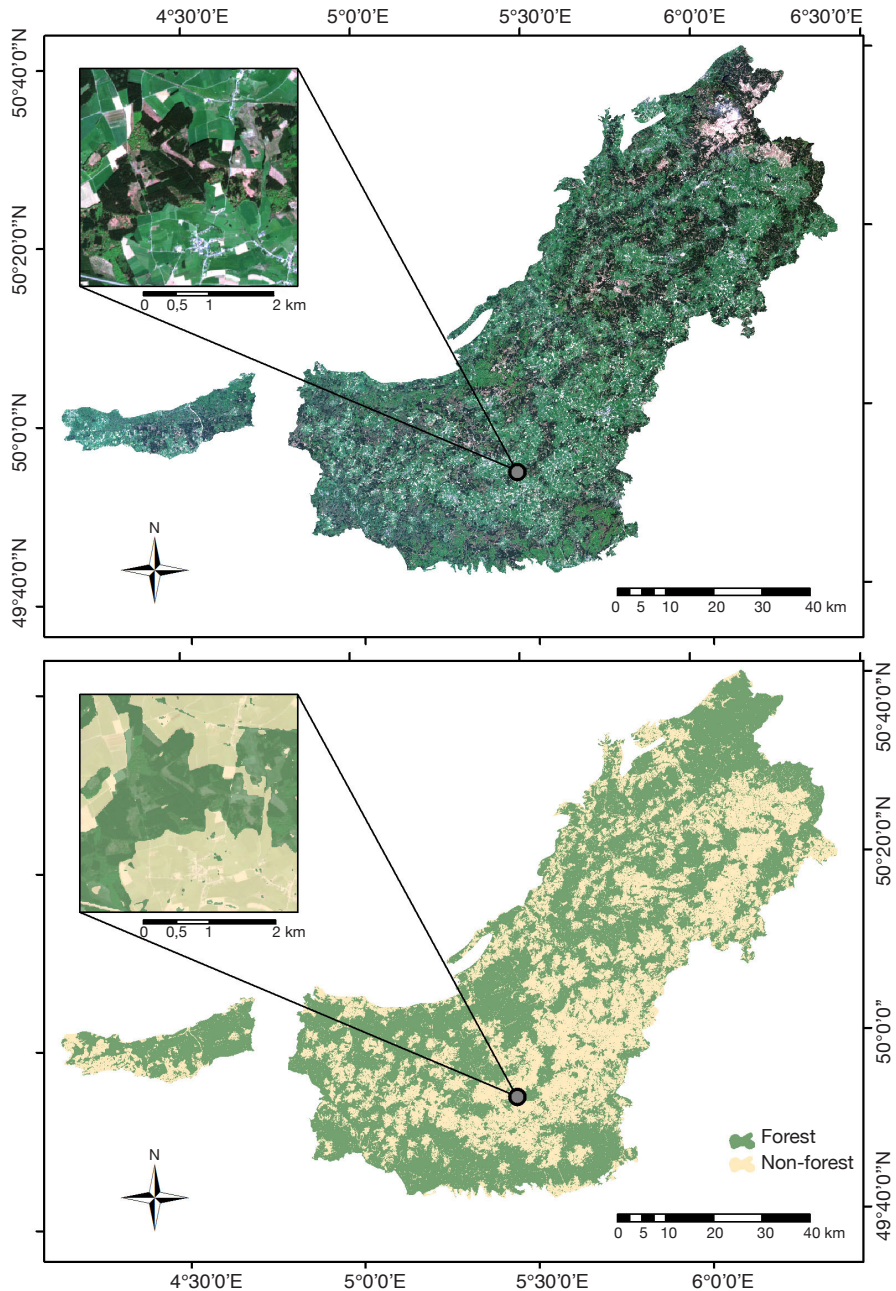
Figure 4. On the top in RGB colour composition, one of the two S2 images (05/08/2015) used in this study. On the bottom, the forest map of the Belgian Ardenne ecoregion generated by merging the three forest classes of the classification result "Objective 1" into one. Both maps present a more detailed view in their top left corner — *En haut en composition colorée RGB, l'une des deux images S2 (08/05/2015) utilisée dans cette étude. En bas, la carte forestière de l'écorégion de l'Ardenne belge, générée en fusionnant les trois classes forestières du résultat de la classification « Objectif 1 » en une seule. Les deux cartes présentent une vue plus détaillée dans leur coin supérieur gauche.*

Accuracy of the best classifier. Achieved accuracies with the S2-3D dataset are presented in detail by a confusion matrix (**Table 6**). The OA was 88.9%. The worse PA concerned the larch (79.9%) and recent clear cut (83.2%) classes. The worst UA were for beech (83.8%) and larch (86.3%).

5. DISCUSSION

5.1. Variable selection

It is interesting to observe the difference between Objectives 1 and 2 in **figure 3**. In Objective 1, the most selected bands were found, in order of number of appearances, B11, B8a, and B12. In Objective 2 the most selected bands were B8a, B5, and B11. These results are in line with the goals of classification models and band properties. Indeed, Objective 1 aimed at distinguishing forest classes (coniferous stands, broad-leaved stands, and recent clear-cuts) from non-forest areas. The second classification objective was separating tree species classes present on the study site. B11 is sensitive to forest above ground biomass and B12 facilitates distinction of live biomass, dead biomass, and soil (**Table 2**), thus B11 and B12 have

more importance in Objective 1 where there are non-forest classes. B5 and B8a are more related to Objective 2; indeed, vegetation classification is the only goal in this case. **Figure 3** shows the importance of shortwave infrared (SWIR) (B11 and B12) and the red-edge band B5 for both models, as mentioned in other studies (Schuster et al., 2012; Fassnacht et al., 2016; Immitzer et al., 2016; Radoux et al., 2016).

Looking at **table 5**, we can see that the most selected variables have a GSD of 20 m. As a consequence, the resolution of the resulting maps was not really 10 m; even more without the use of 3D data. This confirms the relevance of spectral bands sensed by S2 but reminds us that spectral resolution can be more important than spatial resolution for vegetation discrimination at a regional scale.

Selected variables were well distributed between the two S2 images taken on different dates, especially for Objective 2. It appears that image interaction was useful. Choosing the time of image acquisition in relation to species' phenological cycle is a possible way to improve discrimination. Immitzer et al. (2016) test a classification of tree species in Germany for seven classes on a single date. Their results show an OA of 0.64, an accuracy lower than what we found in this study, even for Dataset S2. This was probably

Table 6. Confusion matrix of classification Objective 2 for Dataset S2-3D. The validation of Objective 2 was realized with 10% of the reference data. Classification Objective 2 concerned 11 classes: recent clear cuts (RCC), beech, birch, oak, other broad-leaved stands (OB), Douglas fir, larch, other needle-leaved stands (ON), Scots pine, spruce, young needle-leaved stands (YN). Producer accuracy (PA) and user accuracy (UA) are presented for each class — *Matrice de confusion de la classification Objectif 2 pour le jeu de données S2-3D. La validation de la classification Objectif 2 a été réalisée en utilisant 10% des données de référence. La classification Objectif 2 concernait 11 classes : coupes récentes (RCC), hêtre (Beech), bouleau (Birch), chêne (Oak), autres peuplements feuillus (OB), douglas (Douglas fir), mélèze (Larch), autres peuplements résineux (ON), pin sylvestre (Scots pine), épicéa (Spruce), jeunes peuplements résineux (YN). La précision du producteur (PA) et la précision de l'utilisateur (UA) sont présentées pour chaque classe.*

Prediction	Reference											
	RCC	Beech	Birch	Oak	OB	Douglas fir	Larch	ON	Scots pine	Spruce	YN	UA (%)
RCC	223	2	3	1	2	1	3	1	1	0	4	92.5
Beech	5	238	1	1	8	3	6	11	3	4	4	83.8
Birch	8	5	259	4	2	3	3	3	0	3	1	89.0
Oak	1	1	1	229	2	5	8	0	2	1	1	91.2
OB	6	0	1	5	242	3	4	2	3	2	1	90.0
Douglas fir	2	2	0	3	4	232	16	3	1	1	2	87.2
Larch	8	6	0	1	2	4	214	8	4	0	1	86.3
ON	2	7	0	2	1	7	5	236	0	1	1	90.1
Scots pine	3	2	2	4	2	0	0	0	249	4	2	92.9
Spruce	6	2	0	9	2	7	4	1	4	251	3	86.9
YN	4	3	1	9	1	3	5	3	1	1	248	88.9
PA (%)	83.2	88.8	96.6	85.4	90.3	86.6	79.9	88.1	92.9	93.7	92.5	

partially because of our use of images taken on two dates. It would be interesting to test the use of images taken on several dates during the vegetation period in order to benefit from tree species phenology. Particularly for broad-leaved species, a series of dates from March to May should help to detect differences in foliation period. This is a task for future study; the growing availability of free data from S2 satellites makes this research a possibility.

During the final *VSurf* prediction step, all 3D data were taken into account and were among the best variables for both objectives. The slope was the best for Ojective 2, showing that the presence of certain species in the study site is strongly related to the topography. Fourteen variables were selected for Objective 1 and 18 for Objective 2. Except NDTI and RTVIcore, all the variables in Objective 1 were included in Objective 2. In addition, Objective 2 included additional indices and S2 bands, which helped to discriminate vegetation species. As expected, this suggests that more information is needed to solve a complex problem like separating tree species. Just as the SWIR and red-edge bands were the most selected S2 variable during the *VSurf* interpretation step, almost all the variables selected during the *VSurf* prediction step were a SWIR or red-edge band or a spectral index computed with at least one of these bands.

5.2. Precision of the results

The produced forest map (Objective 1) had a very good precision rate, with an OA of 93.3%. In our reference dataset, used for classifier construction, the non-forest class was composed of different land cover and was less homogeneous than other classes. The non-forest class UA was worse than for the forest class, probably for this reason. In this study, we did not control the behavior of the classifier with small woodland areas like isolated trees or bands of trees. The precision of the map could be negatively impacted by fragmented landscape elements because the spatial resolution of S2 is probably too low for this purpose, and edge pixels represent a large proportion of the total, increasing the bias due to sub-pixel variations (not evaluated here) (Stratoulias et al., 2015; Immitzer et al., 2016; Radoux et al., 2016). Hence, a possible improvement for users of this map could be to choose an appropriate definition for the forest that would remove these problematic elements. According to the Walloon Forest Inventory (Alderweireld et al., 2015), the Belgian Ardenne ecoregion includes 333,850 ha of forest area. Based on the forest map classification and the confusion matrix, an area estimator of forest was computed (Olofsson et al., 2013) at 354,761.3 ha (± 3,695.57 ha) of forest in the Belgian Ardenne

ecoregion. The RFI only considers forest elements bigger than 0.1 ha and wider than 20 m. This limit could partly explain the over-estimation; pixel groups smaller than 10 pixels, correctly classified or not, are common on the forest map.

The results of second objective, concerning tree species discrimination, were encouraging (**Table 6**). The obtained precisions were better than those in previous studies using S2 data (Immitzer et al., 2016) and similar or better than those in studies using data from other sensors with various spatial and spectral resolution (Immitzer et al., 2012). For this number of classes and this study area size, these results are encouraging. This approach demonstrates the possibility of efficiently mapping regional tree species with S2 imagery in the future. Nevertheless, the study did have some limitations, due to its workflow and the reference data used.

First, because of the availability of data the number of different forest stands for some species used to extract pixels was limited (from 31 to 64, **Table 3**). This means that the within-species variance of training data sets was probably too reduced for a large area like the Belgian Ardenne. Furthermore, the DFU cover only public forests that represent 57% of the study area. It will be important for future studies to represent as best as possible the variability of species. Further research could also eventually consider ecological gradients in analyses (*e.g.* water proximity, elevation, sunlight exposure). For instance, the benefit of using ancillary geodata in a classification process has been studied in Forster & Kleinschmit (2014).

Second, we did not manage to account for species mixing at the pixel level. Indeed, the probability to have a single tree or stand exactly covered by a single pixel matching its extent is low (Fassnacht et al., 2016). The simplification done when extracting pixels from supposedly pure stands resulted in interesting conclusions regarding the separate nature of species. But it is not yet sufficient to create a map of species distribution, since the study area includes many mixed pixels. Furthermore, for this study, the most important S2 bands were sensed at 20 m GSD, increasing these effects. As a consequence of these two simplifications, the precision evaluated by independent validation was probably over-estimated for the application of the classifier over the whole study site.

Choosing an object-based approach and processing segmentation with very high resolution images like orthophotos would allow researchers to work at the scale of one stand or tree group (Kumar, 2006). It could partly solve these issues and would give researchers the interesting opportunity to combine advantages from a time series of S2 images and very high-resolution images.

5.3. Contribution of 3D data

In the creation of the forest map, the use of 3D data significantly improved the precision. However, it appears that at a large scale and at this spatial resolution it is possible to get sufficient predictions using only S2 imagery. The best improvements using 3D data were seen in the UA of the forest class and in consequence for the PA of the non-forest class. Information about tree height should, most of the time, limit confusion between other vegetation and forest; the observed trend confirmed this idea. Furthermore, including old clear cuts in the forest map is a complicate task without using anterior CHM's. Taking into account the fact that most of the variables used in the classification have a 20 m GSD, the 10 m spatial resolution of the 3 CHM is probably an advantage for the classification of edges. It could improve the precision at those locations where 20 m pixels have more chance to overlap the edge between forest and non-forest classes. So the quality of geometric limits is probably better for the forest map realized with the S2-3D dataset.

In Objective 2, the global improvement brought by 3D data was less important than in Objective 1. In average, precision did not increase by more than 0.5%. The only interesting exception is the PA of the RCC class, which increased by 5%. As expected, the 3 CHM improved the detection of recent clear cuts. Surprisingly, the detection of YN class did not improve. It appears that their S2 information is already distinguishable from that of other classes without information about height. The use of CHM is not very relevant for the discrimination of tree species at this spatial resolution. In contrast, a derived variable of environment, like the slope (selected as first variable at *VSurf* prediction step), seems to bring more interesting information and improving such an approach could be pertinent.

6. CONCLUSIONS

This paper investigates the new opportunity offered by Sentinel-2 imagery to classify forest and forest species at large scale. Two cloud-free S2 scenes (02/08/2015 and 08/05/2016) were used and a series of spectral indices were computed for each. After variable selection, we applied supervised pixel-based classifications with a random forest classifier. A first model of classification aimed at creating a forest map of the Belgian Ardenne ecoregion. A second tested tree species discrimination for species present on the study site. These two models of classification were processed with both a pure S2 dataset and with additional 3D data and the obtained precisions were compared. The precision of produced forest maps was evaluated with a visually interpreted systematic point grid at intervals of 1,000 m. For the second model, the models were validated with 10% of the reference data.

The evidence from this study suggests that this approach enables accurate classification without 3D data. For Objective 1, classification realized with 3D data was significantly better, with an OA difference of 0.9%. For Objective 2, the improvement in OA was negligible (0.4%). The produced forest map had an OA of 93.3%. The test of tree species discrimination was conclusive and encouraging with an OA of 88.9%. Concerning Objective 2, it is important to remember that the present study has investigated a simplified per-pixel classification with pixels extracted from a limited number of pure stands. As a consequence of these simplifications, the precision evaluated was probably over-estimated for the application of the classifier on the whole study site. Despite these limitations, the results confirmed the great potential of S2 imagery for tree species discrimination. More specifically, the SWIR and red-edge S2 bands are essential, as they were by far the most important in our variable selection process. Their spatial resolution of 20 m can lead to restrictions for detailed analyses. That is why we recommend that further research combines S2 imagery with another data source at very high spatial resolution in order to exploit the undeniable discrimination power of S2 and a better spatial precision. Along the same lines, we achieved similar results both using a 3D dataset and without, but precisions of edges and the detection of small elements seemed to be improved using 3D data. That improvement has not been evaluated in this study. The main gain of using 3D data was the improvement of the forest map and the clear cuts detection. In further research, it would be interesting to generate a forest map including clear cuts, starting from 3D data only at a higher spatial resolution.

The choice of an object-based approach and the use of better acquisition dates are possible methods to improve our classification results. To further our research, we plan to work on the quality of reference data and to develop adequate methods to surpass the test step and create tree species classifiers operational for the production of tree species maps at large scale with an assessment of their precision in the best way.

Bibliography

Agapiou A. et al., 2011. The importance of accounting for atmospheric effects in the application of NDVI and interpretation of satellite imagery supporting archaeological research: the case studies of Palaepaphos and Nea Paphos sites in Cyprus. *Remote Sens.*, **3**(12), 2605-2629.

Alderweireld M., Burnay F., Pitchugin M. & Lecomte H., 2015. *Inventaire forestier wallon. Résultats 1994-2012.* Namur, Belgique : Service Public de Wallonie.

Blackburn G.A., 1998. Quantifying chlorophylls and caroteniods at leaf and canopy scales: an evaluation of some hyperspectral approaches. *Remote Sens. Environ.*, **66**(3), 273-285.

Breiman L., 2001. Random forests. *Mach. Learn.*, **45**(1), 5-32.

Chen P.-F. et al., 2010. New index for crop canopy fresh biomass estimation. *Spectrosc. Spectral Anal.*, **30**(2), 512-517.

Datt B., 1999. Visible/near infrared reflectance and chlorophyll content in *Eucalyptus* leaves. *Int. J. Remote Sens.*, **20**(14), 2741-2759.

Domenech E. & Mallet C., 2014. Change detection in high-resolution land use/land cover geodatabases (at object level). *EuroSDR*, **64**.

European Commission, 2015. *Copernicus: Europe's Eyes on Earth.* Luxembourg: Publications Office.

European Space Agency, 2015. *Sentinel-2a MSI Spectral Responses.xlsx,* https://earth.esa.int/web/sentinel/document-library/latest-documents/-/asset_publisher/EgUy8pfXboLO/content/sentinel-2a-spectral-responses;jsessionid=AA5AEEAE5B3515EFB534D44F239D5FD1.jvm2?redirect=https%3A%2F%2Fearth.esa.int%2Fweb%2Fsentinel%2Fdocument-library%2Flatest-documents%3Bjsessionid%3DAA5AEEAE5B3515EFB534D44F239D5FD1.jvm2%3Fp_p_id%3D101_INSTANCE_EgUy8pfXboLO%26p_p_lifecycle%3D0%26p_p_state%3Dnormal%26p_p_mode%3Dview%26p_p_col_id%3Dcolumn-1%26p_p_col_pos%3D1%26p_p_col_count%3D2, (18/12/2017).

Fassnacht F.E. et al., 2016. Review of studies on tree species classification from remotely sensed data. *Remote Sens. Environ.*, **186**, 64-87.

Filella I. & Penuelas J., 1994. The red edge position and shape as indicators of plant chlorophyll content, biomass and hydric status. *Int. J. Remote Sens.*, **15**(7), 1459-1470.

Forster M. & Kleinschmit B., 2014. Significance analysis of different types of ancillary geodata utilized in a multisource classification process for forest identification in Germany. *IEEE Trans. Geosci. Remote Sens.*, **52**(6), 3453-3463.

Führer E., 2000. Forest functions, ecosystem stability and management. *For. Ecol. Manage.*, **132**(1), 29-38.

Gao B.-C., 1996. NDWI. A normalized difference water index for remote sensing of vegetation liquid water from space. *Remote Sens. Environ.*, **58**(3), 257-266.

Genuer R., Poggi J.-M. & Tuleau-Malot C., 2015. VSURF: An R package for variable selection using random forests. *R Journal*, **7**(2), 19-33.

Genuer R., Poggi J.-M. & Tuleau-Malot C., 2016. *VSURF: variable selection using random forests. R package version 1.0.3.*

Gitelson A.A., Kaufman Y.J. & Merzlyak M.N., 1996. Use of a green channel in remote sensing of global vegetation from EOS-MODIS. *Remote Sens. Environ.*, **58**(3), 289-298.

Guanter L., Gomez-Chova L. & Moreno J., 2008. Coupled retrieval of aerosol optical thickness, columnar water vapor and surface reflectance maps from ENVISAT/MERIS data over land. *Remote Sens. Environ.*, **112**(6), 2898-2913.

Hagolle O., Huc M., Pascual D. & Dedieu G., 2015. A multi-temporal and multi-spectral method to estimate aerosol optical thickness over land, for the atmospheric correction of FormoSat-2, LandSat, VENS and Sentinel-2 Images. *Remote Sens.*, **7**(3), 2668-2691.

Huete A.R., 1988. A soil-adjusted vegetation index (SAVI). *Remote Sens. Environ.*, **25**(3), 295-309.

Immitzer M., Atzberger C. & Koukal T., 2012. Tree species classification with random forest using very high spatial resolution 8-band worldview-2 satellite data. *Remote Sens.*, **4**(9), 2661-2693.

Immitzer M., Vuolo F. & Atzberger C., 2016. First experience with sentinel-2 data for crop and tree species classifications in central Europe. *Remote Sens.*, **8**(3), 166.

Inglada J. et al., 2017. Operational high resolution land cover map production at the country scale using satellite image time series. *Remote Sens.*, **9**(1), 95.

Jacques D.C. et al., 2014. Monitoring dry vegetation masses in semi-arid areas with MODIS SWIR bands. *Remote Sens. Environ.*, **153**, 40-49.

Jensen J.R., 2005. *Introductory digital image processing: a remote sensing perspective.* Upper Saddle River, NJ, USA: Prentice Hall.

Kaufman Y. et al., 1997. Passive remote sensing of tropospheric aerosol and atmospheric correction for the aerosol effect. *J. Geophys. Res.*, **102**(D14), 16815-16830.

Kumar N., 2006. *Multispectral image analysis using the object-oriented paradigm.* Boca Raton, FL, USA: CRC Press.

Lacaux J. et al., 2007. Classification of ponds from high-spatial resolution remote sensing: application to Rift Valley fever epidemics in Senegal. *Remote Sens. Environ.*, **106**(1), 66-74.

Le Maire G., François C. & Dufrêne E., 2004. Towards universal broad leaf chlorophyll indices using PROSPECT simulated database and hyperspectral reflectance measurements. *Remote Sens. Environ.*, **89**(1), 1-28.

Liaw A. & Wiener M., 2002. Classification and regression by randomForest. *R News*, **2**(3), 18-22.

Lichtenthaler H.K. et al., 1996. Detection of vegetation stress via a new high resolution fluorescence imaging system. *J. Plant Physiol.*, **148**(5), 599-612.

Lillesand T.M., Kiefer R.W. & Chipman J.W., 2008. *Remote sensing and image interpretation*. Hoboken, NJ, USA: John Wiley & Sons.

Lindenmayer D.B., Margules C.R. & Botkin D.B., 2000. Indicators of biodiversity for ecologically sustainable forest management. *Conserv. Biol.*, **14**(4), 941-950.

McDermid G. et al., 2009. Remote sensing and forest inventory for wildlife habitat assessment. *For. Ecol. Manage.*, **257**(11), 2262-2269.

McRoberts R. & Tomppo E., 2007. Remote sensing support for national forest inventories. *Remote Sens. Environ.*, **110**(4), 412-419.

Michez A., Piégay H., Lejeune P. & Claessens H., 2017. Multi-temporal monitoring of a regional riparian buffer network (> 12,000 km) with LiDAR and photogrammetric point clouds. *J. Environ. Manage.*, **202**(2), 424-436.

Müller-Wilm U., 2016. *Sentinel-2 MSI. Level-2a prototype processor installation and user manual*. Darmstadt, Germany: Telespazio Vega.

Olofsson P., Foody G.M., Stehman S.V. & Woodcock C.E., 2013. Making better use of accuracy data in land change studies: estimating accuracy and area and quantifying uncertainty using stratified estimation. *Remote Sens. Environ.*, **129**, 122-131.

Pinty B. & Verstraete M.M., 1992. GEMI: a non-linear index to monitor global vegetation from satellites. *Vegetatio*, **101**(1), 15-20.

R Core Team, 2016. *R: a language and environment for statistical computing*. Vienna: R Foundation for Statistical Computing.

Radoux J. et al., 2016. Sentinel-2's potential for sub-pixel landscape feature detection. *Remote Sens.*, **8**(6), 488.

Richards J.A., 2013. *Remote sensing digital image analysis*. Berlin; Heidelberg, Germany: Springer.

Schuster C., Förster M. & Kleinschmit B., 2012. Testing the red edge channel for improving land-use classifications based on high-resolution multi-spectral satellite data. *Int. J. Remote Sens.*, **33**(17), 5583-5599.

Shahi K. et al., 2015. A novel spectral index to automatically extract road networks from WorldView-2 satellite imagery. *Egypt. J. Remote Sens. Space Sci.*, **18**(1), 27-33.

Song C. et al., 2001. Classification and change detection using Landsat TM data: when and how to correct atmospheric effects? *Remote Sens. Environ.*, **75**(2), 230-244.

Sripada R.P., Heiniger R.W., White J.G. & Meijer A.D., 2006. Aerial color infrared photography for determining early in-season nitrogen requirements in corn. *Agron. J.*, **98**(4), 968.

Stratoulias D. et al., 2015. Evaluating Sentinel-2 for lakeshore habitat mapping based on airborne hyperspectral data. *Sensors*, **15**(9), 22956-22969.

Suhet & Hoersch B., 2015. *Sentinel-2 user handbook*. European Space Agency.

Tomppo E., Gschwantner T., Lawrence M. & McRoberts R.E., eds, 2010. *National forest inventories*. Dordrecht, The Netherlands: Springer Netherlands.

Tucker C.J., 1979. Red and photographic infrared linear combinations for monitoring vegetation. *Remote Sens. Environ.*, **8**(2), 127-150.

Van Deventer A.P., Ward A.D., Gowda P.H. & Lyon J.G., 1997. Using thematic mapper data to identify contrasting soil plains and tillage practices. *Photogramm. Eng. Remote Sens.*, **63**, 87-93.

Vogelmann J.E. & Rock B.N., 1985. Spectral characterization of suspected acid deposition damage in red spruce (*Picea* Rubens) stands from Vermont. *In: Proceedings of the Airborne Imaging Spectrometer Data Analysis Workshop, April 8-10, 1985, Jet Propulsion Laboratory, California Institute of Technology, Pasadena, California, United States*, 51-55.

Waser L. et al., 2011. Semi-automatic classification of tree species in different forest ecosystems by spectral and geometric variables derived from Airborne Digital Sensor (ADS40) and RC30 data. *Remote Sens. Environ.*, **115**(1), 76-85.

Wulf H. & Stuhler S., 2015. Sentinel-2: land cover, preliminary user feedback on Sentinel-2a data. *In: Proceedings of the Sentinel-2a expert users technical meeting, 29-30 September 2015, Frascati, Italy*.

(54 ref.)

3

Mapping tree species in pure and mixed forest stands using S2 imagery

1. Preamble

The findings and conclusions presented in Bolyn et al. (2018) enabled the design of a method to achieve the second step of Objective 1. Following the exploratory step, we developed an operational and scalable mapping method adapted to pure and mixed forest stands. Three major changes were made to the approach compared to the first study. First, we abandoned the traditional per-pixel classification (categorical values) for the prediction of tree species proportions (continuous value [0,1]). For the representation of species composition at the pixel level, this means using a vector of proportions whose sum equals 1 (e.g. (0.4, 0.0, 0.6) for three classes) instead of assigning a (dominant) single class label. At the map level, the predictions are then represented as a multi-band grid, one band for each tree species class considered. Second, to train such a model, we replaced the machine learning model (Random Forest) with a deep learning model: a convolutional neural network (CNN). The last major modification was the super-resolution of the S2 images at 2.5 m using the method described in Latte and Lejeune (2020). This research has been published in the peer-reviewed journal *Remote Sensing of Environment (RSE)* (Bolyn et al., 2022).

We published the progress of this research in a popularised article (Bolyn, Latte, Colson, et al. (2020), see appendix A.2). In the latter, the method presented was an intermediate step before implementing an approach using deep learning.

As a supplement to the peer-reviewed article, we provide a set of illustrations for the tree species proportions map in the appendix B.1.

2. Peer reviewed article

Bolyn, C., Lejeune, P., Michez, A., & Latte, N. (2022). Mapping tree species proportions from satellite imagery using spectral–spatial deep learning. *Remote Sensing of Environment*, *280*, 113205. https://doi.org/10.1016/j.rse.2022.113205

Check for
updates

Mapping tree species proportions from satellite imagery using spectral–spatial deep learning

Corentin Bolyn [a,b,*], Philippe Lejeune [a], Adrien Michez [a], Nicolas Latte [a]

[a] *Uliège - Gembloux Agro-Bio Tech. TERRA Teaching and Research Center - Forest Is Life, Passage des Déportés 2, BE-5030 Gembloux, Belgium*
[b] *European Commission, Joint Research Centre (JRC), Ispra, Italy*

ARTICLE INFO

ABSTRACT

Remote sensing can be used to collect information related to forest management. Previous studies demonstrated the potential of using multispectral satellite imagery for classifying tree species. However, methods that can map tree species in mixed forest stands on a large scale are lacking. We propose an innovative method for mapping the proportions of tree species using Sentinel-2 imagery. A convolutional neural network was used to quantify the per-pixel basal area proportions of tree species considering the neighbouring environment (spectral–spatial deep learning). A nested U-shaped neural network (UNet++) architecture was implemented. We produced a map of the entire Wallonia Region (southern Belgium). Nine species or groups of species were considered: *Spruce* genus, *Oak* genus, *Beech*, *Douglas fir*, *Pine* genus, *Poplar* genus, *Larch* genus, *Birch* genus, and remaining species. The training dataset for the convolutional neural network model was prepared using a map of forest parcels extracted from the public forest administration's geodatabase of Wallonia. The accuracy of the predicted map covering the region was independently assessed using data from the regional forest inventory of Wallonia. A robust assessment method for tree species proportions maps was proposed for assessing the (1) majority species, (2) species composition (presence or absence), and (3) species proportions (proportion values). The achieved value of indicator OA_{maj} (0.73) shows that our approach can map the majority tree species in mixed and pure forest stands. Indicators MS (0.89), MPS (0.72) and MUS (0.83) support that the model can predict the species composition in most cases in the study area. *Spruce* genus, *Oak* genus, *Beech*, and *Douglas fir* achieved the best results, with PAs and UAs close to or higher than 0.70. Particularly, high performance was achieved for detecting *Oak* genus and *Beech* in low area proportions: PAs and UAs higher than 0.70 from the 0.4 proportion. Predicted proportions had a R^2_{adj} of 0.50. The proposed method, which uses spectral–spatial deep learning to map the proportions of tree species, is innovative because it was adapted to the complexity of mixed forests and spatial resolution of current satellite imagery. Additionally, it optimises the use of available forest data in the model conception by considering all pixels from pure stands to highly mixed forest stands. When forest inventories are available in a broad sense, that is, georeferenced areas with the proportions of tree species, this method is highly reproducible and applicable at a large scale, offering potential for use in forest management.

1. Introduction

Forest ecosystems provide many services; to maintain their ecological and socio-economic functions, appropriate policies ensuring sustainable management must be implemented. Understanding current challenges and forest evolution at the regional or national level is essential for enacting a well-thought-out forest policy, particularly in the context of global climate change. Tree species are a key source of information for ecologists and forest managers.

In addition to field inventories, remote sensing is useful for collecting information on forested areas. When applied to satellite data,

machine learning methods (Maxwell et al., 2018) and, more recently, deep learning (Yuan et al., 2020) have shown potential in environmental remote sensing research. Tree species classification has evaluated in numerous studies, such as those reviewed in Fassnacht et al. (2016). Open access to high-quality satellite images, including those from Sentinel-2 (S2) satellites, has enabled land cover and land-use mapping in recent years (Phiri et al., 2020).

Most recent studies focusing on medium-resolution satellite imagery involved using pixel-based classification approaches with machine learning methods such as random forests, support vector machines, and artificial neural networks (Zagajewski et al., 2021; Xie

et al., 2021; Bjerreskov et al., 2021; Grabska et al., 2020; Immitzer et al., 2019; Grabska et al., 2019; Hoscilo and Lewandowska, 2019; Persson et al., 2018; Wessel et al., 2018; Bolyn et al., 2018). Two studies were conducted to evaluate the potential of S2 time series using Bayesian inference (Axelsson et al., 2021) and deep neural networks (Conv1D, AlexNet, and LSTM) (Xi et al., 2021). These studies required the availability of a reference database with pixel-level labels for tree species. In general, the necessary pixels were extracted where the forest was known to be pure for a specific species (mono-specific) or when the species was considered as dominant. For example, in some studies (Bjerreskov et al., 2021; Persson et al., 2018), when the reference data were in the form of a field forest inventory, a proportion criterion based on basal area was used to select only plots with a dominant species (typically >70%). There are two reasons for this. First, the spatial resolution of S2 imagery (10 or 20 m depending on the band) does not allow for delineation of the distinct tree crowns of a forest stand. Thus, one pixel may cover several trees of different species in mixed forest stands. Second, even if the spatial resolution is high, field data describing the forest at the tree level over large areas with a sufficiently precise location are typically not available. Therefore, to label pixels with a high level of certainty, a simple solution is to consider only pure forest stands for a specific species.

Although such studies have successfully classified and mapped tree species, a model built using such data for pure forest stands may not show the same performance when applied to mixed stands. Strahler et al. (1986) proposed an explicit framework of remote sensing models in which pixel-based classification is implied considering a discrete scene model, with the scene composed of discrete elements with boundaries. This discrete scene model is nearly always of the "H-resolution" type. Thus, the element may be individually resolved, as the resolution cells of the image are smaller than the elements. Indeed, classification assumes that measurements are samples of energy-exiting objects that are larger than the resolution cells of the image (Strahler et al., 1986). For tree species mapping, the elements of the scene model were trees. Because local variance of an image is linked to the number of mixed pixels, low local variance for pixel-based classification is assumed. Woodcock and Strahler (1987) studied the local variance of an image as a function of resolution. They highlighted that a peak in local variance occurs at a resolution cell size that is somewhat smaller than the size of objects in the scene, which was approximately 1/2–3/4 in their study. Therefore, the imagery used for classification per pixel should have resolution cells smaller than 1/2–3/4 of the tree size to avoid theoretical accuracy limits in mixed forest stands.

Regarding this limitation, the number of studies that include robust evaluation of the resulting tree species map is limited because mixed pixels are not integrated in the validation scheme. Although the same reference data are typically used to train and validate the model, such data cannot fully represent the mapped area, as pixels are extracted only from pure stands. Therefore, purposive sampling and pragmatic site selection may be acceptable for training a classifier; however, a probabilistic sampling design would improve accuracy assessment (Stehman and Foody, 2019).

Several approaches can be used to match the levels of observation to the levels of organisation: dividing a pixel into constituent elements, aggregating the pixels to match a higher level of organisation, or considering the environment of individual pixels without classifying them (Girard and Girard, 2010). Another possibility is to abandon the semantic classification and quantify the proportions of tree species at the pixel level. Mixture models are the most appropriate approach for high local variance conditions (Woodcock and Strahler, 1987). Using this strategy, Gudex-Cross et al. (2017) used spectral unmixing of multi-temporal Landsat images to quantify the basal area percentage of ten tree species/genera using a stepwise linear regression model. The basal area maps were then refined using a set of object-based rules to produce a thematic forest classification.

Table 1

Forest stand types in Wallonia (southern Belgium). From the regional forest inventory, period 1994–2008; (Alderweireld et al., 2015, 2016).

Forest type	Area (ha)	Percentage
Norway spruce stand	163450	34.09%
Oak stand	85200	17.77%
Other broad-leaved stand	56200	11.72%
Beech stand	43750	9.12%
Noble broad-leaved stand	40100	8.36%
Mixed stand Beech–Oak	21200	4.42%
Other needle-leaved	16850	3.51%
Douglas fir stand	13950	2.91%
Pine stand	12600	2.63%
Poplars stand	9800	2.04%
Mixed stand Norway Spruce–Douglas fir	8850	1.85%
Larch stand	7550	1.57%

In recent years, deep learning, particularly convolutional neural networks (CNNs), have been widely used for remote sensing (Ghanbari et al., 2021), primarily for classification and object detection. CNNs are the most common type of NNs for computer vision and image analysis because of their excellent performance and effectiveness. CNNs are particularly robust because of their specific architecture characterised by local receptive fields, shared weights, and subsampling (Kattenborn et al., 2021). Their potential for tree species classification has been tested in some studies and found to achieve high accuracy (Mäyrä et al., 2021; Xi et al., 2021; Cue La Rosa et al., 2021; Illarionova et al., 2021), outperforming traditional machine learning methods.

The objective of this study was to use spectral–spatial deep learning to map tree species proportions over a large area, including all types of forest compositions from pure stands to highly mixed stands, using S2 imagery and available georeferenced forest areas with tree species proportions. There were two challenges to using the proposed method .

- Mapping tree species in pure and mixed forest stands using images with a pixel size too coarse to resolve individual trees ;
- Using forest inventory data that include both pure and mixed stands.

We used a CNN to quantify the per-pixel proportions of the tree species while considering the neighbouring environment. Methods for directly predicting the per-pixel proportions of tree species using both spectral and spatial information are lacking. The method was performed for an entire administrative region, the Wallonia region (southern Belgium), whose forest presents diversity relevant to the study in terms of its structure (mixed and pure forest stands) and tree species composition. A robust and transparent evaluation of the map accuracy was performed using external data from the regional forest inventory (plots) covering the same region.

2. Materials and methods

2.1. Study area

The study area was the Wallonia region (Fig. 1) in the southern part of Belgium, which covers 16,901 km^2, of which 33% is covered by forests (Alderweireld et al., 2015, 2016). 52% of the forest is private and 87% of the forest area is managed for harvesting. The first complete cycle of the regional forest inventory of Wallonia was performed in 1994–2008. An official report (Alderweireld et al., 2015) divided the forest into 12 stand types that are characteristic of the study area (Table 1). The figures from this report illustrate the variety of forests in Wallonia, with a large area of mixed stands containing a variety of tree species. The three most common genera are Spruce, Oak, and Beech.
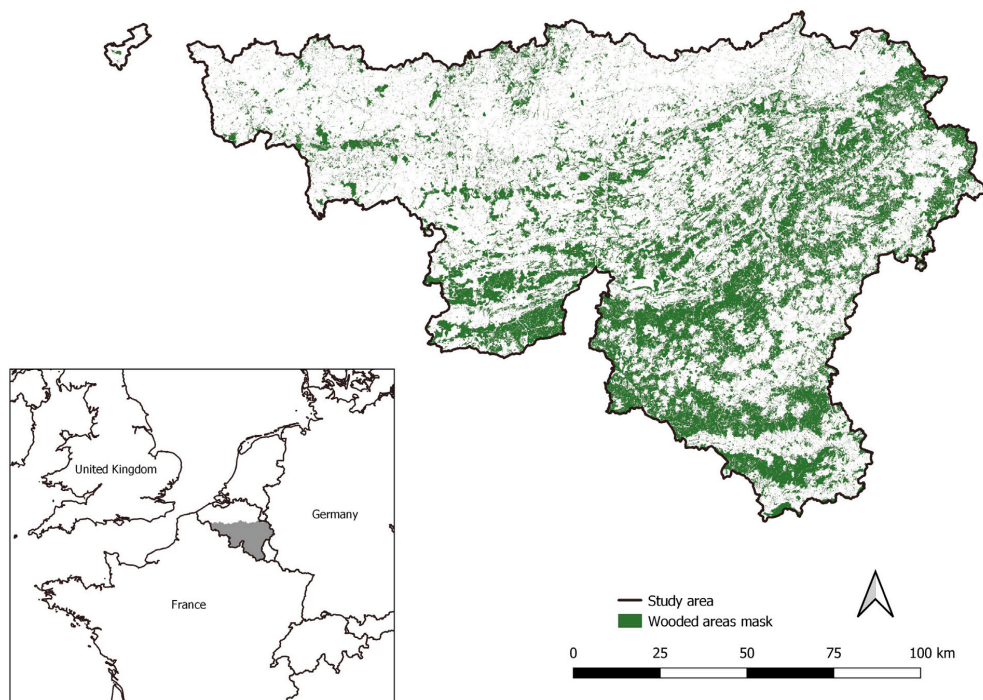
Fig. 1. Geographical location and wooded areas of the study area, Wallonia region (southern Belgium). The study area is presented in grey in the inset map. The wooded areas mask is in green. (For interpretation of the references to colour in this figure legend, the reader is referred to the web version of this article.)

2.2. Workflow and datasets

In this study, classes were not mapped individually but rather as vectors of tree species proportions. The tree species proportions are represented as a vector of nine values in the same order as the tree species classes (Table 3). For each proportion, the values ranged from 0 to 1, and the sum of the vectors was equal to 1. This vector of species proportions was the target variable of a CNN model built to produce the tree species proportions map at 2.5 m within the wooded areas of the study area. A pre-existing map for the reference year 2018, at a spatial resolution of 2 m, was used to mask the wooded areas within Wallonia (Fig. 1). This wooded area mask was made as part of a project aimed at generating a "forest mask"(described and freely available at http://geoportail.wallonie.be). The wooded areas mask corresponded to forest areas more than 20 m wide and 0.5 hectares in area. The 10 bands of the S2 imagery were super-resolved at 2.5 m as described by Latte and Lejeune (2020) and used as predictor variables in the CNN model. Two databases were used as references for the target tree species proportion vectors. The first, named as "forest parcel polygons", was used for model training. The second, named as "assessment plots", was used to assess the accuracy of the map (Fig. 2).

2.2.1. S2 super-resolved imagery

The S2 imagery, level 2 A flat reflectance, which was produced and distributed by the Theia Data Center (https://www.theia-land.fr/en/), was used as predictor data (Hagolle et al., 2020) (Fig. 2). The Wallonia region is covered with eight S2 tiles. To obtain a cloud-free and hole-free mosaic with homogeneous radiometry, surface reflectance synthesis was generated considering the vegetation period (from 15 May to 15 September 2018). For this period, all available tiles with cloud cover of less than 50% were downloaded. A total of 86 tiles

was selected for 13 dates from 18 May to 19 August. The cloud mask computed using MAJA software was used (Baetens et al., 2019). A time-weighted average of the cloud-free pixels was calculated to give more weight to the mid-summer pixels. The dates of the S2 tiles were converted to numerical values corresponding to the day number in the considered time period of 125 days (from 15 May to 15 September 2018). Values from 1 to 125 were rescaled from −6 to 6. The weights of S2 tiles were then calculated as the densities of a normal distribution (mean = 0, sd = 2.5) for the corresponding date values. Finally, the ten S2 bands (four at 10 m and six at 20 m) of the S2 time-weighted mosaic were super-resolved at 2.5 m as described in Latte and Lejeune (2020). PlanetScope scenes "analytic-sr", covering the study area from 26 June to July 02, were used in this process. The super-resolution was not intended to improve the model performance but rather the geometric accuracy of the map, that is, the boundaries and edges of the mapped forest patches, in accordance with the wooded areas mask (2 m, Fig. 1). Indeed, tree species proportions were still modelled using stand-level information for training (see Section 2.2.2).

2.2.2. Forest parcel polygons

A map of forest parcels extracted from the forest administration's geodatabase (Department of Nature and Forests, Public Service of Wallonia, 2017) was used as the target data for model training (Figs. 2 and 3). This database contains almost 120,000 digitised forest polygons distributed over the entire region (Table 3). For each polygon, the basal area proportion of each tree species was estimated by the responsible forest agents. The proportions of tree species classes (Table 3) were calculated by summing the species-specific proportions. The poplar class was poorly represented in the public geodatabase because a large portion of the poplar stands is managed by private owners in the study area. Thus, 178 additional polygons were digitised by visual
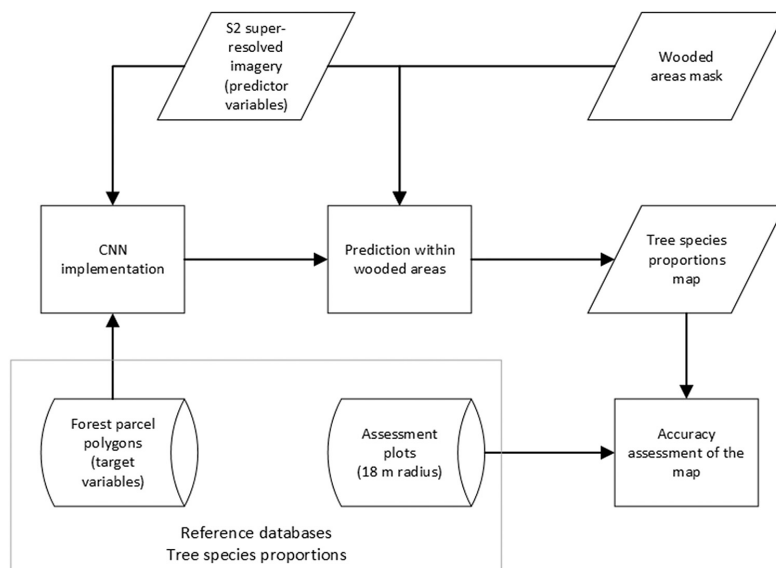
Fig. 2. Workflow of the study.

Table 2
Number of selected plots from the regional forest inventory of Wallonia by year of inventory and their cumulative percentages.

Year	2018	2017	2016	2015	2014	2013	2012	2011	2010	2009	2008
Number of plots	62	295	739	672	714	601	491	408	275	278	211
Cumulative percentage	1	8	23	37	52	65	75	84	90	96	100

interpretation from the orthophotos of the Public Service of Wallonia (http://geoportail.wallonie.be). Only pure plantations were digitised to avoid misclassifications. Poplar plantations are easily recognisable from the sky because of the large and constant distance between plants. A proportion value of 1.0 was assigned to the Poplars class for these polygons.

Using this type of reference polygon to prepare a training dataset improves the reproducibility of the study because these data are often available for forest areas with a formal management plan. Based on the polygon database, the tree species proportions used for model training in the study were calculated using the basal areas of the dominant and understory trees. Notably, diameter at breast height of trees cannot be observed on satellite imagery; thus, we assumed that a CNN model would learn the relationship between the tree crown proportions and basal area proportions, as well as the variation of this relationship between tree species. This likely added uncertainty to the predictions, which is a limitation of this study.

2.2.3. Assessment plots

Another data source, the regional forest inventory of Wallonia (Alderweireld et al., 2015, 2016), was used to independently evaluate the map quality (Fig. 2). Field data from 4,746 plots with an 18 m radius visited since 2008 were used in this assessment (Table 2). More than half of the selected plots were visited after 2013. Plots with young plantations or regenerations, as well as plots without field measurements, were discarded. The selected plots were systematically distributed throughout Wallonia on a one-year basis (Fig. 4).

For each plot, the basal area per hectare (m^2/ha) was calculated by tree species class using field measurements. These values were used to determine the proportions of tree species. A large proportion of these plots were mixed forest stands (a quarter presented a maximum

proportion <= 0.64). The representative dataset of this study area confirmed the need to develop a suitable method for mapping mixed forests. The plots were located using geographic positioning system (GPS).

A few points must be noted regarding the data used to assess the map accuracy. First, there is overlap between the assessment plots and forest parcel polygons. Indeed, forest parcel polygons cover a large part of the public forest, and assessment plots are in both public and private forest stands. In the study area, 52% of the forest is private. This may imply an optimistic bias in the map quality assessment. However, the forest parcel polygons used for training and assessment plots differ in nature. The first database consisted of polygons covering variable areas and provided average information for a complete forest stand (Fig. 3). However, locally, this information is approximately false in the worst case. The second database provides local information for a constant area (radius 18 m). This database was used to locally assess the accuracy of the complete final map predicted by pixel of 2.5 m. Second, there were time lags between measurement of the assessment plots and the period covered by the S2 imagery. Finally, regarding the GPS location of the plots, the root mean squared error (RMSE) reached 3–7 m under the canopy, depending on the forest type (Andersen et al., 2009). For assessment, we therefore assumed that in most of the mapped forest stands, the species composition did not change significantly within a maximum radius of 7 m and over a period of up to ten years (Table 2).

2.2.4. Tree species classes

Nine tree species classes were defined (Table 3) to map the basal area proportions of tree species, which are exhaustive with respect to tree species in the study area. These classes were defined according to the most frequent stand types in Wallonia (Table 1).
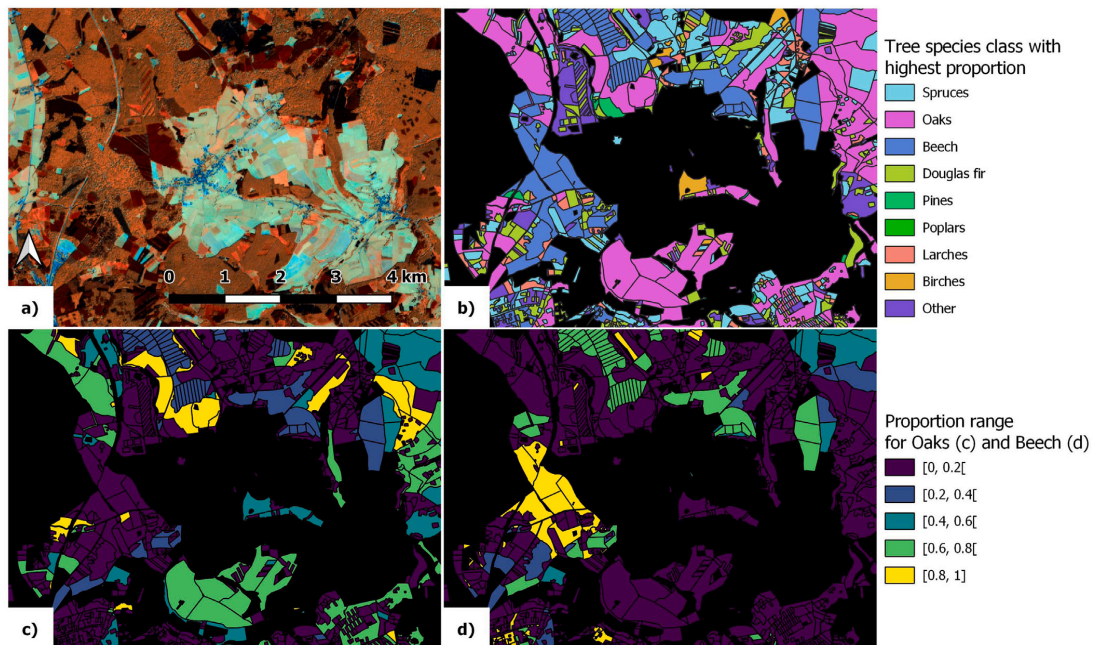
Fig. 3. (a) False colour image of S2 super-resolved imagery (red: B8 A, green: B11, blue: B12). (b) Forest parcel polygons displayed with the tree species class with the highest proportion. (c) Forest parcel polygons displayed with the proportion of Oaks. (d) Forest parcels polygons displayed with the proportion of Beech. (For interpretation of the references to colour in this figure legend, the reader is referred to the web version of this article.)
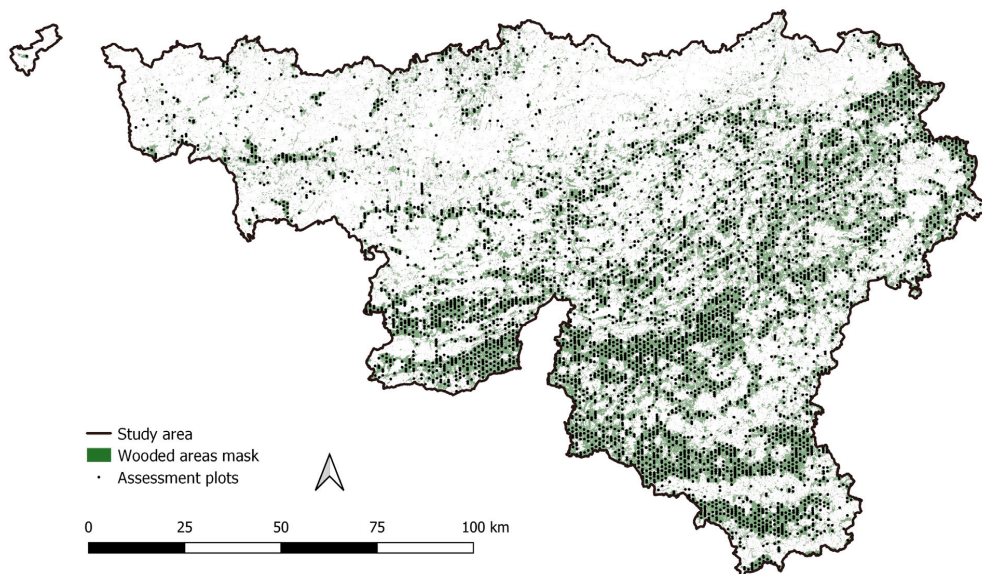
Fig. 4. Accuracy assessment of the tree species proportions map. We selected 4,746 plots of the regional forest inventory of Wallonia (Alderweireld et al., 2016). The wooded areas mask is displayed in green. (For interpretation of the references to colour in this figure legend, the reader is referred to the web version of this article.)

Table 3

Definitions of tree species classes, number of forest parcel polygons used as target data in the model training (map of forest parcels extracted from the forest administration's geodatabase of the Department of Nature and Forests, Public Service of Wallonia) where the class is present, and number of plots used in map assessment (selected from the regional forest inventory of Wallonia) where the class is present. As a discrete element can contain several tree species classes, a forest parcel polygon or an assessment plot can be counted in more than one class.

Tree species class	definition	forest parcel polygons	assessment plots
Spruces	Tree species belonging to the genus *Picea*.	51560	1517
Oaks	Native oak in the study area, *Quercus robur L.* and *Quercus petraea (Mattuschka) Lieblein.*	21657	2285
Beech	*Fagus sylvatica L.*	25804	1454
Douglas fir	*Pseudotsuga menziesii (Mirb.) Franco.*	19119	344
Pines	Tree species belonging to the genus *Pinus*.	6926	264
Poplars	Hybrid black poplar, *Populus x euramericana (Dode) Guinier.*	839	129
Larches	Tree species belonging to the genus *Larix*.	8539	186
Birches	Tree species belonging to the genus *Betula*.	10806	866
Other	Tree species not included in other tree species classes.	32548	1958
Total number of discrete elements		119991	4746

2.3. CNN

2.3.1. Preparation of predictor and target variables

The predictor data (S2 super-resolved imagery, Section 2.2.1) were normalised by considering the entire region using Eq. (1). Normalising the data is highly recommended, as it speeds up learning and convergence and improves the CNN performance. The data were normalised using the following equation:

$$NormVal_b = \frac{Val_b - P_{1st_b}}{P_{99th_b} - P_{1st_b}} \tag{1}$$

where Val_b denotes the values of the considered band b, P_{1st_b} and P_{99th_b} denote the first and 99th percentiles of the values of band b, and $NormVal_b$ denotes the normalised values of the band b.

Based on the entire set of forest parcel polygons (Section 2.2.2), a multi-band raster was generated (same grid as the predictor data) and used as target data in CNN training. Each band of this raster corresponded to a proportion of tree species (sum of all bands equalling to 1). A 'No Data' value was assigned to all pixels not covered by the forest parcels polygons or outside the wooded areas mask.

2.3.2. CNN architecture

To model the tree species proportions in the form of a vector of nine values as a function of the ten super-resolved S2 bands, a U-shaped neural network (UNet) was implemented. The UNet architecture was initially developed by Ronneberger et al. (2015) and is now among the most widely used architectures for pixel-wise image segmentation, including remote sensing (Iglovikov et al., 2017). Typically, the UNet architecture contains two paths: the contraction path (also known as the encoder) and symmetric expanding path (also known as the decoder). The encoder comprises of several convolution and pooling operations (downsampling). The decoder comprises several transposed convolutions (upsampling). Features of the encoder and decoder were concatenated at each level via skip connections. The output showed the same spatial dimensions as the input.

Since 2015, numerous adaptations and improvements of the UNet architecture have been proposed. In this study, we selected a nested UNet, named as UNet++, which significantly improves the segmentation accuracy (Zhou et al., 2018). Compared with the original UNet, UNet++ has two major modifications: redesigned skip pathways and deep supervision. The former reduces the semantic gap between the encoder and decoder features of subnetworks, and the latter enables the outputs of each level to be combined. This architecture was described in detail in Zhou et al. (2018). The data reconstruction part of the architecture was slightly modified to obtain a vector of nine values for which the sum equals 1 for each pixel as the final output (Softmax activation function).

2.3.3. Patches and batches preparation

When using a CNN in remote sensing, the data sample unit is the patch, which can be described as a small multi-band image extracted from a portion of the study area. In this study, the patch size was set as 400 × 400 pixels. To produce a patch dataset for CNN training, each patch extent was generated by randomly selecting a class by randomly selecting a forest parcel polygon where this class is present, regardless of the proportion; in this polygon, a point was randomly generated. This point was the centre of the 400 × 400 pixel window used to extract data from the predictor raster, i.e. the ten S2 bands, and the target raster, representing the proportions of the nine tree species . As explained in Section 2.3.1, the target values were "No Data" for all pixels not covered by the forest parcel polygons.

Because the CNN could not be trained using all patches together, as it would require too much computer memory, these patches were grouped into distinct batches. Each batch was used separately to train the CNN to update the architecture weights progressively. Therefore, preparing patches and batches is an important step. A total of 7,500 batches was generated, with each batch comprised of three randomly generated patches.

The nine tree species classes were highly imbalanced in terms of the area covered in the region (Table 3). This imbalance was not compensated when constructing the training dataset, as the spatial context is an essential component of learning. Nevertheless, the manner by which the patch extents were generated ensured that each tree species class had an equal chance of being represented in a patch.

The data within the patches were augmented by applying rotations (22.5°, 45°, or 67.5°) and flips (vertical and/or horizontal). For each patch, the probability of augmentation was 50%. Data augmentation acts as a regulariser and helps to reduce overfitting.

2.3.4. Training

UNet++ includes weight regularisations to reduce overfitting and improve model generalisation and robustness. For training, the Adam optimiser (Kingma and Ba, 2014) was used, with a relatively low learning rate of $1e^{-4}$. The number of epochs was 5,000 and number of steps per epoch was 50. For each step, one of 7,500 batches was randomly selected. When reaching the learning plateau (i.e., no further model improvement) (Yoshida and Okada, 2019), the learning rate was progressively reduced by a step of −10% every 100 epochs.

A specific loss implementation is defined. The 'No Data' pixels were not used to compute loss. Thus, only pixels with forest parcel polygon data and inside the wooded areas mask (see Section 2.3.1) were used. Five functions were tested: mean absolute error, mean squared error, pseudo-Huber (PH) (Barron, 2019), focal loss (Lin et al., 2017), and Kullback–Leibler divergence (Erven and Harremos, 2014). The best results were obtained using PH (Eq. (2)). The loss of each batch was

computed by averaging the PH values of all selected pixels (all classes considered).

$$PH = \delta^2 \times (\sqrt{1 + (\frac{RS}{\delta})^2} - 1) \qquad (2)$$

where δ (=2) denotes the delta value and RS denotes the residual value for a pixel (true proportion minus predicted proportion).

2.4. Map prediction

Mapping prediction was performed within the wooded areas mask using tiles of 400 × 400 pixels. To avoid undesirable effects at the tile borders resulting from successive convolutions, a grid with an 8-pixel overlap between tiles was used. Before merging the tiles, the 8-pixel overlap of each tile was removed (resulting in 392 × 392 pixels remaining). To further improve the visual aspect, the map was obtained from the average of 16 predictions corresponding to combinations of four shifts (one-quarter left and/or up, or none) and four flips (vertical and/or horizontal, or none).

As the loss function used (Eq. (2)) minimised the error in tree species proportions but did not prevent small error in absent classes (absent class = proportion 0.0), false-positives for small proportions were frequent. Thus, a proportion threshold of 0.2 was applied to improve the consistency of the map. Predicted proportion values below 0.2 were reduced to zero, and the proportions were recalculated to sum to one. The final map was a 9-band raster, with each band corresponding to the proportion of a tree species class.

2.5. Accuracy assessment of the map

2.5.1. Assessment protocol

Classification maps are typically evaluated using a confusion matrix and indices derived from it, such as overall accuracy and producer's and user's accuracies per class (Stehman and Foody, 2019). For this study, because of the specific nature of the prediction, a vector of the proportions of the nine tree species, such traditional methods were not adapted. In the absence of a consensus for assessing compositional data in the literature, we defined a new specific protocol that included new indicators. The evaluation was divided into three parts, each focusing on one specific element: (1) the majority class, (2) species composition (presence or absence), and (3) species proportions (proportion values).

To compare the predicted tree species proportions with those observed in the assessment plots, the predicted values of pixels inside the 18 m radius were extracted and averaged.

2.5.2. Majority class assessment

Plots with a majority class in the field were selected. These plots corresponded to those whose tree species proportion vector contained a class value higher than 0.6 according to the assessment data. Observed and predicted classes with the highest proportion were used to build a traditional confusion matrix and compute three values: the overall accuracy (OA_{maj}), producer's accuracy per class (PA_{maj}), and user's accuracy per class (UA_{maj}). This assessment is most comparable to other studies of tree species classification.

2.5.3. Species composition assessment

The species composition, that is, the presence or absence of tree species classes, was derived from the vector of tree species proportions by applying a simple Boolean filter (vector > 0). Three new indicators were introduced: (1) mean score (MS), (2) mean producer's score (MPS), and (3) mean user's score (MUS). The MS was computed by averaging the proportion of correct attributions within a plot (Eq. (3)). Similar to MS, MPS focused on the presence relative to the reference, and MUS focused on the presence relative to the prediction (Eqs. (4) and (5)):

$$MS = \frac{1}{n} \sum_{i=1}^{n} \frac{c_i}{9} \qquad (3)$$

where n denotes the total number of assessment plots and, for plot i, c_i denotes the number of correct attribution between the presence or absence among the nine classes.

$$MPS = \frac{1}{n} \sum_{i=1}^{n} \frac{t_i}{cr_i} \qquad (4)$$

where n denotes the total number of assessment plots and, for plot i, t_i denotes the number of true-positives among the number of classes cr_i present in the plot i according to the reference.

$$MUS = \frac{1}{n} \sum_{i=1}^{n} \frac{t_i}{cp_i} \qquad (5)$$

where n denotes the total number of assessment plots and, for plot i, t_i denotes the number of true-positives among the number of classes cp_i present in plot i according to the prediction.

The tree species composition was also assessed according to tree species class. Two traditional indicators were used: 1) producer's accuracy (PA, Eq. (6)) and 2) user's accuracy (UA, Eq. (7)).

$$PA_{cl} = \frac{t_{cl}}{pr_{cl}} \qquad (6)$$

where, for the evaluated class cl, t_{cl} denotes the number of true-positives among the number of plots pr_{cl} where the class cl is present according to the reference.

$$UA_{cl} = \frac{t_{cl}}{pp_{cl}} \qquad (7)$$

where, for the evaluated class cl, t_{cl} denotes the number of true-positives among the number of plots pp_{cl} where the class cl is present according to the prediction.

To evaluate the detection accuracy per species as a function of their proportions, Eqs. (6) and (7) were applied to several subsets of assessment plots by proportion ranges (0–0.2, 0.2–0.4, etc.). To determine PA and UA, the plots were sorted based on the reference and predicted proportions, respectively.

2.5.4. Assessment of tree species proportions

The residuals of the predicted proportions were also analysed. The RMSE, variance of residuals (VAR_{res}), variance of reference proportions (VAR_{tot}), and adjusted coefficient of determination (R^2_{adj}) were calculated. First, the nine classes of the tree species proportion vector were considered (4746 plots × 9 classes). Second, RMSE, VAR_{res}, VAR_{tot}, and R^2_{adj} were calculated by class only using values for the class of interest (4746 plots × 1 class).

2.6. Data processing and analysis tools

Preparation and processing of the predictor and target data, as well as deep learning implementation and map accuracy assessment, were performed in R (R Core Team, 2020), mainly using three R packages: raster (Hijmans, 2019), sf (Pebesma, 2018), and keras (TensorFlow backend) (Allaire and Chollet, 2019), and in connection with the GDAL/OGR library (GDAL/OGR contributors, 2020) and Orfeo ToolBox (Inglada and Christophe, 2009; Grizonnet et al., 2017).

3. Results

3.1. Tree species proportions map

Using our method, we produced a map of tree species proportions in the Wallonia region (Fig. 1). The final map covered 16,901 km^2 at 2.5 m spatial resolution (Fig. 5).
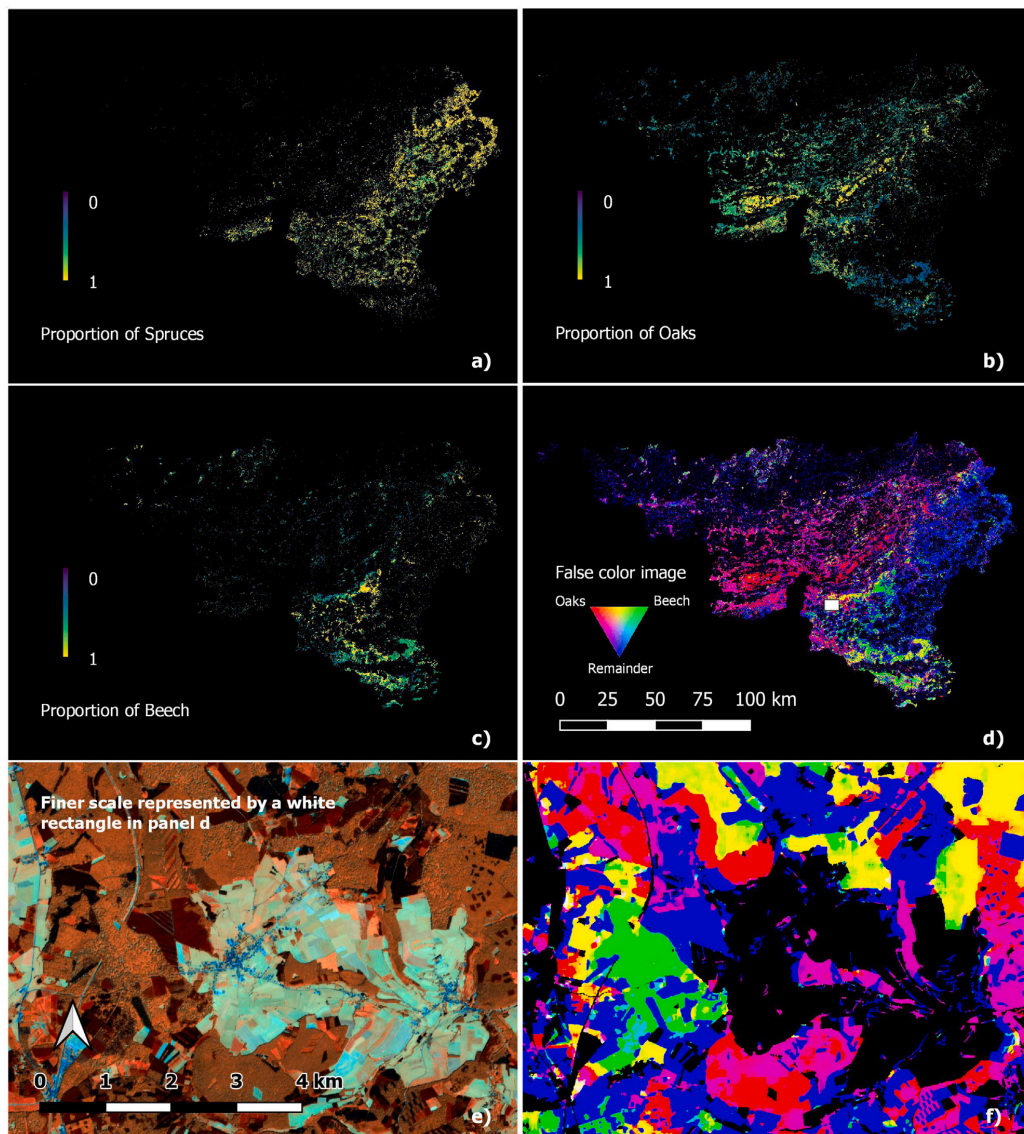
Fig. 5. (a) Tree species proportions map for the Spruces class in the entire study area. (b) Tree species proportions map for the Oaks class. (c) Tree species proportions map for the Beech class. (d) False colour image of the tree species proportions map (red: proportion of Oaks, green: proportion of Beech, blue: sum of proportions for the remaining classes). To display this false colour image, the maximum channel values were set to 0.33. (e) False colour image of the S2 super-resolved imagery (red: B8 A, green: B11, blue: B12) presented for the same extent as panel f. (f) False colour image of the tree species proportions map presented at a finer scale. The extent of the detailed view in panels e and f is represented on the full false colour image (panel d) by a white rectangle. This extent is the same as that in Fig. 3. (For interpretation of the references to colour in this figure legend, the reader is referred to the web version of this article.)

3.2. Accuracy assessment of the map

3.2.1. Majority class assessment

The OA_{maj} was 0.73. The Spruces class had the lowest confusion with a PA_{maj} and UA_{maj} above 0.90 (Table 4). The lowest accuracies were observed for Poplars, Birches, and Other classes. The most frequent classes (Spruces, Oaks, Beech, and Douglas fir) showed the highest accuracies. The main confusion was observed between classes often mixed with each other in the assessment plots; such as Oaks and Beech, and Spruces and Douglas fir.

3.2.2. Species composition assessment

The MS value reached 0.89. The MPS and MUS values were 0.72 and 0.83, respectively.

The Spruces, Oaks, Beech, and Douglas fir classes achieved the best global results, with PAs and UAs close to or higher than 0.70 (Table 5).

Table 4

Confusion matrix built to assess detection of the majority class. Assessment plots with an observed class proportion higher than 0.6 were selected. The confusion matrix was calculated by crossing the observed majority class and predicted majority class. The producer's accuracy (PA_{maj}) and user's accuracy (UA_{maj}) were calculated per class.

Prediction	Validation									UA_{maj}
	Spruces	Oaks	Beech	Douglas fir	Pines	Poplars	Larches	Birches	Other	
Spruces	1024	22	20	20	6	0	1	1	21	0.92
Oaks	10	693	77	2	9	1	0	5	83	0.79
Beech	7	74	467	1	3	2	0	0	25	0.81
Douglas fir	45	4	3	128	3	1	2	0	6	0.67
Pines	5	3	2	3	71	0	7	1	5	0.73
Poplars	0	5	1	1	1	27	2	0	20	0.47
Larches	6	4	2	4	2	1	58	0	3	0.72
Birches	12	45	8	1	8	1	2	24	47	0.16
Other	13	256	59	3	2	20	0	3	273	0.43
PA_{maj}	0.91	0.63	0.73	0.79	0.68	0.51	0.81	0.71	0.57	

Table 5

Number of true-positives (t_{cl}), Number of plot where a class is present according to the reference (pr_{cl}), number of plots where a class is present according to the prediction (pp_{cl}); producer's accuracy (PA) and user's accuracy (UA) by class. See Eqs. (6) and (7).

Class	t_{cl}	pr_{cl}	pp_{cl}	PA	UA
Spruces	1178	1517	1312	0.78	0.90
Oaks	1922	2285	2437	0.84	0.79
Beech	967	1454	1224	0.67	0.79
Douglas fir	233	344	332	0.68	0.70
Pines	134	264	202	0.51	0.66
Poplars	59	129	106	0.46	0.56
Larches	77	186	116	0.41	0.66
Birches	87	866	112	0.10	0.78
Other	1163	1958	1526	0.59	0.76

Table 6

Root mean squared error (RMSE), adjusted coefficient of determination (R^2_{adj}), variance of the residuals (VAR_{res}) and variance of the reference proportions (VAR_{tot}).

Class	RMSE	R^2_{adj}	VAR_{res}	VAR_{tot}
Spruces	0.18	0.80	0.03	0.17
Oaks	0.29	0.19	0.09	0.11
Beech	0.21	0.48	0.05	0.09
Douglas fir	0.13	0.54	0.02	0.04
Pines	0.11	0.28	0.01	0.02
Poplars	0.10	0.05	0.01	0.01
Larches	0.09	0.48	0.01	0.02
Birches	0.17	0.05	0.03	0.03
Other	0.29	0.10	0.08	0.09
Overall	0.19	0.50	0.04	0.07

The Oaks class exhibited the best PA with a value of 0.84, whereas Spruces had the best UA with a value of 0.90. The lowest PA and UA were observed for the Birch and Poplars classes with values of 0.10 and 0.56, respectively.

PAs and UAs increased in the range of proportions for all classes. The best PAs were observed for the Oaks class, with values higher than 0.80 in all proportion ranges above 0.2 (Fig. 6). Except for the Poplars, Larches, and Birches classes, all tree species classes had PAs higher than or equal to 0.75 for the proportion range above 0.6 (Fig. 6). The best UAs were observed for the Oaks, Birches and Other classes with values higher than 0.63 in all proportions above 0.2. In the proportion range of 0.6 to 1.0, the UAs were higher than 0.70 for all classes except Poplars. Only the Oaks and Beech classes achieved high Pas and UAs in low proportions. The PAs and UAs were higher than 0.70 from the 0.4 proportion.

3.2.3. Assessment of tree species proportions

The overall R^2_{adj} value was 0.50. The Spruces class reached the best R^2_{adj}. The lowest R^2_{adj} values were obtained for Poplars, Birches, and Other classes (Table 6).

4. Discussion

The method proposed in this study for mapping tree species proportions using spectral–spatial deep learning expands traditional tree species classification and mapping, as it allows for modelling of the majority class, presence/absence of species, and composition basal area proportions. Furthermore, the method was adapted to the complexity of mixed forests and spatial resolution of current satellite imagery. It also optimises the use of available forest inventory data in the model conception by considering all pixels from pure stands to highly mixed forest stands. This method is highly reproducible and applicable at a large scale in cases where forest inventory data, in a broad sense, are available, that is, georeferenced areas with tree species proportions. The training dataset was derived from a map of forest parcels from the Forest Administration, and the resulting map was assessed and validated using a specific protocol that included new indicators with independent data (plots of the regional forest inventory). The assessment covered the full range of possible forest compositions in the study area ($n = 4{,}746$ sample plots; Fig. 4).

4.1. Map accuracy

The balance between MPS and MUS (0.72 and 0.83 respectively) and the MS value (0.89) support that the model can predict the tree species composition (presence or absence) in most cases in the study area. For the most frequent classes, Spruces, Oaks, Beech, and Douglas fir (Table 1), the high PA and UA values (Table 5) demonstrate that the model can detect these tree species classes for the majority of situations encountered in the study area. For all classes, there was an increasing proportion of false-negatives in the decreasing observed proportions and increasing proportions of false-positives in the decreasing predicted proportions (Fig. 6). This highlights the expected difficulty in building a model that performs well for low proportions, particularly for less common species. Nevertheless, the high values of PA and UA in the low proportion ranges for the Oaks and Beech classes reveal the potential of this approach for mapping mixed forest stands.

Because the majority tree species of a stand is an important parameter in forestry considerations, we also examined whether the model could detect the majority class when one exists. The confusion matrix (Table 4) showed a high OA_{maj} of 0.73. Lower PA_{maj} or UA_{maj} derived from this matrix were compensated by very good accuracies for the most frequent classes (Spruces, Oaks, Beech, and Douglas fir). These higher accuracies show that our approach can map the majority of tree species in mixed and pure forest stands in the study area. Furthermore, we achieved accuracies comparable to those computed for pure stands only in the latest study conducted in European temperate forests (Hemmerling et al., 2021).

The overall RMSE of the predicted proportions was 0.19 for an R^2_{adj} value of 0.50. This result was expected, as the data used to train the model were polygons providing average information for a
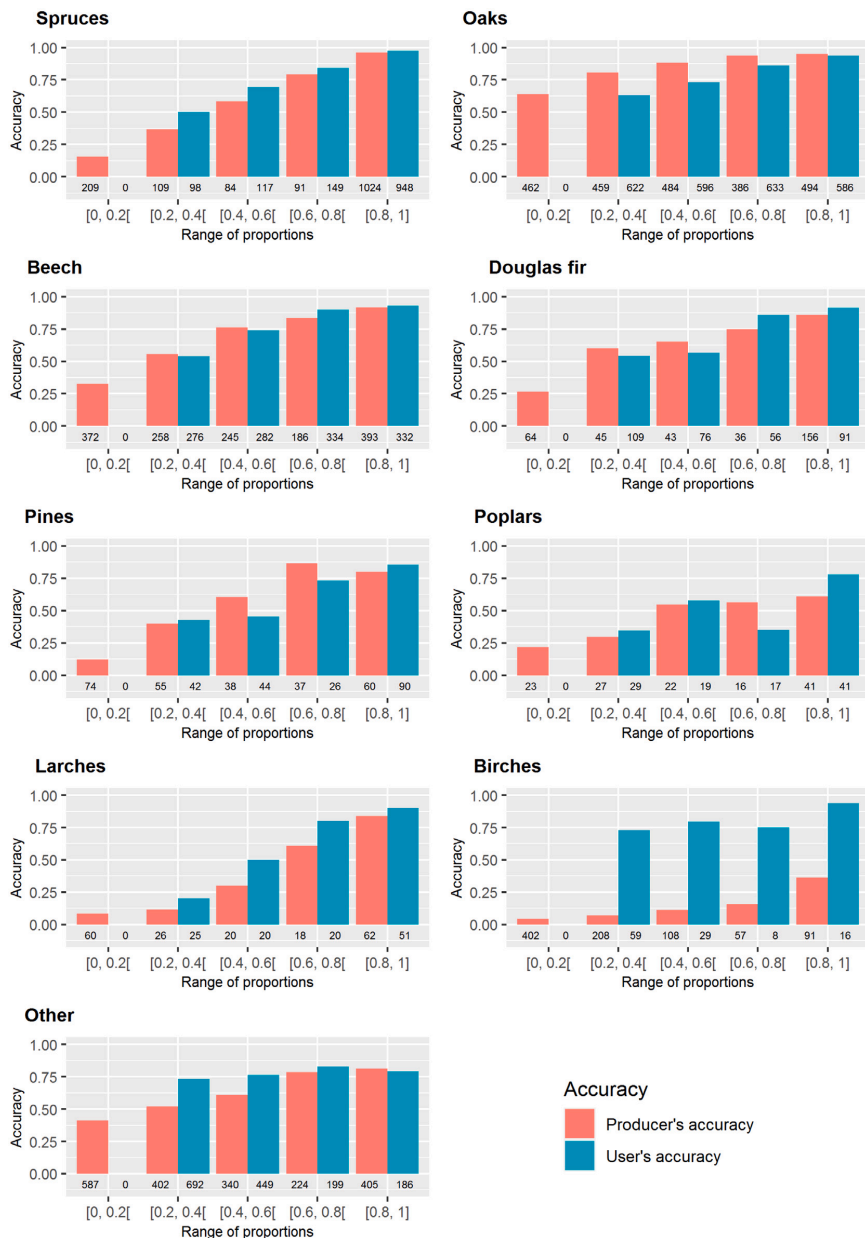
Fig. 6. PAs and UAs by tree species class as a function of the range of proportions. For PAs, the *x*-axis corresponds to the observed proportions. For UAs, it corresponds to the predicted proportions. The number of plots used to calculate the accuracies (pr_{cl} and pp_{cl}, Eqs. (6) and (7)) is shown below the corresponding bars. As described in Section 2.4, predicted proportion values lower than 0.2 were filtered to prevent false-positives. Thus, the UA bar is absent from the 0–0.2 range in all classes.

complete forest stand. Nevertheless, this accuracy was very satisfactory for analysing the tree species composition and majority tree species in the study area. Spruces, the largest class in the study area, achieved an R^2_{adj} value of 0.80. This class is mostly composed of pure or almost pure stands in the study area. This characteristic is reflected in the distribution of the number of assessment plots per proportion range (Fig. 6). Therefore, the variance in its proportions is higher (Table 6), increasing R^2_{adj}. In addition, this class, as the most common tree species, is more likely to be represented in patches used in CNN training, even when not targeted during patch generation (Section 2.3.3).

Gudex-Cross et al. (2017) performed the most comparable and recent study as the current study. Using spectral unmixing of multi-temporal Landsat imagery, the authors quantified the basal area percentage of ten tree species/genera using a stepwise linear regression model. They also performed validation using 50 plots distributed over their study area (Landsat Row 29, Path 14) and achieved R^2_{adj} values from 0.24 to 0.59 depending on the species. Although these statistics were calculated from a proportionally smaller number of observations, they are comparable to our results, highlighting the difficulty of modelling continuous variables, such as the basal area of an individual tree species. To produce a forest thematic map in their study, post-treatment was applied to the percentage basal area rasters obtained from pixel-based spectral unmixing (object-based hierarchical classification scheme). This step requires the definition of arbitrary clustering choices. Because their final forest thematic map was evaluated after this step, comparison was not relevant. Moreover, the quality of the final map depended on the accuracy of the predicted proportions of tree species. Therefore, to ensure consistency and reproducibility, our method can be used to assess tree species composition and majority classes before a hierarchical classification is chosen, such that the direct focus can be placed on the presence or absence of species in the predicted species proportion vector.

4.2. Innovative method for tree species mapping

Compared to the most recent studies using machine learning or deep learning to process satellite images for tree species classification (Xi et al., 2021; Zagajewski et al., 2021; Xie et al., 2021; Bjerreskov et al., 2021; Grabska et al., 2020; Immitzer et al., 2019; Grabska et al., 2019; Hoscilo and Lewandowska, 2019; Persson et al., 2018; Wessel et al., 2018; Bolyn et al., 2018), the proposed method is not limited to spectral information but also includes spatial information, as recently explored by Illarionova et al. (2021). This innovation, enabled by using a CNN, considers the neighbourhood pixels of the targeted pixel for prediction. Therefore, it is an inclusive method for considering groups of pixels for mapping. The prediction was better and more robust because of the nested levels of observation. The mapped object is spatially variable. A forest stand must be considered at several scales of analysis, from the pixel to the whole patch. In contrast to classical segmentation, the CNN allowed us to learn the segmentation parameters directly with regard to the variable to be predicted. The CNN included this step in the model architecture rather than performing pre-processing for object-based analysis.

Predicting tree species proportions at the pixel level based on their surroundings overcame the two challenges of this study. First, it allowed for mapping of the whole forest, including all types of species compositions (pure or mixed stands), even though the resolution of the satellite image was not sufficient to differentiate individual trees. Thus, our method allows reliable characterisation of forest species over large geographical areas and addresses the lack of relevant studies in this field of research raised by Fassnacht et al. (2016).

Second, this approach allowed us to optimise the use of the available forest inventory data in model training and validation by considering all pixels from pure to highly mixed forest stands. The scarcity of spatial data required for remote sensing studies provides an opportunity for a wide range of applications. A recurrent problem is the availability of a representative training dataset. An ideal dataset composed of the precise positioning of tree crowns and their characteristics is rare. However, forest managers often use databases that reference the proportion of tree species per forest plot, stand, or polygon. Thus, Illarionova et al. (2021) proposed an additional strategy. They first trained a CNN model to find homogeneous areas within each forest stand, presenting a tree species class with a proportion higher than 0.5. They then trained a final model for tree species classification in the detected pure areas. Rather than focusing only on homogeneous areas, our reproducible method enables the use of full forest inventory data. Moreover, a

mapping approach via a quantitative variable rather than a qualitative approach can be used to consider the gradients that exist in nature, making this model generalisable to many subjects.

Our method requires some improvements. First, Poplars stands grow and change very rapidly compared to other classes (plantation cycle of 20–25 years). Therefore, in the proportion range 0.8–1.0, the assessment plots data were much more likely to be outdated compared to the other mapped classes. Designing a suitable assessment dataset would improve the analysis of this class.

Second, finding reference data for less frequent classes is an intrinsic problem in model-based mapping. Therefore, in this study, special attention was paid to class balancing during the preparation of patches and batches for CNN training (see Section 2.3.3). Nevertheless, lower results were obtained for minority classes (Poplars, Larches, and Birches). Thus, balancing classes and augmenting data cannot completely compensate for a large lack of data. The best dataset would be that which is most representative of the population variability of every class in the study area. Therefore, new reference data should be collected to improve the model .

Finally, a major improvement to the proposed model would be to add a temporal dimension by upgrading spectral–spatial deep learning to 'spectral-spatial–temporal' deep learning. This is supported by recent studies that highlighted the importance of using S2 time series for tree species classification (Xi et al., 2021; Hemmerling et al., 2021). Their findings suggest that this upgrade would significantly improve the model performance.

4.3. Deep learning for remote sensing mapping

We demonstrated that deep learning is advantageous for remote sensing mapping. As discussed above, the use of spectral–spatial modelling (rather than spectral modelling alone) makes a substantial difference in this field, which necessarily involves spatial considerations. Few studies have been conducted on tree species classification using deep learning with satellite imagery, and previous studies did not use spatial information in their architecture (Xi et al., 2021; D'Amico et al., 2021). In addition, considering the temporal dimension, as discussed above, further research of tree species mapping using spectral–spatial–temporal deep learning is needed.

Another advantage of NNs are their flexibility, as CNN models and frameworks can be retrained using a custom dataset for any use case (O'Mahony et al., 2020). Based on their customisability, it is possible to adapt the architecture, loss function, and output data type. In this study, only this tool could learn from compositional data (i.e. vectors of tree species proportions as target data). In addition, considering the high learning performance of CNNs, they have vast potential for use in modelling complex objects, particularly in remote sensing for forestry or other environmental applications.

Finally, deep learning techniques are powerful only when coupled with sufficient data (O'Mahony et al., 2020). Ideally, well-distributed spatial data with good coverage should be used but are not always available. The proposed method makes the best use of available reference data in forested areas.

5. Conclusion

This study addressed two major challenges in tree species mapping. First, we propose a method for predicting tree species basal area proportions that is adapted to the complexity of mixed forests and satellite spatial resolutions coarser than the size of tree crowns. Second, this method optimises the use of available forest management and inventory data by considering all pixels of pure and mixed forest stands. These two advances enabled the production of a robust tree species map for a large geographical area. Particularly, high performance was achieved for detecting Oaks and Beech tree species classes in areas with low species proportions.

We also proposed a robust assessment method for tree species proportions maps that allows separate assessment of the 1) majority species, 2) species composition (presence or absence), and 3) species proportions (proportion values). When forest inventory data, in a broad sense, are available, that is, georeferenced areas with tree species proportions, the method is highly reproducible and allows for remote sensing studies at scales comparable to field forest inventories and for all types of forest compositions.

The use of spatial information, in addition to spectral information, was crucial for achieving the objectives of the study and resulted in high performance. As recent studies of tree species classification using remote sensing have highlighted the importance of using time series in model performance, we will next include a temporal dimension in the architecture model to take advantage of species phenology.

CRediT authorship contribution statement

Corentin Bolyn: Conceptualization, Methodology, Validation, Visualization, Writing – original draft, Writing – review & editing. **Philippe Lejeune:** Supervision, Writing – review & editing. **Adrien Michez:** Writing – review & editing. **Nicolas Latte:** Conceptualization, Methodology, Software, Writing – review & editing.

Declaration of competing interest

The authors declare that they have no known competing financial interests or personal relationships that could have appeared to influence the work reported in this paper.

Acknowledgements

References

Alderweireld, M., Burnay, F., Pitchugin, M., Lecomte, H., 2015. Inventaire Forestier Wallon - Résultats 1994–2012. SPW, URL: http://orbi.ulg.ac.be/handle/2268/181169.

Alderweireld, M., Rondeux, J., Latte, N., Hébert, J., Lecomte, H., 2016. Belgium (Wallonia). In: Vidal, C., Alberdi, I.A., Hernández Mateo, L., Redmond, J.J. (Eds.), National Forest Inventories. Springer International Publishing, Cham, pp. 159–179. http://dx.doi.org/10.1007/978-3-319-44015-6_8, URL: http://link.springer.com/10.1007/978-3-319-44015-6_8.

Allaire, J.J., Chollet, F., 2019. Keras: R Interface to 'Keras'. URL: https://keras.rstudio.com.

Andersen, H.E., Clarkin, T., Winterberger, K., Strunk, J., 2009. An accuracy assessment of positions obtained using survey- and recreational-grade global positioning system receivers across a range of forest conditions within the tanana valley of interior alaska. West. J. Appl. For. 24 (3), 128–136. http://dx.doi.org/10.1093/wjaf/24.3.128, URL: https://academic.oup.com/wjaf/article/24/3/128/4683488.

Axelsson, A., Lindberg, E., Reese, H., Olsson, H., 2021. Tree species classification using Sentinel-2 imagery and Bayesian inference. Int. J. Appl. Earth Obs. Geoinf. 100, 102318. http://dx.doi.org/10.1016/j.jag.2021.102318.

Baetens, L., Desjardins, C., Hagolle, O., 2019. Validation of copernicus sentinel-2 cloud masks obtained from MAJA, Sen2Cor, and FMask processors using reference cloud masks generated with a supervised active learning procedure. Remote Sens. 11 (4), http://dx.doi.org/10.3390/rs11040433, Number: 4.

Barron, J.T., 2019. A general and adaptive robust loss function. CVPR.

Bjerreskov, K.S., Nord-Larsen, T., Fensholt, R., 2021. Classification of nemoral forests with fusion of multi-temporal sentinel-1 and 2 data. Remote Sens. 13 (5), 950. http://dx.doi.org/10.3390/rs13050950, URL: https://www.mdpi.com/2072-4292/13/5/950.

Bolyn, C., Michez, A., Gaucher, P., Lejeune, P., Bonnet, S., 2018. Forest mapping and species composition using supervised per pixel classification of Sentinel-2 imagery. Biotechnol. Agron. Soc. Environ. 22 (3).

Cue La Rosa, L., Sothe, C., Feitosa, R., Almeida, C., Schimalski, M., Oliveira, D., 2021. Multi-task fully convolutional network for tree species mapping in dense forests using small training hyperspectral data. ISPRS J. Photogramm. Remote Sens. 179, 35–49. http://dx.doi.org/10.1016/j.isprsjprs.2021.07.001.

D'Amico, G., Francini, S., Giannetti, F., Vangi, E., Travaglini, D., Chianucci, F., Mattioli, W., Grotti, M., Puletti, N., Corona, P., Chirici, G., 2021. A deep learning *approach* for automatic mapping of poplar plantations using Sentinel-2 imagery. GISci. Remote Sens. 58 (8), 1352–1368. http://dx.doi.org/10.1080/15481603.2021.1988427, URL: https://www.tandfonline.com/doi/full/10.1080/15481603.2021.1988427.

Erven, T.v., Harremos, P., 2014. Rényi divergence and Kullback-Leibler divergence. IEEE Trans. Inform. Theory 60 (7), 3797–3820. http://dx.doi.org/10.1109/TIT.2014.2320500, Number: 7.

Fassnacht, F., Latifi, H., Stereńczak, K., Lefsky, M., Straub, C., Waser, L., Ghosh, A., Modzelewska, A., 2016. Review of studies on tree species classification from remotely sensed data. Remote Sens. Environ. 186, 64–87.

GDAL/OGR contributors, 2020. GDAL/OGR Geospatial Data Abstraction Software Library. Open Source Geospatial Foundation, URL: https://gdal.org.

Ghanbari, H., Mahdianpari, M., Homayouni, S., Mohammadimanesh, F., 2021. A meta-analysis of convolutional neural networks for remote sensing applications. IEEE J. Sel. Top. Appl. Earth Obs. Remote Sens. 14, 3602–3613. http://dx.doi.org/10.1109/JSTARS.2021.3065569, URL: https://ieeexplore.ieee.org/document/9376238/.

Girard, M.C., Girard, C.M., 2010. Traitement Des Données de Télédétection. Dunod, Paris, OCLC: 1091131298.

Grabska, E., Frantz, D., Ostapowicz, K., 2020. Evaluation of machine learning algorithms for forest stand species mapping using Sentinel-2 imagery and environmental data in the Polish Carpathians. Remote Sens. Environ. 251, 112103. http://dx.doi.org/10.1016/j.rse.2020.112103.

Grabska, E., Hostert, P., Pflugmacher, D., Ostapowicz, K., 2019. Forest stand species mapping using the sentinel-2 time series. Remote Sens. 11 (10), 1197. http://dx.doi.org/10.3390/rs11101197.

Grizonnet, M., Michel, J., Poughon, V., Inglada, J., Savinaud, M., Cresson, R., 2017. Orfeo ToolBox: open source processing of remote sensing images. Open Geospatial Data Softw. Stand. 2 (1), 15. http://dx.doi.org/10.1186/s40965-017-0031-6, Number: 1.

Gudex-Cross, D., Pontius, J., Adams, A., 2017. Enhanced forest cover mapping using spectral unmixing and object-based classification of multi-temporal Landsat imagery. Remote Sens. Environ. 196, 193–204. http://dx.doi.org/10.1016/j.rse.2017.05.006.

Hagolle, O., Colin, J., Kettig, P., d'Angelo, P., Auer, S., Doxani, G., Desjardins, C., Inglada, J., 2020. Sentinel-2 surface reflectance products generated by THEIA and DLR: methods, validation and applications. ISPRS Ann. Photogramm. Remote Sens. Spatial Inf. Sci. Publisher: Copernicus Publications.

Hemmerling, J., Pflugmacher, D., Hostert, P., 2021. Mapping temperate forest tree species using dense Sentinel-2 time series. Remote Sens. Environ. 267, 112743. http://dx.doi.org/10.1016/j.rse.2021.112743, URL: https://linkinghub.elsevier.com/retrieve/pii/S0034425721004636.

Hijmans, R.J., 2019. Raster: Geographic Data Analysis and Modeling. URL: https://CRAN.R-project.org/package=raster.

Hoscilo, A., Lewandowska, A., 2019. Mapping forest type and tree species on a regional scale using multi-temporal sentinel-2 data. Remote Sens. 11 (8), 929. http://dx.doi.org/10.3390/rs11080929.

Iglovikov, V., Mushinskiy, S., Osin, V., 2017. Satellite imagery feature detection using deep convolutional neural network: A kaggle competition. ArXiv abs/1706.06169.

Illarionova, S., Trekin, A., Ignatiev, V., Oseledets, I., 2021. Tree species mapping on sentinel-2 satellite imagery with weakly supervised classification and object-wise sampling. Forests 12 (10), 1413. http://dx.doi.org/10.3390/f12101413, URL: https://www.mdpi.com/1999-4907/12/10/1413.

Immitzer, M., Neuwirth, M., Böck, S., Brenner, H., Vuolo, F., Atzberger, C., 2019. Optimal input features for tree species classification in central europe based on multi-temporal sentinel-2 data. Remote Sens. 11 (22), 2599. http://dx.doi.org/10.3390/rs11222599.

Inglada, J., Christophe, E., 2009. The Orfeo Toolbox remote sensing image processing software. In: 2009 IEEE International Geoscience and Remote Sensing Symposium. vol. 4, http://dx.doi.org/10.1109/IGARSS.2009.5417481, pp. IV–733. Journal Abbreviation: 2009 IEEE International Geoscience and Remote Sensing Symposium Num Pages: IV-736.

Kattenborn, T., Leitloff, J., Schiefer, F., Hinz, S., 2021. Review on Convolutional Neural Networks (CNN) in vegetation remote sensing. ISPRS J. Photogramm. Remote Sens. 173, 24–49. http://dx.doi.org/10.1016/j.isprsjprs.2020.12.010, URL: https://www.sciencedirect.com/science/article/pii/S0924271620303488.

Kingma, D., Ba, J., 2014. Adam: A method for stochastic optimization. In: International Conference on Learning Representations.

Latte, N., Lejeune, P., 2020. PlanetScope radiometric normalization and sentinel-2 super-resolution (2.5 m): A straightforward spectral-spatial fusion of multi-satellite multi-sensor images using residual convolutional neural networks. Remote Sens. 12 (15), 2366. http://dx.doi.org/10.3390/rs12152366.

Lin, T.Y., Goyal, P., Girshick, R.B., He, K., Dollár, P., 2017. Focal loss for dense object detection. In: 2017 IEEE International Conference on Computer Vision. ICCV, pp. 2999–3007.

Maxwell, A., Warner, T., Fang, F., 2018. Implementation of machine-learning classification in remote sensing: An applied review. Int. J. Remote Sens. 39, 2784–2817. http://dx.doi.org/10.1080/01431161.2018.1433343.

Mäyrä, J., Keski-Saari, S., Kivinen, S., Tanhuanpää, T., Hurskainen, P., Kullberg, P., Poikolainen, L., Viinikka, A., Tuominen, S., Kumpula, T., Vihervaara, P., 2021. Tree species classification from airborne hyperspectral and LiDAR data using 3D convolutional neural networks. Remote Sens. Environ. 256, 112322. http://dx.doi.org/10.1016/j.rse.2021.112322, URL: https://www.sciencedirect.com/science/article/pii/S0034425721000407.

O'Mahony, N., Campbell, S., Carvalho, A., Harapanahalli, S., Hernandez, G.V., Krpalkova, L., Riordan, D., Walsh, J., 2020. Deep learning vs. traditional computer vision. In: Arai, K., Kapoor, S. (Eds.), Advances in Computer Vision. vol. 943, Springer International Publishing, Cham, pp. 128–144. http://dx.doi.org/10.1007/978-3-030-17795-9_10, URL: http://link.springer.com/10.1007/978-3-030-17795-9_10. Series Title: Advances in Intelligent Systems and Computing.

Pebesma, E., 2018. Simple features for R: Standardized support for spatial vector data. R J. 10 (1), 439–446. http://dx.doi.org/10.32614/RJ-2018-009, Number: 1.

Persson, M., Lindberg, E., Reese, H., 2018. Tree species classification with multitemporal sentinel-2 data. Remote Sens. 10 (11), 1794. http://dx.doi.org/10.3390/rs10111794.

Phiri, D., Simwanda, M., Salekin, S., Nyirenda, V.R., Murayama, Y., Ranagalage, M., 2020. Sentinel-2 data for land cover/Use mapping: A review. Remote Sens. 12 (14), 2291. http://dx.doi.org/10.3390/rs12142291, URL: https://www.mdpi.com/2072-4292/12/14/2291. Number: 14 Publisher: Multidisciplinary Digital Publishing Institute.

R Core Team, 2020. R: A Language and Environment for Statistical Computing. R Foundation for Statistical Computing, Vienna, Austria, URL: https://www.R-project.org/.

Ronneberger, O., Fischer, P., Brox, T., 2015. U-net: Convolutional networks for biomedical image segmentation. In: Navab, N., Hornegger, J., Wells, W.M., Frangi, A.F. (Eds.), Medical Image Computing and Computer-Assisted Intervention. MICCAI 2015, In: Lecture Notes in Computer Science, Springer International Publishing, Cham, pp. 234–241. http://dx.doi.org/10.1007/978-3-319-24574-4_28.

Stehman, S.V., Foody, G.M., 2019. Key issues in rigorous accuracy assessment of land cover products. Remote Sens. Environ. 231, 111199. http://dx.doi.org/10.1016/j.rse.2019.05.018, URL: https://www.sciencedirect.com/science/article/pii/S0034425719302111.

Strahler, A.H., Woodcock, C.E., Smith, J.A., 1986. On the nature of models in remote sensing. Remote Sens. Environ. 20 (2), 121–139. http://dx.doi.org/10.1016/0034-4257(86)90018-0, URL: https://linkinghub.elsevier.com/retrieve/pii/0034425786900180.

Wessel, M., Brandmeier, M., Tiede, D., 2018. Evaluation of different machine learning algorithms for scalable classification of tree types and tree species based on sentinel-2 data. Remote Sens. 10 (9), 1419. http://dx.doi.org/10.3390/rs10091419.

Woodcock, C.E., Strahler, A.H., 1987. The factor of scale in remote sensing. Remote Sens. Environ. 21 (3), 311–332.

Xi, Y., Ren, C., Tian, Q., Ren, Y., Dong, X., Zhang, Z., 2021. Exploitation of time series sentinel-2 data and different machine learning algorithms for detailed tree species classification. IEEE J. Sel. Top. Appl. Earth Obs. Remote Sens. 14, 7589–7603. http://dx.doi.org/10.1109/JSTARS.2021.3098817, URL: https://ieeexplore.ieee.org/document/9495140/.

Xie, B., Cao, C., Xu, M., Duerler, R., Yang, X., Bashir, B., Chen, Y., Wang, K., 2021. Analysis of regional distribution of tree species using multi-seasonal sentinel-1&2 imagery within google earth engine. Forests 12 (5), 565. http://dx.doi.org/10.3390/f12050565.

Yoshida, Y., Okada, M., 2019. Data-dependence of plateau phenomenon in learning with neural network — Statistical mechanical analysis. In: Wallach, H., Larochelle, H., Beygelzimer, A., Alché-Buc, F., Fox, E., Garnett, R. (Eds.), Advances in Neural Information Processing Systems 32. Curran Associates, Inc., pp. 1722–1730.

Yuan, Q., Shen, H., Li, T., Li, Z., Li, S., Jiang, Y., Xu, H., Weiwei, T., Yang, Q., Wang, J., Gao, J., Zhang, L., 2020. Deep learning in environmental remote sensing: Achievements and challenges. Remote Sens. Environ. 241, 111716. http://dx.doi.org/10.1016/j.rse.2020.111716.

Zagajewski, B., Kluczek, M., Raczko, E., Njegovec, A., Anca, D., Kycko, M., 2021. Comparison of random forest, support vector machines, and neural networks for post-disaster forest species mapping of the Krkonoše/karkonosze transboundary biosphere reserve. Remote Sens. 13 (13), 2581. http://dx.doi.org/10.3390/rs13132581.

Zhou, Z., Rahman Siddiquee, M.M., Tajbakhsh, N., Liang, J., 2018. UNet++: A nested U-net architecture for medical image segmentation. In: Stoyanov, D., Taylor, Z., Carneiro, G., Syeda-Mahmood, T., Martel, A., Maier-Hein, L., Tavares, J.a.M.R., Bradley, A., Papa, J.a.P., Belagiannis, V., Nascimento, J.C., Lu, Z., Conjeti, S., Moradi, M., Greenspan, H., Madabhushi, A. (Eds.), Deep Learning in Medical Image Analysis and Multimodal Learning for Clinical Decision Support. Springer International Publishing, Cham, pp. 3–11.

4

Automated classification of trees outside of the forest

1. Preamble

This section presents developments in relation to Objective 2. We used a CHM derived from ALS data to produce a vegetation map. The latter was the start of an automated detection of TOF and their classification as a function of their shape and distribution in the landscape. This research has been published in the peer-reviewed journal *Remote Sensing* (Bolyn et al., 2019).

We have also published this research in a popularised article (Bolyn, Latte, Fourbisseur, et al. (2020), see appendix A.1). In the latter, we present the implementation of the TOF mapping method and a complementary analysis for two Belgian municipalities.

2. Peer reviewed article

Bolyn, C., Lejeune, P., Michez, A., & Latte, N. (2019). Automated classification of trees outside forest for supporting operational management in rural landscapes. *Remote Sensing*, *11*(10), 1146. https://doi.org/10.3390/rs11101146

Article

Automated Classification of Trees outside Forest for Supporting Operational Management in Rural Landscapes

Corentin Bolyn * , **Philippe Lejeune, Adrien Michez** and **Nicolas Latte**

Uliège-Gembloux Agro-Bio Tech. TERRA Teaching and Research Center—Forest Is Life, Passage des Déportés 2, BE-5030 Gembloux, Belgium; p.lejeune@uliege.be (P.L.); adrien.michez@ulg.ac.be (A.M.); Nicolas.Latte@ulg.ac.be (N.L.)

* Correspondence: cbolyn@doct.uliege.be; Tel.: +32-81-62-2678

check for updates

Abstract: Trees have important and diverse roles that make them essential outside of the forest. The use of remote sensing can substantially support traditional field inventories to evaluate and characterize this resource. Existing studies have already realized the automated detection of trees outside the forest (TOF) and classified the subsequently mapped TOF into three geometrical classes: single objects, linear objects, and ample objects. This study goes further by presenting a fully automated classification method that can support the operational management of TOF as it separates TOF into seven classes matching the definitions used in field inventories: Isolated tree, Aligned trees, Agglomerated trees, Hedge, Grove, Shrub, and Other. Using publicly available software tools, an orthophoto, and a LIDAR canopy height model (CHM), a TOF map was produced and a two-step method was developed for the classification of TOF: (1) the geometrical classification of each TOF polygon; and (2) the spatial neighboring analysis of elements and their classification into seven classes. The overall classification accuracy was 78%. Our results highlight that an automated TOF classification is possible with classes matching the definitions used in field inventories. This suggests that remote sensing has a huge potential to support the operational management of TOF as well as other research areas regarding TOF.

1. Introduction

Trees have important and diverse roles that make them essential outside of the forest. Around the world, trees outside the forest (TOF) have a significant impact on national biomass and carbon stocks [1,2]. Locally, they host biodiversity and, as part of the landscape, they represent elements of connectivity for many species relying on trees [3,4]. Goods and environmental services supplied by this resource are essential for people in many regions. The Food and Agriculture Organization of the United Nations (FAO) considers forests and TOF as essential for global food security and nutrition, as people directly and indirectly depend on them. They directly rely on this resource through the consumption and sale of foods harvested, and indirectly through forest-related employment, forest ecosystem services, and forest-based biodiversity [5].

Increased consideration has been progressively given to TOF over the past several decades. In Europe, for example, through agri-environment measures, the European Commission "provides payments to farmers who subscribe, on a voluntary basis, to environmental commitments related to the preservation of the environment and maintaining the countryside" (see https://ec.europa.eu/agriculture/envir/measures_en for further information). At present, TOF are often included in

national forest inventories [6]. Nevertheless, monitoring designs are still not adapted to TOF properties, which generally leads to low accuracy. In their review about TOF monitoring, Schnell et al. [6] concluded that, instead of increasing sample size, combining field surveys with prior remote sensing methods is a good approach that could improve TOF estimates without unacceptably increasing costs.

Remotely sensed data have been used in many studies in order to make a global assessment of TOF. In most cases, remote sensing of TOF was only an intermediate processing step to develop a requiring the spatial characterization of TOF for applications such as biomass estimation. Thus, the detection and classification of TOF were often not automated or were done only by applying a simple approach. Some studies mainly used visual interpretation methods to map and classify TOF [7–11]. Other studies implemented automatic processes, often divided into two tasks. The first task consists of mapping the vegetation and separating trees in the forest (TIF) from TOF. The second task consists of classifying different kinds of TOF on the basis of their geometrical properties.

For instance, regarding TOF mapping, Straub et al. [12] used full-waveform laser scanner data acquired by a airborne laser scanning (ALS) system to detect the vegetation with the local density of laser reflection. To separate forest from non-forest areas, they used estimates of height, tree crown cover, size of a vegetation region, and width of a vegetation region. Also with a wall-to-wall ALS dataset, Maack et al. [13] applied a simpler approach. They computed the mean height in a 4 m × 4 m window and used a threshold of 2 m in combination with existing OpenStreetMap (OpenStreetMap Foundation, Sutton Coldfield, UK) data to detect TOF areas. Using multi-spectral aerial imagery (R, G, B, and NIR), Meneguzzo et al. [14] made a comparative study of TOF mapping using two different methods: first, an unsupervised per-pixel classifier; and, secondly, an object-based image analysis. Both methods were found to be appropriate for mapping TOF and could complete ground-based inventory. Using high-resolution satellite imagery, Singh and Chand [15] computed a normalized difference vegetation index (NDVI) to differentiate vegetated from non-vegetated areas with a pixel-based approach. An unsupervised ISODATA classification algorithm was used to separate TOF from other elements. With the same data type, Pujar et al. [16] used an object-based approach. A first coarse scale of segmentation was used to classify land cover. A second fine scale of segmentation was used to detect TOF in the detected agricultural landscape.

Concerning the TOF geometrical classification, Straub et al. [12] classified TOF on the basis of their form and size into two classes: Single tree objects or Connected groups of trees. Singh and Chand [15], Pujar et al. [16], and Seidel et al. [10] made a more detailed geometrical classification into three classes: Single objects, Linear objects, and Ample objects. Singh and Chand [15] classified TOF in these three classes by visual interpretation. Pujar et al. [16] realized it using spectral and geometric segment parameters computed during the segmentation process in an object-based approach. The overall accuracy was 76%, and the kappa coefficient was 0.59. Finally, starting from a TOF map entirely digitized by visual interpretation, Seidel et al. [10] classified TOF using the diameter of the smallest enclosing circle of each polygon as well as a measure of elongation (E).

An automated classification of TOF in three geometrical classes is relevant, as each of these TOF types structure the landscape in a different way. However, a more sophisticated classification method that can support the operational management of TOF in rural landscapes is missing. Indeed, most of the time, field inventories classify TOF elements in finer categories that consider more classification criteria, such as the length of an element, its width, or the number of trees. Furthermore, several TOF elements can often be considered as a single group in such categories. Then, the spatial context has to be used in an automated processing in order to enable a characterization of TOF classes that matches with the definitions used in field inventories. To the best of our knowledge, no study in the literature presents a method to automatically classify fine TOF categories using neighboring and the possible spatial combinations of TOF elements. The objective of this study was to fill this gap by developing a classification method for classes frequently used in rural landscape inventories. In order to ensure that the chosen TOF definitions are relevant for field inventories on a large scale, targeted TOF classes were defined on the basis of European agri-environment measures. In order to suggest a realistic

and operational approach, the algorithm was entirely developed by means of publicly available software tools.

2. Materials and Methods

2.1. Study Site

Three adjacent municipalities from southern Belgium were selected as a pilot area (20,076 ha) for this study: Gesves, Assesse, and Ohey (Figure 1). These municipalities combine agricultural and forest contexts and are densely covered by TOF. Table 1 shows the distribution between landcover classes according to the CORINE Land Cover database 2012 (see https://land.copernicus.eu/pan-european/corine-land-cover).
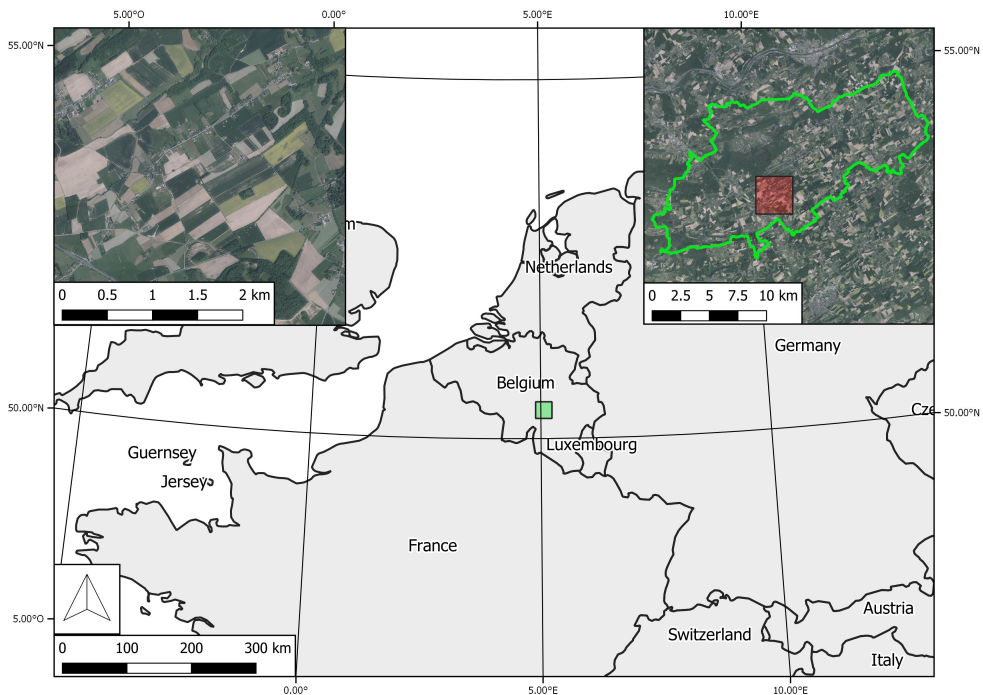
Figure 1. Localisation of the study site (green square). The study site edges (green lines) are shown in the top-right corner (orthophoto 2012–2013, Public service of Wallonia). A more detailed view is presented in the top-left corner, located by the red square in the top-right corner view.

Table 1. Distribution of areas (ha) by land cover class according to the CORINE Land Cover database 2012.

Land Cover	Area (ha)
Agricultural areas	13,057.80
Artificial surfaces	2605.73
Forest and semi-natural areas	4411.99

2.2. Remotely Sensed Data

Two publicly available datasets (see http://geoportail.wallonie.be) were used in this study:

1. LIDAR data. The study site was covered by two survey flights on 17 December 2013 and 18 January 2014. The average point density of small-footprint discrete airborne LIDAR data was

0.8/m^2. A canopy height model (CHM) was computed (LIDAR digital surface model—LIDAR digital terrain model) with 1 m ground sampling distance (GSD);

2.   Orthophotos for which the survey flight took place on 7 June 2013 for the study site. Data were acquired by a VEXCEL UltraCam Xp camera (Vexcel Imaging GmbH, A-8010 Graz, Austria) at 0.25 m GSD. A normalized difference vegetation index (NDVI) was computed at 1 m GSD.

The LIDAR CHM and the NDVI were aligned and stacked into one multiband raster covering the extent of the study site.

2.3. Tools

All the processing steps presented in Section 2 were realized using publicly available software tools. R software [17] was used to develop algorithms and to realize statistical treatments. The *sf* package of R [18] was used to develop vector operations. Simple manipulations on raster were realized using the *raster* package of R [19]. Advanced processing on raster were realized using the Orfeo Toolbox (OTB) software (see https://www.orfeo-toolbox.org).
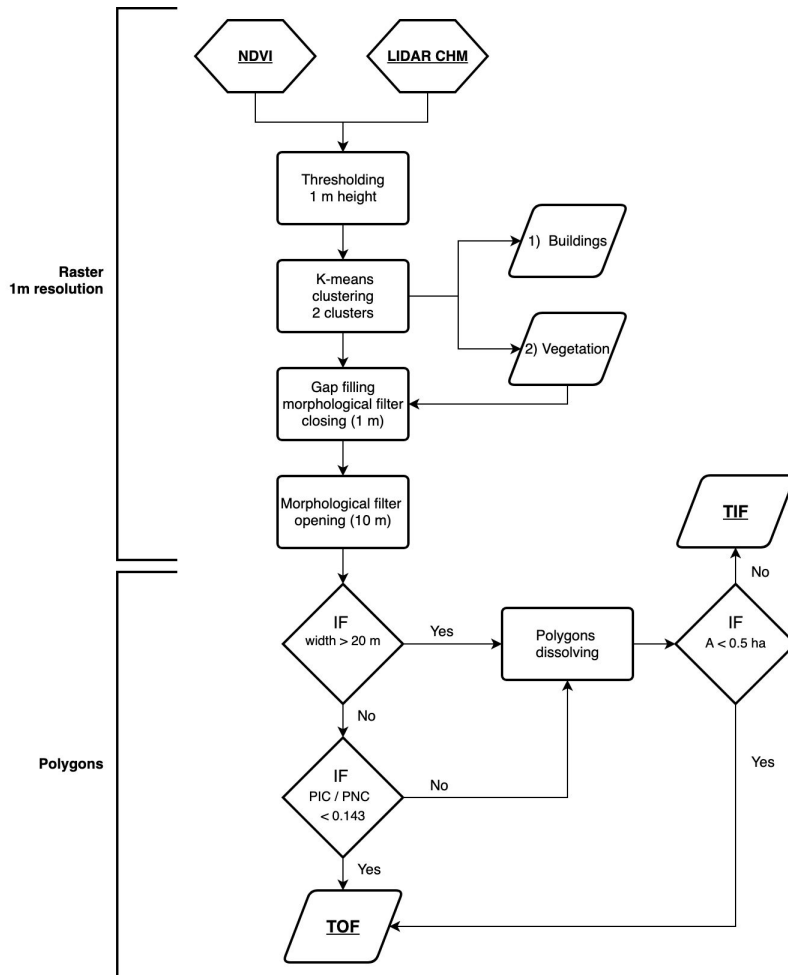
2.4. TOF Mapping

The first part of the processing was applied on raster data (Figure 2, upper part). First, the multi-band raster was masked for LIDAR CHM values smaller than 1 m in height. Through this means, we isolated elevated elements from the ground. Then, an unsupervised classification K-means clustering was applied on the NDVI to separate buildings and vegetation. Only pixels attributed to the cluster grouping higher NDVI values were conserved to make the vegetation raster.

Starting from the vegetation raster, the goal was to conserve only TOF elements. In other words, the elements that did not meet a forest definition were kept. According to the FAO's definition of forest [20], the forest was defined as a continuous vegetation element larger than 0.5 ha and wider than 20 m.

Small gaps were filled using the binary morphological operation from OTB software (parameters: closing, 1 m in X and Y). The width criterion of the forest definition was tested using a binary morphological operation (parameters: opening, 10 m in X and Y). This processing divided the pixels into two classes: pixels making part of an element wider than 20 m, and pixels making part of an element not wider than 20 m. Afterwards, the raster was polygonized and all subsequent processings were applied to features (Figure 2, bottom).

Polygons not wider than 20 m were subjected to a second test before being classified as TOF. When touching a polygon wider than 20 m, the perimeter in contact (PIC) was compared to the perimeter not in contact with the other polygon (PNC). If the perimeter ratio (PIC/PNC) was lower than 0.143, the polygon was classified as TOF. This value was empirically defined in order to include the elongated polygons in contact with forest. Considering a rectangular element, polygons were considered as elongated if the width/length ratio was smaller than 1/3. For the perimeter ratio (PIC/PNC), it corresponded to 1/7 or 0.143. All polygons with a PIC/PNC ratio higher than 0.143 were dissolved with the polygons in contact.

Afterwards, the area criteria of forest definition was tested on polygons classified wider than 20 m. Polygons smaller than 0.5 ha were classified as TOF. Others were classified as TIF.

Figure 2. Flowchart of the trees outside the forest (TOF) mapping. CHM: canopy height model; NDVI: normalized difference vegetation index; TIF: trees in the forest.

2.5. TOF Classification

2.5.1. Targeted TOF Classes

As a European region, the public service of Wallonia (Southern Belgium) has defined control instructions to allocate European agri-environment measures funds. Inspired by its definitions, seven classes were targeted in this paper as being the best compromise between field reality in the European context and a geographic information system (GIS) method. The classes are based on geometric and spatial criteria coming from agri-environment measures definitions adapted for GIS processes. Using GIS, TOF are seen from the sky as crown polygons. According to the following definitions, a woody patch was defined by a nonlinear element having an area smaller than 400 m²:

1. Isolated tree: a patch that represents only a single tree crown and that has an area greater than 12.6 m². For a disk, it corresponds to a diameter of 4 m. The distance between its crown extremity and hedges, groves, and forest is greater than 5 m. The distance between its crown extremity and other patches is larger than 10 m. The circularity (C) is greater than 0.75 ($Circularity = 4\pi A / P^2$ where A is the area of the polygon, and P is the perimeter);

2. Aligned trees: linear group of minimum five patches. The distance between crowns is less than 10 m;
3. Agglomerated trees: group of patches not meeting the criteria of aligned trees. The distance between consecutive tree crowns is smaller than 10 m;
4. Hedge: linear continuous element with a minimum length (L) of 10 m and a maximum mean width (W) of 20 m. The elongation (E) is higher than 3 ($E = L/W$ where E is the elongation, L is the length, and W is the width). Neighboring hedge elements are merged if their distance is less than 5 m;
5. Grove: continuous but nonlinear element, the area (A) of which is higher than 400 m²;
6. Shrub: patch not assigned to other classes, having a distance of less than 5 m to a neighboring hedge, grove, or forest, and a distance of less than 10 m to a neighboring patch. This class corresponds to shrubs, trees not meeting the criteria to be an isolated tree, and groves smaller than 400 m²;
7. Other: TOF not meeting the criteria of any previous definitions.

As an example, targeted classes 1 to 6 are illustrated with an orthophoto in Figure 3.

Figure 3. Illustration of the targeted classes for the TOF classification: 1: Isolated tree, 2: Aligned trees, 3: Agglomerated trees, 4: Hedge, 5: Grove, 6: Shrub. Orthophoto 2018, Public service of Wallonia.

2.5.2. Overall TOF Classification Flowchart

The classification processing was divided into two steps (Figure 4). First, TOF polygons were classified into three geometrical classes: Grove, Linear element, and Patch. Then, the neighboring of Linear elements and Patches was analyzed in order to attribute final TOF classes: Isolated tree, Aligned trees, Agglomerated trees, Hedge, Shrub, and Other.
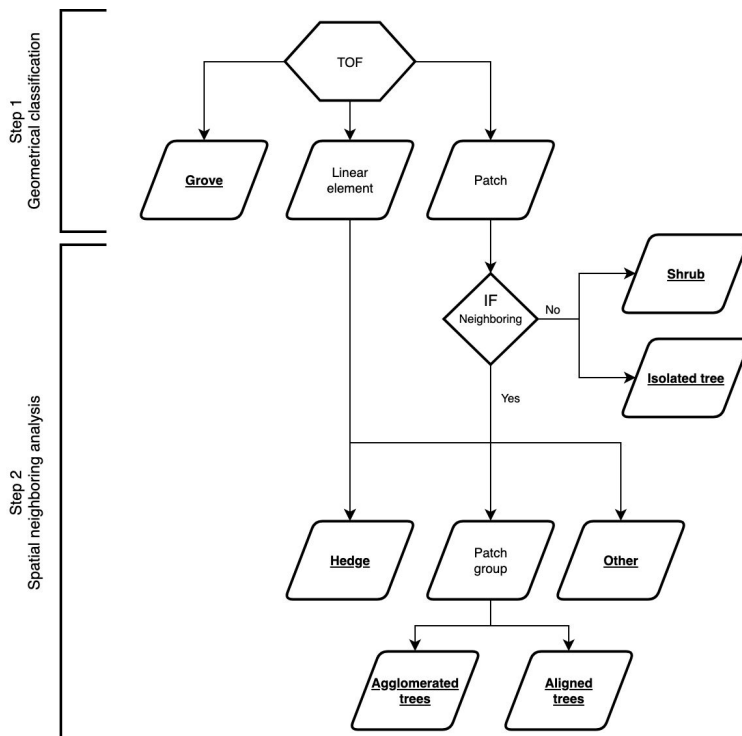
Figure 4. Overall flowchart of the TOF classification divided into two steps: geometrical classification and spatial neighboring analysis. Targeted classes are marked in bold and underlined.

2.5.3. Step 1: Geometrical Classification of TOF Polygons

The goal of this step was to describe the geometry of each TOF polygon based on four parameters: Length (L), Width (W), Elongation (E), and Circularity (C).

Figure 5 describes the classification decisions according to these four parameters. Each polygon was classified into one of the following three classes: Linear element, Grove, and Patch. Among these classes, only the Grove class is a TOF class targeted in this study. Linear element and Patch are intermediate classes that could be combined with another neighboring TOF polygon before the attribution of a targeted class. The analysis of the spatial neighboring is the second step of the TOF classification.

Circularity (C) was computed on smoothed TOF polygons. A positive buffer (+4 m) followed by a negative buffer (−4 m) were applied to smooth the polygon edges formed by 1 m pixel limits. For polygons not wider than 20 m (according to the morphological filter) with circularity lower than 0.5, a centerline was generated in order to evaluate Length (L), Width (W), and Elongation (E). For other polygons, Length, Width, and Elongation were set to 0.

Centerline generation is presented in Figure 6: in addition to the smoothing, TOF polygons were simplified in order to optimize the generation of a skeleton. TOF edges were simplified using the standard Douglas–Peucker algorithm. The tolerance parameter value was set to 0.2 and the preserve topology option was used. By this means, the large number of vertexes was reduced. Furthermore, the edges of the polygons were partitioned into 1-m segments. Then, polygon vertexes were used to generate Voronoi polygons. Voronoi polygon edges were converted into a linestring layer. Only Voronoi edges 0.1 m inside the TOF polygons were conserved.

In order to find the centerline among segments, a filtering process was applied on every line segment. The angle between a line segment and its nearest TOF edge segment (the line formed by

two vertexes) was computed. If this angle was greater than 150°or smaller than 30°, it was conserved. Inside a TOF polygon, if the skeleton was cut into several parts after this step, parts were linked by their nearest vertexes. Finally, line segments were merged to create the centerline.
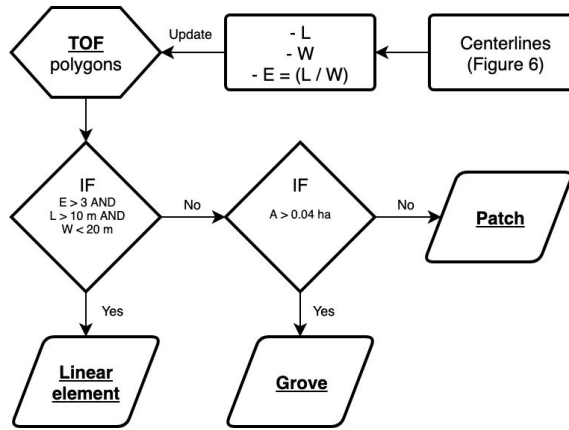

Figure 5. Flowchart of the first step of classification: geometrical classification of TOF polygons.
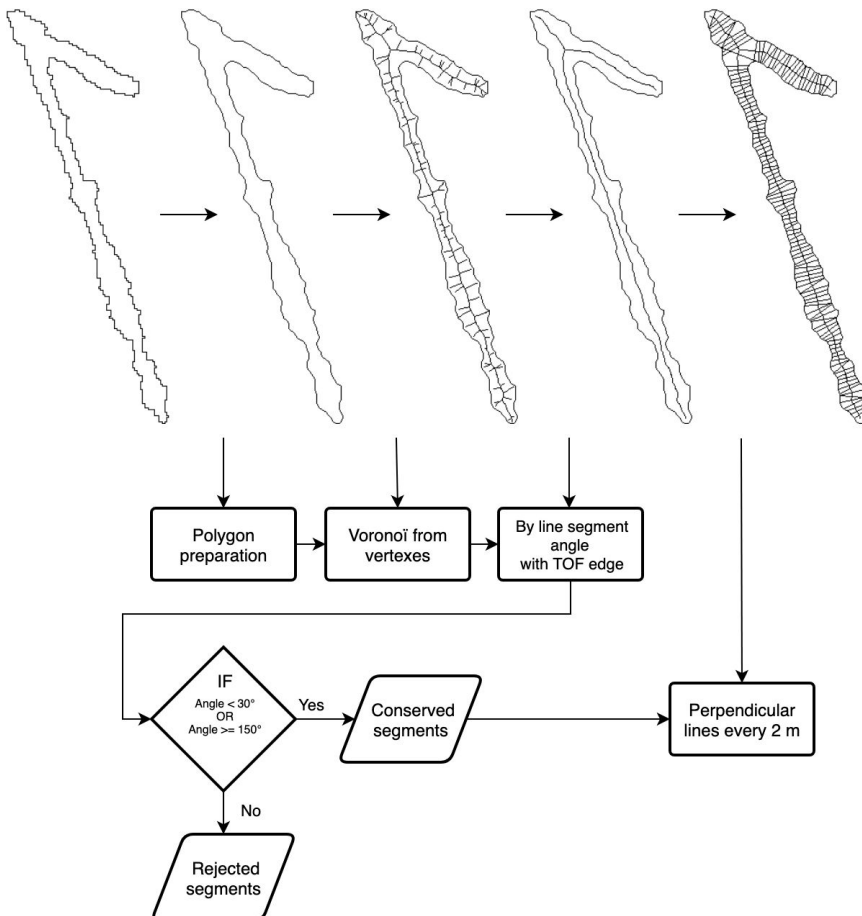

Figure 6. Flowchart of the centerline generation.

For each TOF centerline segment, perpendicular lines were computed every 2 m and were intersected with their TOF polygon. To avoid estimating width in junctions, perpendicular lines were not conserved when intersecting more than one centerline segment.

For a TOF polygon, Length (L) was computed as the total length of the TOF centerline, and Width (W) was computed as the mean of all the perpendicular line lengths.

2.5.4. Step 2: Spatial Neighboring Analysis

For every feature of the Linear element class and of the Patch class, distances from other features were analyzed from edge to edge. For the Patch class, the potential spatial combinations with other elements in proximity are given in Table 2.

**Table 2.** Spatial combinations for the Patch class, in decreasing order of priority.

Neighboring Test	1. Patch 10 m Around	2. Linear Element 5 m Around	3. Forest or Grove 5 m Around
New class	Patch group	Hedge	Other

A new class was attributed to Patch TOF having a proximity with these other elements. If several proximities occurred for the same TOF, the order of priority was respected to attribute the new class. For possibilities 1, 2, and 3, the new attributed classes were: Patch group, Hedge, and Other. Thus, a patch near to nothing except the forest or a grove was classified as Other. Furthermore, for possibilities 1 and 2, all the TOF polygons in the same spatial neighboring were grouped into a new multipolygon feature.

Linear element polygons and Hedge multipolygons less than 5 m from each other were grouped into multipolygon features and classified as Hedge.

Patches that were not close to any element were classified as Isolated tree if their area was higher than 12.6 m² and if Circularity was higher than 0.75. If these two conditions were not met for an isolated Patch, it was classified as Shrub.

The last treatment classified Patch group multipolygons in two classes: Aligned trees and Agglomerated trees. The number of patches by feature and their aligned disposition were used to make this final classification (Figure 7). The minimum patch number to classify a Patch group into Aligned trees was five. In order to determine if patches were aligned, line segments were generated to link their centroids stepwise, and the angles formed between these segments were then computed. If at least 75% of these angles were greater than 135°, patches were considered as being aligned. For these two classes, the number of patches by feature was saved.
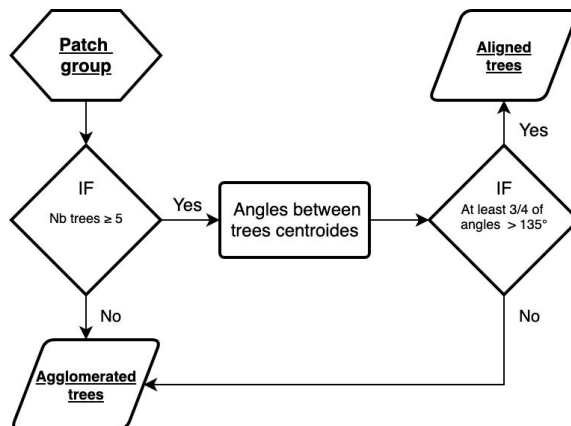
Figure 7. Flowchart of the Patch groups classification into two classes: Aligned trees and Agglomerated trees.

2.5.5. Accuracy Assessment

The TOF classes were primarily designed to inventory TOF agricultural landscapes. For this reason, the accuracy of TOF classification was evaluated in agricultural parcels referenced in the Belgian public database (see http://geoportail.wallonie.be). A visual interpretation of the orthophoto was realized for 10% of the mapped TOF elements located within 5 m of the agricultural parcels layer. The goal was to assess the accuracy of the classification algorithm applied on a TOF map. The accuracy of the TOF mapping was not directly assessed. The 10% sample was randomly selected. Each sample element was visually classified into one class by a skilled operator. If a difference occurred between the automated classification and the visual classification, it was then specified whether the error was due to the TOF classification or to the TOF mapping. Indeed, the TOF classification was based on the geometrical and spatial properties of TOF polygons. Then, if there was some error in the TOF mapping, the algorithm could provide a classification for the polygon which seemed accurate according to its given properties but which was actually erroneous and did not match with the reality observed in the field. When a TOF element was not vegetation but a commission of the TOF map, it was classified as "NO".

Based on this visual interpretation, a confusion matrix was generated and the overall accuracy was computed. Production (PA) and consumer (CA) accuracies were computed by class. This accuracy assessment was called "complete validation". Starting from the same dataset, observations with an error associated to the TOF mapping were removed. A second confusion matrix was then generated and accuracy indices (overall accuracy, PA, and CA) were computed. This second accuracy assessment was called "filtered validation".

3. Results

For a visualization zone, Figure 8 shows the results of the TOF mapping as well as those of step 1 and step 2 of the TOF classification.

Table 3 shows areas (ha) covered by the TIF and TOF classes on the study site.

Table 3. Areas (ha) covered by trees in the forest (TIF) and trees outside the forest (TOF) on the study site.

Class	Area (ha)
TIF	5169.35
TOF	1040.65

Table 4 shows areas (ha) covered by the targeted classes on the study site.

Table 4. Distribution of areas (ha) by targeted class on the study site.

Class	Area (ha)
Agglomerated trees	74.26
Aligned trees	2.35
Grove	339.16
Hedge	596.58
Isolated tree	9.75
Other	6.28
Shrub	12.27

As shown in Table 5, production accuracies (PAs) and consumer accuracies (CAs) computed with the complete validation were satisfactory. The overall accuracy was 78.4%. The TOF classification was overall conclusive. Nevertheless, the minimum PA was 0.35 for the Aligned trees class and the minimum CA was 0.58 for the Shrub class.
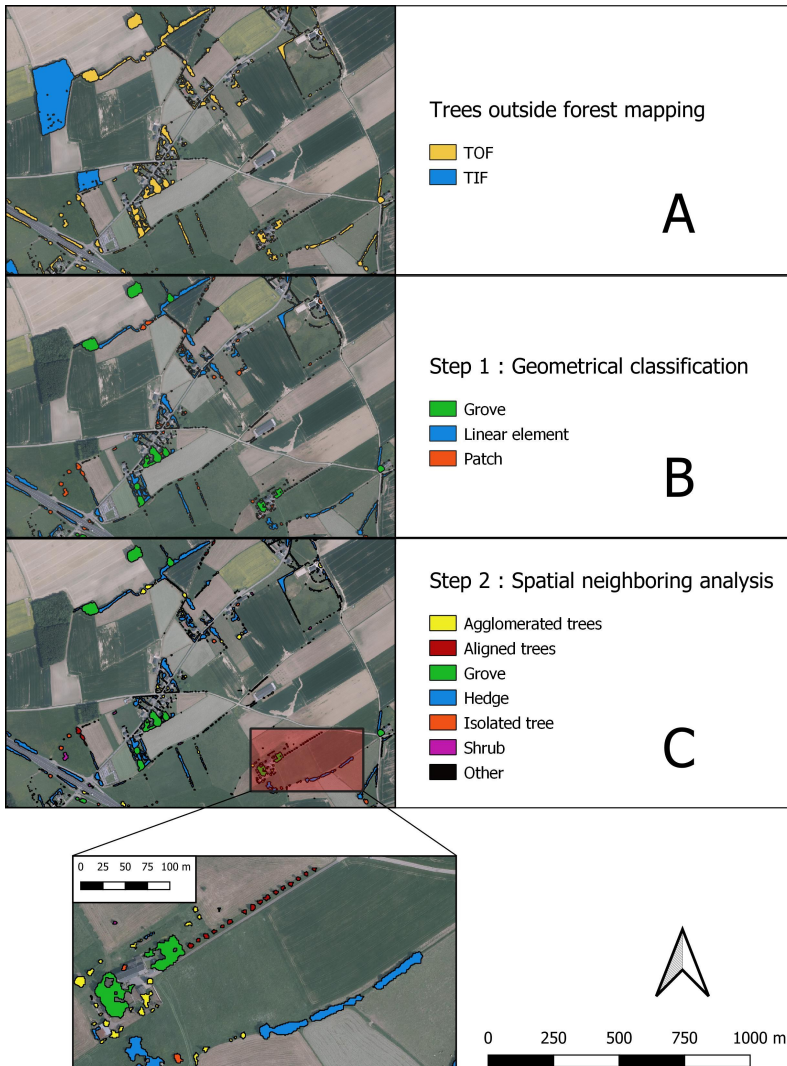
Figure 8. Visualization zone of the results. (**A**) the trees outside the forest mapping. Two classes in the legend: trees outside the forest (TOF) and trees in the forest (TIF); (**B**) step 1 of the TOF classification—geometrical classification of TOF polygons; (**C**) step 2 of the TOF classification—spatial neighboring analysis. For step 2, a more detailed view is presented on the bottom. Background map: orthophoto 2012–2013, Public service of Wallonia.

PA and CA were higher for the filtered validation (without errors due to the TOF mapping) with a minimum PA of 0.90 for the Grove class and a minimum CA of 0.89 for the Aligned trees class (Table 5). The overall accuracy was 92.6%. The algorithm of TOF classification made the intended decisions in most cases when considering a reference dataset free from TOF mapping error.

Table 5. Production accuracies (PAs) and consumer accuracies (CAs) of the classification by TOF class, computed for the complete validation dataset and the filtered validation dataset.

	PA		CA	
	Complete	**Filtered**	**Complete**	**Filtered**
Agglomerated trees	0.79	0.98	0.80	0.97
Aligned trees	0.35	1.00	0.73	0.89
Grove	0.78	0.90	0.95	0.97
Hedge	0.86	0.95	0.85	0.93
Isolated tree	0.76	0.99	0.83	0.92
Other	0.92	0.92	0.76	0.97
Shrub	0.90	0.92	0.58	0.95

For the complete validation dataset, the overall error of classification was 21.63%; 17.30% were due to the TOF mapping, according to the visual interpretation. The number of validation observations are presented by class in Table 6.

Table 6. Number of observations by class in complete and filtered validation datasets.

	Agglomerated Trees	**Aligned Trees**	**Grove**	**Hedge**	**Isolated Tree**	**Other**	**Shrub**	**Total**
Complete	266	11	122	335	124	45	253	1156
Filtered	220	9	120	305	112	35	155	956

As shown in the confusion matrix built with the complete validation dataset (Table 7), the lowest PA of the Aligned trees class was associated with the confusion with the Agglomerated trees class. The lowest CA of the Shrub class was mainly associated with the confusion with the Agglomerated trees class, the Isolated tree class, and the false detection of vegetation (NO class in Table 7).

Table 7. Confusion matrix of the TOF classification, built with the complete validation dataset. Observations are sorted by reference class in columns, and by prediction class in rows.

Prediction	Reference							
	Agglomerated Trees	**Aligned Trees**	**Grove**	**Hedge**	**Isolated Tree**	**NO**	**Other**	**Shrub**
Agglomerated trees	213	12	1	27	1	8	0	4
Aligned trees	1	8	0	2	0	0	0	0
Grove	3	0	116	3	0	0	0	0
Hedge	10	1	28	285	0	5	3	3
Isolated tree	5	0	1	2	103	4	0	9
NO	0	0	0	0	0	0	0	0
Other	5	0	3	1	0	1	34	1
Shrub	32	2	0	11	31	30	0	147

4. Discussion

The classification of the seven TOF classes achieved an overall accuracy of 78.4%. This result demonstrates that it is possible to design a fully automated mapping of accurate TOF types that matches the definitions used in field inventories. Accuracies were satisfactory in comparison to similar existing studies. Furthermore, previous studies stopped at step 1 of classification. Using high-resolution satellite imagery, Pujar et al. [16] automatically mapped three TOF classes (Point, Line, and Patch) with an overall accuracy of 75.1% in an agricultural landscape. In their study based on full-waveform laser scanner data, Straub et al. [12] classified four classes: Non-tree vegetation, Forest, Non-forest vegetation—group of trees, Non-forest vegetation—single trees. For the "group of trees" class, the PA was 0.68 and the CA was 0.78. For the "single trees" class, the PA was 0.52 and the CA was 0.69.

The TOF classification deeply depends on TOF polygons' shape and neighboring. As a consequence, a large part of classification errors were not due to the process itself but to omission,

commission, or poor delineations of elements in the TOF mapping. Working on an ideal TOF mask, the developed algorithm predicted the intended class in most cases.

With respect to the aligned trees, the performance of the classification algorithm proved to be highly sensitive to the TOF mapping results. Along an aligned element group, just one missing detection could divide the line into two independent parts no longer meeting the conditions (Figure 7). The worst PA (0.35) of the Aligned trees class confirmed the latter finding (Table 5). Sometimes, aligned trees can be present on both sides of a street. If the street is not wide enough, these two entities were grouped as a single TOF element by the process. A GIS street layer would allow aligned trees to be correctly separated in post-processing in such a case. More generally, the use of an existing GIS layer to test intersection or proximity with structuring elements of the landscape (streets, rivers, etc.) is an interesting perspective to better characterize TOF resources seen from above.

As expected, the most frequent classification error concerned the Shrub class. Indeed, most commissions of TOF detected in the TOF mapping (NO class in Table 7) necessarily had typical properties of the Shrub class as they often corresponded to small but elevated urban elements which can easily be confused with vegetation due to a confusing NDVI signal. Additionally, Agglomerated trees with small height were often classified as Shrub because not all the trees were detected. It appears that the chosen method for vegetation detection is less efficient below a 3-m height and that it produces omissions and poor or incomplete delineations of TOF. Most of the time, this had the effect of classifying separated trees into the Shrub class. Finally, the defined rules applied to differentiate the isolated tree class and the Shrub class are based on an area value and a circularity value. This method appears to be too simple, and it failed in some cases—particularly when the TOF polygon was poorly delineated. More development could be made in order to integrate the certitude that there is one single tree into the existing rules.

In their conclusion, Straub et al. [12] suggested method development in order to classify elongated groups of trees connected with the boundary of the forest as TOF. This was implemented in step 1 through the application of a morphological filter using the distance from the boundary to detect narrow parts of a raster. Nevertheless, this method sometimes revealed unexpected behavior: if there was a gap in the vegetation raster (even as small as one pixel), the distances were then calculated from that gap and the vegetation which was in contact with the gap could be considered as having a width smaller than 20 m while it was actually wider. As a consequence, it could be erroneously classified as TOF.

Separating the vegetation outside the forest in well-defined categories can be regarded as a challenging task. The goal is to reach the best compromise that serves the study objectives. In that way, definitions were built to represent structuring elements of agricultural lands related to agri-environment measures. That is why the results were conclusive in agricultural land, and therefore less adapted to urban areas where the variability of shapes and the number of possible combinations of elements are higher than in agricultural lands. This caused more exceptions and confusion between the defined classes.

5. Conclusions

An accurate and automated classification of trees outside the forest (TOF) that can support the operational management of TOF in rural landscapes was realized. An algorithm was developed for seven classes matching the definitions used in field inventories. The use of the neighboring and possible spatial combinations of TOF elements allowed us to detect complex landscape elements. The overall accuracy of the classification was 78%. This study was entirely carried out by means of publicly available software tools and simple operations in such a way that it improves the reproducibility of the method and shows the potential of geographic information systems and remote sensing for TOF applications. This study demonstrates that automated TOF classification is possible with classes matching the definitions used in field inventories. This suggests that remote sensing has a huge potential to support the operational management of TOF as well as other research areas regarding TOF.

Abbreviations

The following abbreviations are used in this manuscript:

A	Area
ALS	Airborne laser scanning
C	Circularity
CHM	Canopy height model
CA	Consumer accuracy
E	Elongation
FAO	Food and Agriculture Organization of the United Nations
GIS	Geographic information system
GSD	Ground sampling distance
L	Length
NDVI	Normalized Difference Vegetation Index
OTB	Orfeo Toolbox software
PA	Production accuracy
PIC	Perimeter in contact
PNC	Perimeter not in contact
TIF	Trees in the forest
TOF	Trees outside the forest
W	Width

References

1. Schnell, S.; Altrell, D.; Ståhl, G.; Kleinn, C. The contribution of trees outside forests to national tree biomass and carbon stocks—A comparative study across three continents. *Environ. Monit. Assess.* **2015**, *187*. [CrossRef] [PubMed]
2. Zomer, R.J.; Neufeldt, H.; Xu, J.; Ahrends, A.; Bossio, D.; Trabucco, A.; van Noordwijk, M.; Wang, M. Global Tree Cover and Biomass Carbon on Agricultural Land: The contribution of agroforestry to global and national carbon budgets. *Sci. Rep.* **2016**, *6*. [CrossRef] [PubMed]
3. McCollin, D.; Jackson, J.; Bunce, R.; Barr, C.; Stuart, R. Hedgerows as habitat for woodland plants. *J. Environ. Manag.* **2000**, *60*, 77–90. [CrossRef]
4. Rossi, J.P.; Garcia, J.; Roques, A.; Rousselet, J. Trees outside forests in agricultural landscapes: Spatial distribution and impact on habitat connectivity for forest organisms. *Landsc. Ecol.* **2016**, *31*, 243–254. [CrossRef]
5. FAO members adopt first global action plan for forest genetic resources. *Unasylva* **2013**, *64*, 72–74.
6. Schnell, S.; Kleinn, C.; Ståhl, G. Monitoring trees outside forests: A review. *Environ. Monit. Assess.* **2015**, *187*. [CrossRef] [PubMed]
7. Marchetti, M.; Garfì, V.; Pisani, C.; Franceschi, S.; Marcheselli, M.; Corona, P.; Puletti, N.; Vizzarri, M.; di Cristofaro, M.; Ottaviano, M.; Fattorini, L. Inference on forest attributes and ecological diversity of trees outside forest by a two-phase inventory. *Ann. For. Sci.* **2018**, *75*, 37. [CrossRef]
8. Plieninger, T.; Schleyer, C.; Mantel, M.; Hostert, P. Is there a forest transition outside forests? Trajectories of farm trees and effects on ecosystem services in an agricultural landscape in Eastern Germany. *Land Use Policy* **2012**, *29*, 233–243. [CrossRef]

9.   Plieninger, T. Monitoring directions and rates of change in trees outside forests through multitemporal analysis of map sequences. *Appl. Geogr.* **2012**, *32*, 566–576. [CrossRef]

10.   Seidel, D.; Busch, G.; Krause, B.; Bade, C.; Fessel, C.; Kleinn, C. Quantification of Biomass Production Potentials from Trees Outside Forests—A Case Study from Central Germany. *Bioenergy Res.* **2015**, *8*, 1344–1351. [CrossRef]

11.   Seidel, D.; Hähn, N.; Annighöfer, P.; Benten, A.; Vor, T.; Ammer, C. Assessment of roe deer (*Capreolus capreolus* L.) – vehicle accident hotspots with respect to the location of 'trees outside forest' along roadsides. *Appl. Geogr.* **2018**, *93*, 76–80. [CrossRef]

12.   Straub, C.; Weinacker, H.; Koch, B. A fully automated procedure for delineation and classification of forest and non-forest vegetation based on full waveform laser scanner data. *Int. Arch. Photogramm. Remote Sens. Spat. Inf. Sci.* **2008**, *37*, 1013–1019.

13.   Maack, J.; Lingenfelder, M.; Eilers, C.; Smaltschinski, T.; Weinacker, H.; Jaeger, D.; Koch, B. Estimating the spatial distribution, extent and potential lignocellulosic biomass supply of Trees Outside Forests in Baden-Wuerttemberg using airborne LiDAR and OpenStreetMap data. *Int. J. Appl. Earth Observ. Geoinf.* **2017**, *58*, 118–125. [CrossRef]

14.   Meneguzzo, D.; Liknes, G.; Nelson, M. Mapping trees outside forests using high-resolution aerial imagery: A comparison of pixel- and object-based classification approaches. *Environ. Monit. Assess.* **2013**, *185*, 6261–6275. [CrossRef] [PubMed]

15.   Singh, K.; Chand, P. Above-ground tree outside forest (TOF) phytomass and carbon estimation in the semi-arid region of southern Haryana: A synthesis approach of remote sensing and field data. *J. Earth Syst. Sci.* **2012**, *121*, 1469–1482. [CrossRef]

16.   Pujar, G.; Reddy, P.; Reddy, C.; Jha, C.; Dadhwal, V. Estimation of trees outside forests using IRS high resolution data by object based image analysis. *Int. Arch. Photogramm. Remote Sens. Spat. Inf. Sci.* **2014**, *40*, 623–629. [CrossRef]

17.   R Core Team. *R: A Language and Environment for Statistical Computing*; R Foundation for Statistical Computing: Vienna, Austria, 2018.

18.   Pebesma, E. Simple Features for R: Standardized Support for Spatial Vector Data. The R Journal. 2018. Available online: https://journal.r-project.org/archive/2018/RJ-2018-009/ (accessed on 18 March 2019).

19.   Hijmans, R.J. Raster: Geographic Data Analysis and Modeling. R package Version 2.8-4. 2018. Available online: https://CRAN.R-project.org/package=raster (accessed on 18 March 2019).

20.   FAO. *FRA 2015 Terms and Definitions*; FAO: Rome, Italy, 2015.

5

Conclusion

1. Major findings

The aim of this thesis was to develop methods for monitoring tree resource using remote sensing. Although their nature may remain identical, their characteristics, the functions that society assigns to them and the information needs are different when considering trees inside or outside the forest. We defined two objectives to address the specificity of TIF and TOF, while placing them in the current research context. The first objective was to develop a method for mapping tree species in pure and mixed stands in European temperate forests using S2 imagery. The second objective was to develop a tool for the automated classification of TOF, with a typology close to that used by managers and administrations.

1.1. Objective 1: mapping tree species in the forest

We can divide our research on forest mapping into two steps: first, the exploration of S2 capacities for forest mapping and tree species classification through a simple workflow (chapter 2). Second, the development of an operational method for mapping tree species over extended areas in European temperate forests (chapter 3).

1.1.1. Exploring the Sentinel-2 opportunity

In the exploratory study (chapter 2 section 2), the tree species analysis only considered the classification of pure pixels extracted from pure forest stands for a selected species. It did not attempt to deal with the problem of mixed forest stands, nor to evaluate the behaviour of a pure-pixel classifier in mixed forest stands. We tested the feasibility of a self-sufficient tree species mapping using S2, without using a pre-existing forest map. To achieve this, we trained two separate models. The first aimed at mapping forest areas, the second at classifying the main tree species of the study area. We used Random Forest for both models.

We selected two cloud-free S2 images covering the entire study area, the Ardenne ecoregion of Belgium (chapter 2 section 2, Figure 1): 2 August 2015 and 8 May 2016. We then generated a series of spectral indexes for each of them (chapter 2 section 2, Table 2). A specificity of this study was the time gap between the first S2 image and the second one. Change classes (recent clear-cuts (RCC) and young needle-leaved stands (YN)) allowed to account for forest cover loss during this period. Classes of the "forest map" model were: broad-leaved stands, needle-leaved stands, RCC and non-forest areas. Classes of the "tree species" model were: beech, birch (Betula sp.), oak, broadleaved stands (OB), Douglas fir, larch, Scots pine (Pinus sylvestris L.), spruce, YN, other needle-leaved stands (ON) and RCC.

Before training the models, we performed a variable selection using the VSURF R package (Genuer et al., 2016). The full process was performed a first time using only S2 data: $(2 \times (10_{bands} + 34_{indexes}) = 88_{variables})$. We ran it a second time after adding four 3D variables: 3 CHMs (data acquisition dates were 2006-2007, 2009-2010 and

2012-2014 respectively) and 1 SLOPE layer. The aim was to improve the detection of RCC and young stands. To create the training dataset, we extracted pixels covered by forest parcel polygons that were considered as pure stands (proportion > 0.8) (chapter 2 section 2, Table 3). We validated the forest map (generated by the first model) with an independent systematic point grid (1 km x 1 km, n = 5,744 points) generated by visual interpretation. For the tree species classification (second model), we randomly selected 10% of the reference pixels for validation.

The accuracy achieved highlighted the high potential of S2 imagery for mapping tree species within the forest. Indeed, the overall accuracy (OA) of the forest map model was 0.92 using only S2 data. Still using S2 only, the tree species classification achieved an OA of 0.89 with a mean user's accuracy (UA) also of 0.89. The use of 3D variables slightly improved accuracy (chapter 2 section 2, Tables 4 and 6). The results showed that CHMs were not essential variables to achieve the objectives of this study at this spatial resolution (10m). However, CHMs were selected as first variables in both models and improved the detection of RCC as expected. The very encouraging results of this classification test demonstrated the feasibility of mapping tree species in European temperate forests using S2 imagery.

The process of variable selection allowed for an interesting discussion. Regarding the S2 bands, we highlighted the importance of the red-edge (B5) and SWIR (B11, B12) bands for tree species classification (chapter 2 section 2, Figure 3). The net dominance of the selected variables at 20 m spatial resolution confirmed the theoretical properties of the S2 bands (chapter 2 section 2, Table 1). However, it also showed that the 10m S2 bands are not the most relevant for this application. For the tree species classification, the interpretation step of VSURF selected 95% of the variables involving a 20m band. We then considered 20 m as the true limiting spatial resolution for further studies. Although two images were not enough for a proper time series study, we observed an equal distribution of variables selected from the first and second S2 images. This equal use illustrated the complementarity of data in the classification process and suggested a potential for S2 time series in tree species classification. Finally, an interesting observation was the variable selected as the most important for the "tree species" model: SLOPE. This variable was the only environmental parameter in the dataset. Its selection reflected a strong relationship between slope and the presence of one or several tree species, highlighting the potential of environmental or contextual variables for species mapping.

This study (chapter 2) investigated a simplified per-pixel classification based on a limited number of "pure" forest parcels for training. Very encouraging results confirmed the capacity of S2 to separate frequent Belgian tree species based on their spectral signature. Our conclusions prepared us to go beyond the testing step. Based on our findings, we then worked on the design of a tree species mapping method adapted to an extended area deployment using S2 data.

1.1.2. From per-pixel classification to tree species proportion mapping

The second study (chapter 3) addressed the challenge of up-scaling tree species mapping using satellite imagery. Achieving this required mapping all types of forest composition, from pure stands to highly mixed stands, and building a representative training dataset well distributed over the study area. We used spectral-spatial deep learning to develop a model that predicts tree species proportions instead of mapping classes individually (chapter 3 section 2, Figure 2). This made it possible to map tree species in mixed stands, where the pixel size of images is too coarse to delineate trees. Our model was also able to use proportion vectors for training. As georeferenced areas with tree species proportions are a common type of forest inventory, this allowed a highly representative training dataset to be built.

We used a CNN (UNet++) to predict, pixel by pixel, a vector of tree species proportions (sum equal to 1) considering the surrounding environment. The predictor images were surface reflectance syntheses generated considering the vegetation period from 15 May to 15 September 2018. We super-resolved the ten S2 bands at 2.5 m as described in Latte and Lejeune (2020). The model was trained using a map of forest parcel polygons extracted from the geodatabase of the Public Forest Administration of Wallonia (chapter 3 section 2, Figures 2 and 3). Nine species or species groups were considered: Spruce genus, Oak genus, Beech, Douglas fir, Pine genus, Poplar genus, Larch genus, Birch genus and the remaining species (chapter 3 section 2, Table 3). As a result, we successfully produced a map of tree species proportions in the forest of the Walloon Region (Southern Belgium, chapter 3 section 2, Figures 1 and 5).

A parallel achievement of this thesis was the proposal of an evaluation protocol specific to proportions maps (chapter 3 section 2, article section 2.5). In the latter, we divided the evaluation into three parts, each focusing on a specific element: (1) majority class, (2) species composition (presence or absence), and (3) species proportions (proportion values).

We used 4746 plots (chapter 3 section 2, figure 4 and table 3) of the Walloon regional forest inventory (Alderweireld et al., 2015) to evaluate our map. The indicators of our evaluation protocol show that our approach was successful. In terms of species composition, the mean score (MS) value (0.89) and the balance between mean producer's score (MPS) and mean user's score (MUS) (0.72 and 0.83 respectively) confirm that the model correctly predicted species composition in most cases. The best results were observed for Spruce genus, Oak genus, Beech, and Douglas fir. These classes are the most abundant in the study area (chapter 3 section 2, Table 1). They reached producer's accuracy (PA)s and UAs close to or higher than 0.70 (chapter 3 section 2, Table 5). We highlighted that PAs and UAs decreased with the proportion of species (chapter 3 section 2, Figure 6). In spite of this difficulty, Oak genus and Beech achieved high performances with low area proportions. PAs and UAs were higher than 0.70 from the 0.4 proportion. This result showed the ability of our approach to handle mapping in

mixed forest stands.

The majority class assessment was the most comparable analysis to the usual per pixel classification approach. In fact, we predicted the dominant class per pixel, as a classification approach implies. Therefore, the confusion matrix (chapter 3 section 2, Table 4) revealed essential information: how does our model behave in assigning a dominant class, as most previous studies did. With the difference that the evaluation occurred regardless of whether the forest stand in question was pure or mixed. The indicator overall accuracy of majority class assessment (OA_{maj}) had a value of 0.73. This shows that in most cases the predictions for the study area were reliable. We observed higher producer's accuracy of majority class assessment (PA_{maj}) and user's accuracy of majority class assessment (UA_{maj}) (chapter 3 section 2, table 4) for the most common classes (spruce, oak, beech and Douglas fir). The accuracies achieved were high for the most common species, demonstrating the potential of a tree species proportion model for predicting the dominant species. Compared to "pure" pixel classification in two recent tree species classification studies conducted in Germany (Hemmerling et al., 2021; Welle et al., 2022), the accuracies achieved in our majority class assessment were similar or lower, depending on the tree species class. This result was expected, as we assumed that it would be more difficult to identify the dominant species in a mixed stand than in a pure stand.

Finally, the model's ability to predict proportions (R^2_{adj} 0.50, RMSE 0.19) would ideally be improved. However, this was limited by the nature of the forest parcel polygons used for training. Their proportion values are estimated for large areas (chapter 3 section 2, Figure 3). The values are then approximated and may be locally inaccurate. In this study, the accuracy achieved was satisfactory and proves that deep learning is able to exploit forest parcel polygons (e.g. from a forest management plan) to predict tree species composition over extended areas. For comparison, Gudex-Cross et al. (2017) realised a study on spectral unmixing of multitemporal Landsat imagery and calculated the basal area percentage of ten tree species classes. They achieved comparable R^2_{adj} from 0.24 to 0.59 depending on the tree species.

We used the super-resolved S2 images (Latte & Lejeune, 2020) as a predictor variable for the design of our model. This increase in spatial resolution (from 10-20 m to 2.5 m) improved the delineation of forest patches on the predicted map. However, it did not improve our accuracy metrics when compared to a version of the CNN model trained without using super-resolution S2 imagery. This was partly expected, as in both cases the training data was extracted using stand level information (forest plot polygons). Furthermore, 2.5 m is not yet fine enough to solve the problem of mixed pixels in mixed forest stands.

We have developed a method that can use satellite imagery to map tree species in all types of species composition, from pure to highly mixed forest stands. The latter works even when the spatial resolution of the image is too coarse to distinguish individual

trees. Furthermore, this approach allows for the valorisation of forest inventory data available in the form of tree species proportions. Thus, we propose an efficient method adapted to forest characterisation over extended areas using current satellite imagery and data. In terms of the accuracies achieved, we have demonstrated that the high versatility of deep learning is advantageous for remote sensing mapping.

1.2. Objective 2: automated classification of trees outside of the forest

We developed a tool to map TOF and classify them into groups defined on the basis of European agri-environmental measures (chapter 4). The idea was to use remote sensing and map TOF with a typology close to that used by managers and administrations. The classes were: Isolated tree, Aligned trees, Agglomerated trees, Hedge, Grove, Shrub and Other (chapter 4 section 2, Figure 3).

First, we developed a workflow to separate TOF from TIF starting from a vegetation mask (chapter 4 section 2, Figure 2). Second, we developed an algorithm to classify TOF in two steps: (1) the geometrical classification; (2) the spatial neighbouring analysis (chapter 4 section 2, Figure 4). The geometrical classification analysed the shape of each individual TOF polygon to classify it as a grove, linear element or patch. The spatial neighbouring analysis iteratively scanned possible spatial combinations of linear elements or patches. The final classes were assigned based on the properties of the potential TOF combinations.

We used the tool in the municipalities of Assesse, Gesves and Ohey (chapter 4 section 2, Figure 8) and randomly selected 10 % of the mapped TOF located within agricultural parcels to assess the accuracy of the automated TOF classification. The validation reference dataset was created by visual interpretation using orthophotos. In this study we focused on the classification process rather than on improving the initial vegetation map. For this reason, the calculation of accuracy indices was carried out twice. First, using the full reference dataset. Second, filtering for errors due to poor tree delineation on the vegetation mask, according to visual interpretation. The "filtered" indicators, which focused only on the behaviour of the classification algorithm, were no longer representative of the true quality of the map.

The first evaluation of the TOF classification showed an OA of 0.78. This high value proved the efficiency of an automated method for TOF inventory. When focusing on well delineated TOF polygons, the OA increased to 0.93. This showed that the TOF classification method performed as expected (chapter 4 section 2, Table 5). The study highlighted that our TOF classification algorithm is operational and its performance depends on the quality of the vegetation mask used as input. The aligned trees class was particularly sensitive to errors. Its PA (including all reference data) was 0.35. In fact, if a single tree is not detected within an aligned group, the line is split into two parts that no longer meet the conditions (chapter 4 section 2, Figure 7). The most

sensitive class to commission was shrub. This class had a UA value of 0.58. The large definition of this class made it easy to confuse it with the others (chapter 4 section 2, Table 7). Indeed a small area and no defined shape was the appearance of numerous commissions in the vegetation map (e.g. small urban elements) and poorly delineated TOF.

The performance of our algorithm depends on the quality of the input vegetation mask. In particular, the differentiation of TOF classes is based on shape and spatial criteria. An automated classification of TOF into elements corresponding to the definitions used in field inventories in rural landscapes is possible with high accuracy. This highlights the potential of remote sensing to support TOF management.

2. Further discussion

2.1. The limits of dominant species mapping

Performing studies under ideal conditions was an informative first step in exploring S2 imagery for forest mapping. However, it is appropriate to test the approach at its limits in a second step. In this sense, there is a lack of studies that evaluate the performance of their mapping workflow outside of their ideal training areas. Studies that developed a pixel-based classification model to detect the dominant species did not evaluate the behaviour of such a model in mixed forest. Assumptions for such an approach should be presented and evaluated. Indeed, the concept of dominant species per 10m or 20m pixel can be confusing. First of all, what is the expected class assignment for a mixed pixel? However, assessing accuracy in mixed forest stands is a challenge in itself, as the availability of sub-pixel reference data to make an assessment is generally very low.

A series of studies on tree species classification (Axelsson et al., 2021; Bjerreskov et al., 2021; Grabska et al., 2019, 2020; Hoscilo & Lewandowska, 2019; Immitzer et al., 2019; Persson et al., 2018; Wessel et al., 2018; Xi et al., 2021; Zagajewski et al., 2021) followed our first publication (Bolyn et al., 2018). They based their reference database for model training and validation on pure forest stands. They confirmed the great potential of S2 for tree species mapping. The study of Grabska et al. (2020) allows a good comparison, as it was carried out on a large area in the Polish Carpathians (about 20,000 km^2) for 8 tree species classes in common with our study, and with a high level of detail regarding the method and their map evaluation protocol. Using S2 imagery and some environmental variables, they achieved an OA of 0.87 and high area-adjusted PAs and UAs for most of their classes.

In these studies, one option for assessing the behaviour of pure pixel classification in mixed stands would have been to assess whether the proportions of classes in the predicted pixels were correct at the forest stand level. However, this would still require stand delineation, adding complexity and potentially leading to arbitrary decisions.

Alternatively, if the number of classes to be mapped is limited, it is possible in the model design to add defined mixed classes that retain a thematic sense. For example, the first model presented in chapter 2 had only two forest classes: deciduous and coniferous. It would have been appropriate to include a mixed forest class. However, this was not relevant in this study as the forest classes were merged into a single class in post-processing.

The dominant species model provides partial information and leads to a dead end at some level. In addition, a strength of the satellite data method is its up-scalability: a case study based on an ideal data set and in a relatively small area loses its significance because it is condemned to remain at that scale. That is why we have adopted a pragmatic approach, adapted to the current context of forest research. Instead of fitting data to state-of-the-art models, we designed a model that fits the data. This had three consequences: first, there was no need to modify or filter the training data; second, the model was applicable everywhere; third, we were able to make a real evaluation of the map. The recent studies on tree species classification proved the discriminative power of S2. The next step was to develop a pragmatic and operational method for tree species mapping over extended areas.

2.2. *Predicting tree species proportions using a CNN*

To deal with the issue of mixed forest stands, we trained a CNN (UNet++) to predict, pixel by pixel, a vector of tree species proportions (sum equal to 1), taking into account the surrounding environment. To predict a vector whose sum is 1, we modified the UNet++ architecture by using Softmax as the final activation function. "Softmax is an activation function that scales numbers/logits into probabilities. The output of a Softmax is a vector (say v) with probabilities of each possible outcome. The probabilities in vector v sums to one for all possible outcomes or classes." (Elijah Koech, 2023). Its mathematical expression applies the standard exponential function to each element and normalises the calculated values (Equation 5.1).

$$S(y)_i = \frac{exp(y_i)}{\sum_{j=1}^{n} exp(y_j)} \qquad (5.1)$$

Where y is an input vector to the function S, of n elements for n classes, and y_i denotes the ith element of the input vector.

"The softmax function is often used to normalize the output of a network to a probability distribution over predicted output classes" (Wikipedia, 2023). To train the model, we used the pseudo-Huber loss function (chapter 3 section 2, Equation 2) by calculating, for the 9 classes, the residual values of a pixel as the difference between the true proportions (according to forest parcels polygons) and the predicted proportions. Therefore, the target variable in our study was a vector of proportions rather than probabilities.

The proposed workflow raised important considerations regarding the different scales of forest perception involved in the prediction process and map evaluation. The map prediction was realised by pixels of 2.5 m. There were 3 other working scales involved in the method: the forest parcel, the CNN convolution windows in a patch and the assessment plot. The target variable, i.e. the proportion values used in model training, was provided by the polygons of the forest parcels (chapter 3 section 2, Figures 2 and 3). The size of these management units varies and can be several hectares. The CNN patches were 1000 m side by side (400 × 400 pixels). We used the U-shaped UNet++ architecture, which consists of 4 encoder (downsampling) blocks and 4 decoder (upsampling) blocks (Ronneberger et al., 2015; Zhou et al., 2018). Each block consists of two 3×3 convolutions followed by a 2×2 pooling (with stride 2). In our study, this means that the convolution covering the largest area, between the encoder and decoder network, was a window of 120 m side (3× 40 m), covering an area of 1.4 ha. Finally, we used inventory plots to evaluate the generated tree species proportions map. The plot diameter was 36 m (Figure 5.1).

This model workflow can be summarised as follows: the forest parcel information was used in a CNN to learn the prediction of tree species proportions per pixel (2.5 m). We can assume that the pixel prediction was based on the environment in a window of 120×120 m. This window was large enough to extract forest stand features. We then expected the model to predict the proportions of tree species for an area identified as a stand. However, we performed the evaluation of the predicted map at the plot level (36 m diameter). Therefore, we evaluated the map at a fine scale and assessed the extent to which the CNN model learned to predict tree species proportions locally. The tree species proportions used for model training and map validation were calculated from the basal areas of the dominant and understory trees. The assumption of our study, tested by the map evaluation, was therefore that the model would learn the relationship between canopy proportions (tree crowns seen from the sky) and basal area proportions, as well as the variation of this relationship between tree species. As this relationship can be complex, this was probably a learning limitation of our model.

Another solution to the problem of mixed forest stands could have been an object-based approach. Indeed, metrics computed by object could potentially describe the properties of mixed forest stands and allow classification of forest types and, eventually, prediction of tree species proportions. This could allow more control over model behaviour. However, it requires expertise to set up a segmentation algorithm with a number of assumptions (on object size, homogeneity criteria, etc.). Once the segmentation is done, how to choose the pixel aggregation indices to best capture the object properties in relation to the model prediction goal? Also, since image segmentation tends to group pixels into homogeneous objects, this approach might be more suitable for classification into defined forest types than for predicting tree species proportions. Another issue would be the spatial correspondence between the segmentation and the reference data used to train a model. To ensure that objects are fully covered by refer-
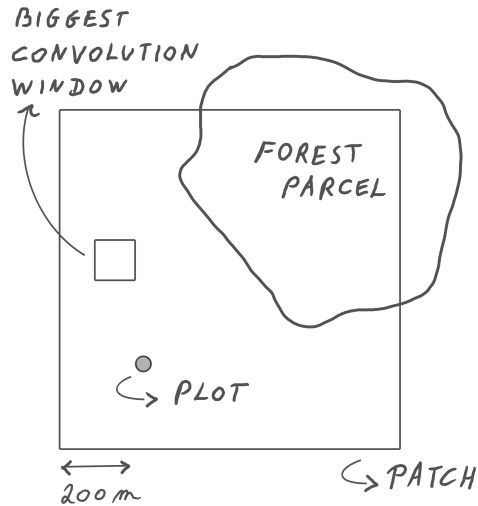
Figure 5.1: Illustration of the CNN patch size in relation to the three scales of forest perception involved in the method presented in chapter 3: the forest parcel, the CNN convolution windows and the assessment plot. The drawings are freehand but respect the orders of magnitude.

ence areas, one solution could be to segment small objects, but at the risk of missing the desired forest stand information. In our view, one advantage of our approach was to include segmentation in the model design. Using a CNN, a deep learning model for segmentation, allowed both spatial and spectral information to be used in learning to map tree species. In this way, we avoided pre-processing assumptions and fully exploited our reference dataset for segmentation and proportions prediction.

2.3. The benefits of deep learning

In the current context, the use of deep learning still requires the training of specific skills. There are a number of technical aspects to be understood when coding an architecture. However, the range of possibilities offered by deep learning tools provides freedom in modelling.

In the context of our mapping research, a deep learning approach offers key advantages. First, the model can learn complex spectral and spatial relationships from reference observations. Second, we have control over what the input and output of the designed model are; this was crucial in the design of the tree species proportion model, which was trained using forest parcel polygons. Finally, it is possible to adapt the loss function, which drives the learning, to the needs of the study.

At the same time, by using a deep learning model, we lose control over the exact

behaviour of the predictor variables. For example, the way in which the spatial component is used in the prediction of our tree species proportions map remains unclear. Based on the forest parcels polygons used in training, the model probably learned to identify pixels belonging to the same forest stand. It may also have learned some patterns of frequent proximity of forest stand types. However, we can only try to answer these questions by observing the final prediction.

Then, the use of deep learning may not be appropriate for simple tasks, as it may be pointless to simply improve accuracy in applications where machine learning models are already successful. If we do not consider performance, the real benefit is to add new components in modelling to go further in the use of predictive variable interaction and to develop operational tools for the end user. In the mapping application, the use of the spatial dimension is of course crucial.

2.4. Interest in supplementing spectral imagery with other sources

Our first tree species mapping study (chapter 2) used CHMs and slope in the design of a predictive model. Both CHMs and slope played an important role in classification. There was no doubt that CHMs are an asset for vegetation mapping and change detection. Similarly, an environmental variable such as slope is relevant to analyse the distribution of a species in the landscape.

Although slope, and more broadly any environmental variable, is related to the presence of a tree species, landscape management plays too important a role in this relationship. It is therefore dangerous to use such a predictive variable for mapping. It introduces a bias, especially if a selective and relatively small training dataset is used, which may not be representative enough of the training area to avoid side effects. It also reduces the reproducibility of the method, as management traditions vary from one region to another. As the accuracies obtained were very satisfactory (chapters 2 and 3) using only spectral information, we discourage the addition of environmental variables in a machine or deep learning model aimed at generating forest maps in European temperate forests. Indeed, we consider that the "black box" nature of machine learning is not compatible with the potential side effects of such variables. Their use would be more appropriate for well controlled post-processing of the map or for enriching it with new information.

The study presented in chapter 2 used two S2 images separated by one year. This time interval implied the addition of change classes to the mapping. The height information provided by the CHMs is related to the age of the forest stand and helped in mapping clear-cuts, even if the CHMs were earlier than the satellite imagery. However, the ideal dataset would also include CHMs acquired at the same time as the spectral images. In chapter 2, the LiDAR dataset was not used to its full potential. In fact, it is possible to generate many metrics from 3D point clouds and CHM rasters that provide a rich description of forest structure. Such indices are an asset for tree species discrim-

ination. Using only CHMs (whether LiDAR or photogrammetric) when mixing 3D and spectral data underexploits their complementarity. However, the development of an all-in-one model with many variables reduces the reproducibility of studies, as the availability of LiDAR or photogrammetric datasets is specific to a region. On the other hand, developing simple tools based on free data such as S2 increases the chances of up-scaling a method. Therefore, for forest mapping, we recommend either to exploit the full potential of LiDAR/photogrammetry in combination with satellite imagery, or to divide the research effort into two tasks: (1) using 3D data (where available) to map forest areas and clearcuts at very high spatial resolution; (2) using satellite imagery such as S2 to map tree species.

2.5. The challenges of land-use mapping

The mapping of trees outside the forest was entirely concerned with land use classes in this thesis. The first step in our research was to clearly define the target classes of the TOF map under development. Separating land use classes using simple geometric rules quickly became a challenge when looking at the result and listening to the comments of the project partners. Field visits showed how many parameters people take into account and how much they use exceptions when assigning a class. For example, is a hedge that widens a lot over a section still a single element, or a grove that crosses two hedges? This is a matter of judgement. However, it did highlight that there is a common understanding of trees as a landscape structuring element, but an exhaustive and exclusive typology is lacking for the development of a mapping tool.

Therefore, improving the TOF mapping tool in the future will first require improving our TOF typology. Indeed, automated classification has achieved high performance (chapter 4). If the future development of this mapping tool is perfectly adapted to user needs, it will be a great success.

3. Perspectives

3.1. Objective 1: mapping tree species in the forest

3.1.1. Analysis of the spectral signature of tree species classes

Our two studies on tree species mapping showed limitations in the interpretation of accuracy indicators. In the first study (chapter 2), the results were rather optimistic because the pixels used in training and validation were extracted from the same polygon dataset. In the second study (chapter 3), we assessed the accuracy of the tree species map using an independent dataset, the assessment was robust and representative of the study area. However, in terms of species composition, the assessment did not allow the distinction between errors due to the model and those due to the limit of discriminative power of S2. In other words, the confusion between some tree species

and the prediction of a mixed forest composition could coexist in the behaviour of the model. In particular, the indicators showed a lower accuracy to detect the presence of birch and poplar classes, even in "pure" stands (proportion higher than 0.8, chapter 3 section 2, Figure 6). Neither of our studies included a direct analysis of the spectral signature of the tree species classes considered. Such an analysis has the potential to better interpret the separability of classes based on pixel spectral values alone. Before attempting to improve our species mapping model, a better understanding of the predictor data is beneficial to identify and address limitations of the current method. Both studies used the same source (forest parcel polygons extracted from the Forest Administration's geodatabase, Department of Nature and Forests, Public Service of Wallonia, 2017) to create a reference dataset and build their model. Based on the sample of reference polygons used in chapter 3, spectral curves of "pure "tree species classes could be analysed for pixels falling in polygons with a proportion higher than 0.8. From another perspective, we could average the spectral values per polygon and perform the same analysis at the forest parcel level. This would also allow us to use all forest parcels with a tree species class proportion higher than 0.6 and then analyse the separability of the majority class (chapter 3 section 2, Table 4) based on the S2 spectral signal.

3.1.2. Exploiting the time dimension

Exploring how the temporal dimension could help to discriminate tree species using multispectral imagery is obviously an interesting research topic. Recent studies have highlighted the role of time series in tree species classification (Hemmerling et al., 2021; Xi et al., 2021). Going beyond the study presented in chapter 3, adding the time dimension to the spectral and spatial dimensions intuitively provides a huge amount of information. Each patch used in the deep learning process would contain values in four dimensions: latitude, longitude, time and S2 band. This creates a very high discrimination potential that could improve the separation of tree species classes by phenology.

However, there are challenges to developing such a method. Firstly, pixels in an extended study area would not be covered by the same S2 satellite time series due to the acquisition frame. This raises the issue of image normalisation. Secondly, in European temperate forests, the number of occurrences of a time series corrupted by cloud cover or shadow can be very high. These two obstacles need to be taken into account for the development of a scalable and reproducible method in the continuation of our work. One possibility is to resample image tracks on the same time grid (Inglada et al., 2015, 2017). Each time value of a pixel is calculated by linear interpolation of the cloud-free time series. This method modifies the original data and may introduce noise. Nevertheless, our present method also generated a synthesis image using all S2 tracks of the vegetation period. The alternative presented here interpolates missing values instead of aggregating the available ones. Such a dataset has the potential to

test the concept of a spectral-spatial-temporal deep learning model.

3.1.3. Improving the model training dataset

In the study presented in chapter 3, the reference dataset used for training consisted of forest parcel polygons extracted from the forest administration's geodatabase (Department of Nature and Forests, Public Service of Wallonia, 2017). As a consequence, the observations came only from public forests. Firstly, it would be interesting to assess whether the mapping models behave differently in private forests. Secondly, we should enrich the current dataset with observations located in private forests. As we have developed a method using polygons with tree species proportions, the task of collecting new data is easier than in the past. In fact, using plots from a management plan would only require some digitisation work.

Less common species classes achieved lower accuracies in the final map. As suggested above, the addition of a temporal dimension could help to improve discrimination. However, the lack of representation of some species may be the cause. In this case, we should increase their representation when improving the reference dataset.

The method presented in chapter 3 can work for other study areas. As deep learning takes advantage of many observations, it is beneficial to create a reference dataset that covers a larger region. Building a common training dataset for tree species mapping could help research in this area and lead to the production of valuable maps across countries. Our method is based on forest parcels polygons. As long as a geodatabase of public forests exists, several regions or countries could join efforts to develop better tree species maps. In this idea, the creation of a win-win partnership between the respective universities, administrations and stakeholders remains an issue, in addition to a legal context that is not always favourable to public data sharing. In addition, extending the study area too much can also add complexity to the design of a model. For the same tree species, there may be differences in phenology from one region to another, variety and phenotype may differ, and forest context characteristics may change significantly. Therefore, representative datasets should be collected by region to compensate for their specificities. Also, the development of a model by natural area versus a single large area should both be tested to determine which is the best option.

Another approach to enriching the reference dataset is crowdsourcing. As an example, See et al. (2015) used crowdsourced validation data from Geo-Wiki in the conception of an hybrid global land cover map. During the development of a first version of the tree species map (see appendix A.2), we set up a website where partners in this research project could draw polygons on a map. In addition to satellite RGB imagery and orthophotos, we added the latest version of the tree species map. The idea was to allow iterative improvement of the model as stakeholders drew plots where they knew the model was wrong. During this thesis, this approach was implemented in too short a time and the web application was sent to too small a group. In addition, people were instructed to draw pure forest stands because the mapping method was then based on

pure pixels. This limited the ability to share expertise, but is now solved by a model trained on tree species proportions. With a view to building a tree species dataset over a large area, such a platform could be maintained to centralise non-official data (from project partners, forest owners, students, etc.). However, it will only be useful if it is maintained and managed over time and disseminated frequently to the appropriate people.

3.1.4. Potential uses of the tree species proportion map

The raster of tree species proportions can itself be used as input in scientific applications. However, a tree species proportion map raises questions about estimating area based on predictions. Indeed, using the pixel counting approach would mean counting pixels of a class and weighting them by their proportion. Due to the accuracy of the predicted proportions, this approach would be biased. Furthermore, the bias in the area estimation induced by the spatial resolution itself (Waldner & Defourny, 2017) is not negligible in our approach because we have kept a coarse resolution, qualified as L-resolution by Strahler et al. (1986). Therefore, a better approach would be to estimate the area using the reference classification, in other words a sample-based area estimation, where the role of the map is to reduce the standard errors of the area estimates (Olofsson et al., 2013; Stehman & Foody, 2019). This would require first creating a thematic map by applying threshold rules to the proportions of tree species that define the desired forest types.

In addition to using the raw proportions map, foresters could apply any new typology based on thresholds of tree species proportions that define forest types (such as those defined in national forest inventories). The new map generated would be more readable and the derived area estimates could be comparable to those based on inventories (if the appropriate typology is used). This approach can be applied to any field. For example, an ecologist might be interested in establishing a typology to target habitats associated with the presence of certain tree species and then produce a map of forest habitats.

Another option is to aggregate the map information before using it (average of the proportions in a given area). Considering our two previous examples, foresters could aggregate the proportions according to their own forest management parcels. In the field of ecology, the LifeWatch Wallonia-Brussels project proposes an interesting database describing homogeneous landscape units with percentages of land use and a combination of topographic, contextual, climatic and ecosystem dynamics variables ("LifeWatch-WB ecotope database | Lifewatch regional portal", 2023). enriching such a map describing potential habitats with tree species proportions would be an interesting valorisation.

3.2. Objective 2: automated classification of trees outside of the forest

3.2.1. Scalability of the tool

The current version of the TOF mapping and classification algorithm is still a prototype. It has been developed on samples of LiDAR acquisitions. So far, the tool has been used on request to produce output at the scale of a municipality. This processing already represents gigabytes of 3D point clouds and generates a geodatabase of thousands of TOF polygons. The tool will reach its full potential when applied to an extended area. A first target for its deployment is the Walloon region (southern Belgium), which was completely covered by an ALS acquisition in 2013-2014. In addition, a second flight in 2021-2022 has been realised and is available on the geoportal of Wallonia. Upscaling of the approach would be feasible with a few modifications. However, an optimisation of the algorithm may be necessary to improve processing time and memory management.

Once stabilised for use over extended areas, the functions of the TOF mapping method should be compiled into an R package (algorithms have been written in R language with dependencies on the sf and lidR packages). This, together with transparent documentation, will facilitate the use, dissemination and improvement of the tool. Ideally, we would make a stable version of this package available to the community on the Comprehensive R Archive Network (CRAN, R repository) and on a developer platform. In addition to the associated peer-reviewed article (chapter 4 section 2), this would greatly increase the use of the method and consequently the feedback.

3.2.2. Method improvement

Unlike the method described in chapter 4, the latest version of the TOF mapping tool no longer uses an NDVI index to separate buildings from vegetation. This part of the process now works directly on 3D point clouds by filtering points with coplanarity or colinearity. Alternatively, the internal classification of the LiDAR dataset can be used if it is available with sufficient quality. CHM generation has been implemented, giving the freedom to generate the most appropriate CHM and allowing better adaptation to the specificities of ALS acquisitions. We preferred to use the pit-free algorithm from Khosravipour et al. (2014) as it provides a clever way to fill pits in the canopy without aggregating pixels. Using a single data source avoids time gaps and registration problems between data sources. While limiting the number of inputs creates a strong and simple tool, orthoimages and CHMs are more common datasets and require less expertise from potential users of the tool. Therefore, to increase its applicability, it may be beneficial to maintain and improve a version of the TOF classification tool based on these data sources. In the same spirit, users should be able to use their own created TOF mask and process only the TOF classification functions.

It would be relevant to try to improve or replace some of the processing steps that

separate TOF from TIF by using the functionalities of Morphological Spatial Pattern Analysis (MSPA) (Soille & Vogt, 2022; Soille & Vogt, 2009)), an image processing software implemented in the free software GTB (GuidosToolbox). Based on geometric concepts, this application divides the foreground area (in our case the vegetation) of a binary image into seven classes: Core, Island, Perforation, Edge, Loop, Bridge and Branch. This classification provides rich information about the landscape that could help in several steps of our workflow. In particular, our method struggled to distinguish between TOF and TIF in some contexts (e.g. fragmented forest and forest edges). Improving this part of the workflow would then be beneficial.

3.2.3. Going further in the characterisation

The developments presented in chapter 4 used ALS acquisition with an average point density of 2 pulses/m^2. Today, for comparable acquisition costs, the density of 3D point clouds is better. The latest ALS dataset in Wallonia (Southern Belgium) has a density of 10 points/m^2. This represents the first perspective of improvement for this TOF mapping application: an expected improvement in the delineation of TOF, especially smaller ones.

In terms of classification algorithms, the class of agglomerated trees could be further subdivided. Further research should focus on the development of algorithms able to detect plantations and orchards within this group. Indeed, these two landscape elements deserve special attention compared to random groups of trees, as they are part of the agricultural system or forest management. It would also be interesting to add a contextual step at the end of the workflow. This would look for the proximity of rivers, roads, lakes, etc. in order to go deeper into the characterisation of the TOF features.

While the method is based on an ALS dataset whose acquisitions are punctual, CHMs can also be generated by photogrammetry (Michez et al., 2020) which has a much better return time in European countries. This makes it possible to analyse the TOF resource as a function of time. In Belgium, the Public Service of Wallonia plans to acquire orthophotos every year from 2015. Therefore, we could look for TOF disparitions with a 1-year step in this study area. A simple example of disparition analysis is presented in the appendix A.1.

Apart from the classification of TOF types, the identification of TOF species is a challenging but relevant research topic. Spectral metrics based on S2 images by TOF element could be used as predictor variables to predict the species. In this task, the design of a reference dataset will be the first obstacle outside the forest, as species are even less inventoried for TOF. ALS data was the initial input for our TOF mapping method. In terms of species mapping, a more complete approach could actually include TIF. We would then map all trees in the study area, TOF and TIF, using ALS data and produce a comprehensive tree map. In such a unified approach, we would perform LiDAR-based tree segmentation within forest areas. Tree species mapping within the forest would then be performed using object-based classification by tree.

The tree species model trained in the forest, where more data is currently available for training, could then be tested on TOF to predict species in addition to the type of TOF classification presented in this thesis.

4. Research in the field of remote sensing oriented towards concrete applications

In this thesis we have worked on the use of remote sensing for the development of operational tools for tree monitoring. This is in contrast to another part of remote sensing research, which focuses on the analysis of remote sensor signals and their relationship with the physical properties of the objects being sensed. Our research was also not primarily focused on improving or developing new algorithms for processing remote sensing data. Instead, we have developed methods to take the best of existing algorithms and remote sensing datasets to provide operational tools.

In such an approach, the research objectives are guided by the identification of needs and confronted with the characteristics of the available datasets in the study area. The aim then becomes how to take the best of existing technologies and find a solution to their limitations in order to deliver a high quality map to the end user. This final map product must be evaluated with consistency. This last requirement may be difficult to achieve in some contexts. However, a map without accuracy assessment (in addition to model performance) loses its meaning and usefulness. We encourage remote sensing research related to concrete applications, as it stimulates innovation where it is needed in a research area that is by nature applied. Finally, the sharing of algorithm codes and reference datasets, where possible, is a plus for transparency. It also has the potential to accelerate progress in this research area, where artificial intelligence is playing an increasingly important role.

A

Related popularized publications

1. Mapping and characterization of trees outside of the forest using LiDAR technology

This article presents for two Belgian municipalities the implementation of the method detailed in chapter 4. It also proposes complementary analysis that can be derived from the generated TOF map.

Bolyn, C., Latte, N., Fourbisseur, A., Colson, V., Baudry, O., & Lejeune, P. (2020). Cartographie et caractérisation des arbres hors forêt à l'aide de la technologie LiDAR [Publisher: Forêt Wallonne asbl]. *Forêt.Nature*, *155*. Retrieved January 24, 2021, from https://orbi.uliege.be/handle/2268/250834

FORÊT
•NATURE

Tiré à part du Forêt.Nature n° 155, p. 34-46

CARTOGRAPHIE ET CARACTÉRISATION DES ARBRES HORS FORÊT À L'AIDE DE LA TECHNOLOGIE LIDAR

Corentin Bolyn (GxABT, ULiège)**, Nicolas Latte** (GxABT, ULiège)**, Anne Fourbisseur** (Carah)**,
Vincent Colson** (CAPFP, OEWB)**, Olivier Baudry** (AWAF)**, Philippe Lejeune** (GxABT, ULiège)

Cartographie et caractérisation des arbres hors forêt à l'aide de la technologie LiDAR

Corentin Bolyn[1] | **Nicolas Latte**[1] | **Anne Fourbisseur**[2] | **Vincent Colson**[3] | **Olivier Baudry**[4] | **Philippe Lejeune**[1]

[1] Gembloux Agro-Bio Tech (ULiège)
[2] Carah Asbl
[3] Cellule d'Appui à la Petite Forêt Privée (OEWB)
[4] AWAF asbl

Comment suivre et évaluer des éléments aussi disparates que des haies, arbres isolés, bosquets… dans un paysage ouvert et à large échelle ? C'est tout l'enjeu de cette étude menée par Gembloux Agro-Bio Tech sur base de données LiDAR en Wallonie et en France.

RÉSUMÉ

Il est aujourd'hui admis qu'une part importante de la ressource ligneuse se trouve en dehors de la forêt. Les « arbres hors forêt » ont un rôle important dans notre environnement grâce à leurs multiples fonctions : production de bois, préservation de la biodiversité, qualité paysagère… Bien que l'évolution récente des politiques environnementales tendent à leur donner plus d'importance, ils restent peu étudiés et ne font que rarement l'objet d'un inventaire ou d'un suivi à l'échelle régionale ou nationale. Face au besoin d'outils pour l'évaluation de cette ressource, une méthode de cartographie et de description des éléments arborés situés hors forêt a été développée. Elle repose sur l'utilisation de données LiDAR aérien

Les arbres sont des éléments omniprésents dans notre environnement. La forêt couvre à elle seule 30 % du territoire wallon. Cette ressource ligneuse, dont les enjeux de gestion sont considérables, est relativement bien décrite et connue au travers d'inventaires spécifiques et de nombreuses études.

Depuis quelques décennies, l'idée que la ressource ligneuse ne se concentrait pas uniquement en forêt a fait son chemin, faisant émerger le concept d'arbres hors forêt (encart 1). Les nombreuses fonctions que les éléments arborés remplissent en dehors de la forêt sont de plus en plus reconnues. Globalement, ils produisent du bois apte à différentes valorisations, qu'il s'agisse du bois énergie ou de filières avec davantage de valeur ajoutée. Par leur production de bois, ces éléments ont donc également un impact significatif sur le stockage de carbone. Localement, ils abritent une biodiversité importante et, à l'échelle du paysage, ils représentent des éléments de connectivité (corridors écologiques) pour de nombreuses espèces. Ces éléments arborés protègent également les sols de l'érosion et y stockent du carbone à long-terme, maintiennent la qualité de l'eau et protègent des inondations, du vent et des intempéries. Enfin, ils constituent un élément paysager à valeur socioculturelle, marqueur des territoires et de leur histoire[5]. Tirant profit de ces nombreux avantages, les techniques agroforestières associent des plantations ligneuses à des cultures agricoles aux effets bénéfiques réciproques[3].

L'ensemble des biens et services environnementaux fournis par cette ressource sont essentiels pour la population de nombreux pays. À ce titre, la FAO considère la forêt et les arbres hors forêt comme essentiels pour la sécurité alimentaire mondiale[4].

Les arbres hors forêt sont cependant beaucoup moins étudiés que ceux des forêts et ne font que rarement l'objet d'un inventaire ou d'un suivi à l'échelle régionale ou nationale. Or, l'évolution récente des politiques environnementales tendent à leur donner un rôle de premier plan. À travers les mesures agroenvironnementales, la Commission européenne finance les agriculteurs qui souscrivent, sur une base volontaire, à des engagements liés à la préservation de l'environnement et à l'entretien du paysage. Dans le même temps, la Wallonie octroie des subventions pour la plantation de haies, vergers et alignements d'arbres, reconnaissant leurs fonctions écosystémiques fondamentales. Dans ce contexte, le développement d'outils pour l'évaluation et le suivi de la ressource ligneuse hors forêt prend tout son sens.

Une des activités de recherche du projet Interreg Va France-Wallonie-Vlaanderen ForetProBos avait pour

au travers d'une série d'algorithmes intégrée dans une procédure automatique. Les éléments arborés de plus de 2 mètres de hauteur sont cartographiés avec une résolution de 1 mètre et catégorisés en cinq classes en fonction de leurs dimensions et de leur organisation spatiale. Les utilisations de cette couche cartographique sont nombreuses : calcul de statistiques, analyses spatiales, étude de la dynamique temporelle… À titre d'exemple, nous présentons les résultats obtenus sur trois sites : les communes rurales de Ohey et de Paliseul en Wallonie, et un périmètre regroupant douze communes françaises situées au Nord-Est de Valencienne.

objectif de développer une méthode de cartographie et de description des éléments arborés hors forêts en exploitant des données de télédétection. L'objectif de cet article est de présenter cette méthode et d'illustrer les résultats qu'elle produit pour deux communes rurales wallonne (Ohey et Paliseul) et un périmètre regroupant 12 communes françaises au Nord-Est de Valenciennes.

Comment cartographier les arbres hors forêt ?

La délimitation et la cartographie d'éléments ligneux situés hors forêt (nommés AHF dans la suite de l'article) nécessitent de recourir à des données à très haute résolution spatiale pour délimiter des éléments ligneux qui peuvent être de petite taille et les différencier de leur environnement immédiat constitué de végétation herbacée, de substrats non végétaux ou d'éléments construits par l'homme.

La méthode de cartographie qui a été développée repose exclusivement sur l'utilisation de données de type LiDAR aérien (encart 2). Ces données présentent une résolution spatiale de l'ordre de 1 mètre et fournissent des estimations précises de la hauteur des éléments présents à la surface du sol.

Sur cette base, il a donc été possible de considérer la hauteur minimale comme principal critère de délimitation des éléments ligneux. Celle-ci a été fixée à 2 mètres, pour séparer les AHF de la végétation non ligneuse. Ce choix méthodologique impose d'être capable ensuite de séparer les éléments ligneux des autres objets non végétaux de hauteur supérieure à 2 mètres mais également de séparer les éléments ligneux en et hors forêt.

Une chaîne de traitement automatisée a été développée pour générer une couche décrivant les limites et les caractéristiques des éléments ligneux situés hors forêt au départ du nuage de points LiDAR. De manière synthétique, la méthode qui a été développée se compose de quatre étapes principales.

Étape 1 : identification des points « sol » et normalisation du nuage de points. La première étape vise à identifier les points LiDAR qui correspondent au sol et se baser sur l'altitude de ceux-ci pour définir la hauteur des autres points par rapport au niveau du sol. Cette opération est qualifiée de normalisation du nuage de points. Ces derniers sont désormais caractérisés par des coordonnées (x, y, h), la hauteur h remplaçant l'altitude z.

Étape 2 : identification des points correspondant à des éléments ligneux. Les points dont la hauteur est su-

Encart 1.
Définitions et typologie des éléments ligneux présents dans le paysage

Établir une définition et une classification des arbres hors forêt nécessite avant tout de préciser ce qu'est une forêt. Nous avons considéré la définition de la FAO (organisation des Nations Unies pour l'alimentation et l'agriculture) qui considère les forêts comme étant « des terres occupant une superficie de plus de 0,5 hectare avec des arbres atteignant une hauteur supérieure à 5 mètres et un couvert forestier de plus de 10 %, ou avec des arbres capables d'atteindre ces seuils in situ ». Cette définition englobe les éléments linéaires, comme les brise-vents ou les corridors d'arbres, d'une surface de plus de 0,5 hectare, et d'une largeur de plus de 20 mètres.

Sur base de la superficie, du taux de couverture des cimes (projection des cimes au sol) et de la hauteur des arbres, la FAO divise ainsi le territoire en trois occupations du sol : la forêt, les autres terres boisées et les autres terres. Sur cette base, les arbres hors forêt correspondent aux éléments ligneux du paysage situés dans les autres terres.

Typologie des arbres hors forêt
Certaines mesures agroenvironnementales liées à la Politique Agricole Commune de l'Union européenne concernent les éléments ligneux du paysage. À ce titre, leurs critères d'admissibilité fournissent des définitions précises pour certains éléments ligneux présents en zone agricole[6] :
- Les haies et bandes boisées : tronçon de minimum 10 mètres de long, largeur de moins de 10 mètres. Si alignement d'arbres : diamètre de la couronne supérieur à 4 mètres et espace entre couronnes de moins de 5 mètres.
- Arbre isolé : arbre dont les couronnes sont situées à plus de 5 mètres de tout autre arbre, circonférence de plus de 40 cm à 1,5 mètre de hauteur.
- Buisson et arbuste isolé : 1,5 mètre de hauteur et situé à plus de 5 mètres de tout autre élément.

- Bosquet : superficie de maximum 4 ares composée de plantes ligneuses majoritairement indigènes, soit arbres, buissons ou arbustes et située à plus de 5 mètres de tout autre élément.
- Arbres fruitiers : de haute tige ; pas de notion de taille de couronne ou de distance entre couronnes.

Ces définitions ne couvrent pas l'ensemble des configurations pouvant être rencontrées. Elles ont été adaptées et complétées pour garantir le caractère exhaustif de la cartographie produite. Cette adaptation intègre un critère lié à la source de données utilisée (LiDAR aérien), celui-ci concerne la hauteur retenue pour sélectionner les points du nuage correspondant à des éléments ligneux ; il a été fixé à 2 mètres. La conséquence implicite de ce choix est que seuls les éléments ligneux dépassant cette hauteur sont cartographiés.

Dans les définitions qui sont présentées ci-après transparaissent également des considérations relatives à l'agencement spatial des éléments ligneux. Des visites de terrain ont été réalisées pour valider les critères fixés.

Les différentes classes qui ont été retenues se définissent comme suit :
- Bosquet : élément continu non linéaire dont la surface est supérieure à 400 m².
- Groupes d'arbres : groupe d'éléments ligneux séparés de moins de 10 mètres et non structuré en alignement (vergers par exemple).
- Alignements : alignement de minimum 5 éléments ligneux séparés de moins de 10 mètres.
- Haies : élément linéaire continu avec une longueur minimum de 10 mètres et une largeur maximum de 20 mètres. Le rapport entre la longueur et la largeur est supérieur à 3. Les tronçons de haie distant de moins de 5 mètres constituent la même haie.
- Arbres isolés : élément ligneux constitué d'un seul arbre, situé à plus de 5 mètres de tout autre élément cartographié. La couronne projetée au sol couvre minimum 12,6 m², ce qui correspond à un disque de 4 mètres de diamètre.
- Buisson : élément ligneux isolé, situé à plus de 5 mètres d'un bosquet, d'une haie ou de la forêt, et à plus de 10 mètres d'un autre élément ligneux. Cette classe comprend les buissons, les arbustes et les bosquets dont la surface est inférieure à 400 m².
- Autres : rassemble les éléments de plus de 2 mètres de haut qui ne répondent pas aux critères précédents.

Définition de forêt, autres terres boisées et autres terres
Source : FAO 2001
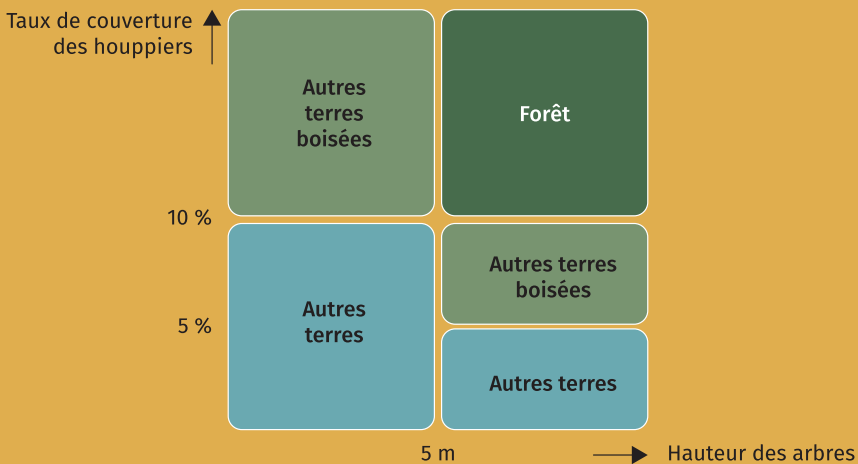
périeure à la valeur seuil de 2 mètres sont analysés. Ces points correspondent à de la végétation ligneuse ou à différents éléments construits par l'homme : bâtiments, ponts, éoliennes, pylônes, câbles électriques, etc. Les caractéristiques géométriques des points relatifs à toutes ces constructions sont exploitées au travers de différents filtres pour conserver uniquement les points correspondant aux surfaces couvertes d'éléments ligneux. Ces points sont ensuite convertis en segments (polygones « shapefile ») regroupant tous les pixels (de 1 x 1 mètre) contenant au moins un point LiDAR classé comme « ligneux ». On dispose à ce stade d'un premier produit cartographique qui représente l'ensemble des surfaces couvertes d'éléments ligneux d'une hauteur supérieure à 2 mètres.

Étape 3 : séparation entre forêt et ligneux hors forêt. La séparation des éléments ligneux forestiers et non forestiers s'opère en considérant la définition générale de la forêt de la FAO, basée sur une surface et une largeur minimales (encart 1). A priori, cette étape peut sembler simple à réaliser mais, en réalité, elle est plus difficile qu'il n'y paraît. En particulier, pour appliquer le seuillage sur la largeur minimale de 20 mètres. Dans un premier temps, les éléments ligneux sont divisés en tout point sur base de la largeur. Pour respecter la continuité des éléments ligneux, il est ensuite nécessaire d'analyser chaque subdivision pour annuler celles dont la taille trop petite n'est pas pertinente, comme un court rétrécissement dans une

bande boisée, un élargissement sur une faible distance dans une haie, ou un élément linéaire de petite longueur en continuité avec la forêt.

Le résultat de cette troisième étape est une couche cartographique présentant l'emprise des éléments ligneux hors forêt (figure 1).

Étape 4 : classification des éléments ligneux situés hors forêt. Cette étape vise à classifier les éléments de la couche produite à l'étape précédente, en considérant leurs caractéristiques en termes de dimension et d'agencement spatial (encart 1). La typologie est mise en œuvre en deux étapes[1]. La première étape considère uniquement les critères de dimension : surface, largeur, longueur et hauteur. Le calcul de la longueur des éléments boisés repose sur un algorithme complexe qui génère un squelette au sein de chaque polygone, sur lequel s'appuient ensuite des sections perpendiculaires permettant de mesurer la largeur. À ce stade du processus, trois catégories sont identifiées : les éléments ligneux de petite taille, les bosquets (surface de plus de 400 m²) et les éléments allongés (longueur minimum de 10 mètres, largeur maximum de 20 mètres, rapport longueur sur largeur supérieur à 3). Un dernier algorithme, mettant en œuvre des critères de proximité termine la séparation des différents éléments pour correspondre à la typologie finale comprenant six catégories présentée dans l'encart 1 (figure 2).

Figure 1. Illustration de la classification des éléments considérés comme en forêt (en vert) et hors forêt (en bleu).

Figure 2. Illustration de l'application de la typologie sur les éléments ligneux de plus de 2 mètres de hauteur.

- Bosquet
- Groupe d'arbres
- Alignement
- Haie
- Arbre isolé
- Buisson

Des analyses complémentaires

La couche cartographique finale peut être utilisée directement (visualisation, gestion, etc.) mais aussi pour réaliser des analyses spatiales complémentaires. Par exemple, des critères de proximité peuvent être définis pour raccrocher les AHF à certains éléments structurant du paysage, comme les voiries ou les cours d'eau. Il est également possible de mesurer le niveau de connectivité entre éléments ligneux, forestiers et non forestiers.

La détection des changements est également intéressante à considérer dans une perspective de gestion durable des AHF à l'échelle du paysage : l'enlèvement ou l'installation d'éléments ligneux devraient pouvoir être cartographiés et quantifiés au cours du temps. Pour assurer correctement ce suivi, il convient de disposer de mise à jour régulière de la couverture LiDAR. Dans le cas de la Wallonie, la prochaine acquisition devrait être disponible d'ici 1 à 2 ans. Dans l'attente de ces données, nous avons considéré une

solution alternative moins précise, mais néanmoins intéressante. Elle consiste à utiliser le Modèle Numérique de Surface (MNS) dérivé du traitement des images aériennes acquises pour la production de la couche ortho-image 2019 disponible sur le Géoportail de Wallonie. Ce MNS, d'une résolution de 50 cm, combiné avec un Modèle Numérique de Terrain, peut être utilisé pour estimer la hauteur des éléments ligneux en 2019 et ainsi déceler ceux dont la hauteur a fortement diminué (c'est-à-dire inférieure à 1 mètre en 2019), traduisant une probable suppression. Considérant la résolution et la précision de ce MNS, cette analyse s'est focalisée sur les éléments dont la hauteur initiale (en 2014) était supérieure à 4 mètres. Pour les mêmes raisons, l'exercice de détection de nouveaux éléments arborés n'a pas été envisagé.

Quelle précision espérer ?

La méthode qui est présentée fonctionne de manière automatique dans la mesure où elle repose exclusivement sur la mise en œuvre d'algorithmes appliqués

Encart 2. **Le LiDAR aérien : une source de données très précieuse et très précise pour cartographier et mesurer les arbres et les forêts**

Le LiDAR (pour Light Detection and Ranging) est un système de télédétection qui produit des représentations de la surface terrestre sous la forme de nuages de points 3D. Lorsque le système est embarqué sur un avion, un hélicoptère ou encore un drone, on parle de LiDAR aérien, par opposition au LiDAR terrestre où le système fonctionne au niveau du sol.

Au cours du vol, l'émetteur génère des impulsions laser à très haute fréquence (supérieure à 100 kHz). Celles-ci balaient le sol ou les éléments présents à sa surface. Les échos renvoyés permettent de calculer la position (x, y, z) des objets qui se situent sur la trajectoire de l'impulsion : branches, houppier, tronc, toits...) et finalement du sol. Les précisions des positions ainsi obtenues sont comprises entre 20 et 30 cm en planimétrie (x et y) et entre 15 et 20 cm pour l'altitude (z).

Les caractéristiques du faisceau laser, ainsi que les paramètres de vol (fréquence, altitude et plan de vol) conditionnent la densité du nuage de points produit. Celle-ci peut varier de moins de un point à plusieurs centaines de points par mètre carré. L'obtention de densités élevées nécessite une vitesse et

une altitude de vol plus faibles imposant le recours à un hélicoptère ou à un drone.

L'application d'un algorithme spécifique permet de traiter le nuage de points et d'identifier les points « sol ». Ceux-ci sont utilisés pour générer un modèle numérique de terrain décrivant le modelé du terrain. Cela permet ensuite de « normaliser » le nuage de points c'est-à-dire de calculer pour chaque point sa hauteur par rapport au niveau du sol.

Le Service Public de Wallonie a réalisé entre 2013 et 2014 une acquisition par LiDAR aérien couvrant l'ensemble du territoire régional. Celle-ci a été réalisée en huit blocs à une densité moyenne légèrement supérieure à deux points par mètre carré, ce qui correspond à une base de données qui comporte un nuage constitué de plus de quarante milliards de points ! Les caractéristiques techniques des vols réalisés sur les différents blocs sont telles que seules les données de cinq blocs couvrant deux tiers de la région sont exploitables pour détecter correctement les arbres hors forêt.

Cette couverture LiDAR régionale a déjà été valorisée dans des applications forestières. C'est notamment
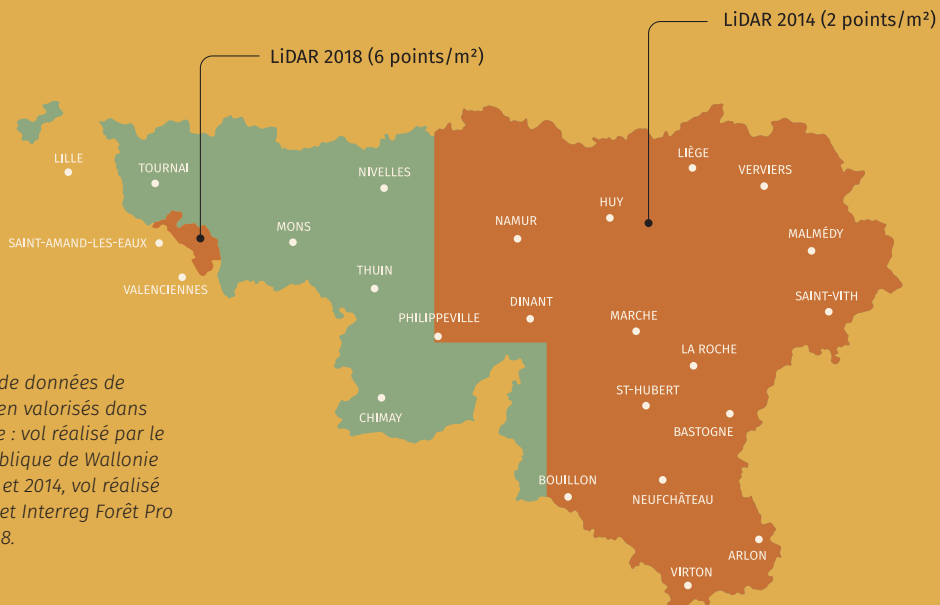
Deux jeux de données de LiDAR aérien valorisés dans cette étude : vol réalisé par le Service Publique de Wallonie entre 2013 et 2014, vol réalisé par le projet Interreg Forêt Pro Bos en 2018.

Acquisition des données par vol LIDAR

le cas dans l'outil Forestimator[2] qui réalise, sans mesure de terrain, des estimations de la hauteur dominante pour des plantations de résineux. Il a été montré que la précision de ces estimations est du même ordre de grandeur que celles basées sur des mesures réalisées sur le terrain.

Par ailleurs, le projet Interreg Forêt Pro Bos a commandé en 2018 un vol LiDAR sur trois sites pilotes situés dans les départements de l'Aisne, de la Marne et du Nord, pour une superficie totale de 434 km². Les nuages de points produits présentent une densité moyenne de six points par mètre carré.
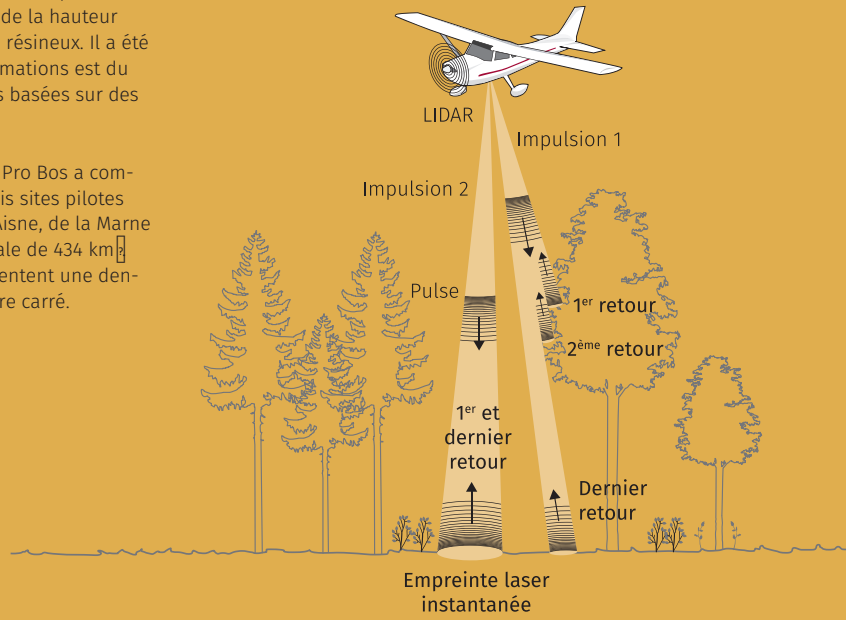
Nuage de points LiDAR aérien classé en trois catégories : le sol (en gris), la végétation (en vert) et les éléments construits par l'homme (en rouge et jaune).
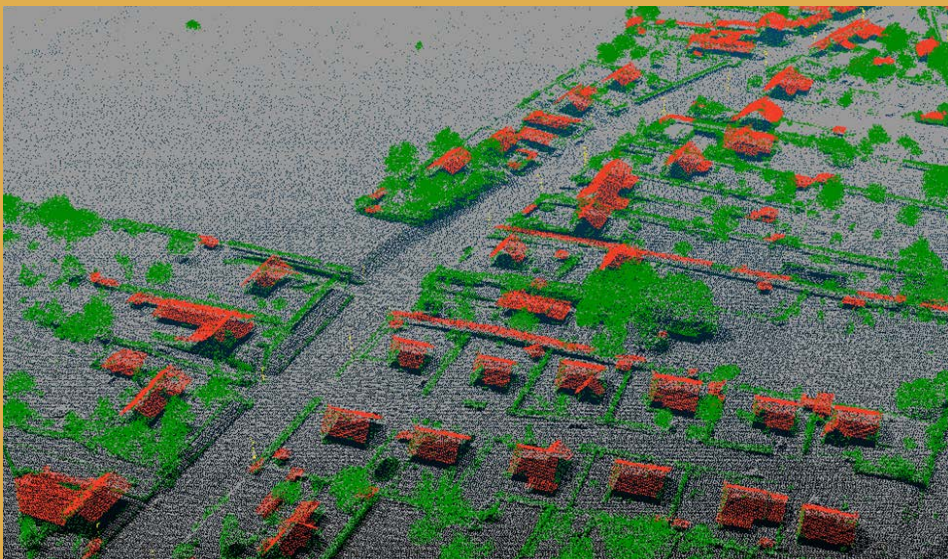
aux données de départ. Comme toute approche automatique, celle-ci n'est pas exempte d'erreurs. Les principales sources d'erreur proviennent de la confusion entre éléments ligneux et non ligneux de plus de 2 mètres de hauteur (principalement des bâtiments), surtout en zone d'habitat. Une seconde source d'erreur est liée aux lignes électriques qui surplombent des éléments ligneux et entraînent une surestimation de la hauteur de ces derniers. En Wallonie, le fait de disposer d'une nouvelle couche LiDAR, avec une densité de points plus élevée devrait permettre de corriger la plupart de ces confusions.

Une évaluation par photointerprétation de la classification des éléments ligneux en zone agricole portant sur près de mille éléments a démontré que la précision atteignait 93 %.

Analyse de la cartographie des AHF

Afin d'illustrer la diversité des informations pouvant être dérivées de cette cartographie, nous avons réalisé une analyse des données produites sur trois sites : deux communes rurales en Wallonie (Ohey et Paliseul) et un périmètre regroupant douze communes françaises au Nord-Est de Valenciennes (Condé-sur-l'Escaut).

Le tableau 1 présente les statistiques globales relatives aux éléments ligneux forestiers et non forestiers pour les trois sites. Le caractère forestier de la commune de Paliseul ressort clairement avec un taux de boisement forestier de 44,5 %. Dans les trois sites, les haies dominent les éléments non forestiers, avec des pourcentages supérieurs à 60 % pour les communes wallonnes, voire même à 70 % pour le site français. La densité de haies varie entre 1,7 km/km² pour Paliseul et 6,1 km/km² pour Condé-sur-l'Escaut.

L'analyse de la distribution des AHF en fonction des affectations du territoire a été réalisée pour les deux communes wallonnes en croisant la carte des éléments ligneux avec le plan de secteur (figure 3). On constate que la majorité des AHF se trouvent en zone agricole (57 % pour Ohey et 44 % pour Paliseul). Cependant, le taux de présence des éléments ligneux dans la zone agricole reste marginal car ces éléments couvrent à peine 3 % de la surface de cette partie du territoire.

Les détections de changements dans les deux communes wallonnes au départ du MNS de 2019 ont été réalisées en considérant uniquement les éléments dont la hauteur initiale (2014) était supérieure à 4 mètres. La figure 4 présente la distribution par classe de hauteur des éléments ligneux hors forêt ob-

Tableau 1. Statistiques globales relatives aux éléments ligneux forestiers et non forestiers pour les trois sites (Ohey, Paliseul et Condé-sur-l'Escaut).

Type d'élément		Ohey (5 668 ha)				Paliseul (11 127 ha)				Condé-sur-L'Escaut (11 192 ha)			
		Surface (ha)	Surface (%)	Longueur (km)	Nombre d'arbres	Surface (ha)	Surface (%)	Longueur (km)	Nombre d'arbres	Surface (ha)	Surface (%)	Longueur (km)	Nombre d'arbres
Arbres hors forêt	Bosquets	51,0	20,8			58,4	18,2			155,5	14,5		
	Groupes d'arbres	24,1	9,8		6 157	44,2	13,8		14 716	125,6	11,8		8 658
	Alignements d'arbres	0,8	0,3		326	0,9	0,3		412	2,4	0,2		160
	Haies	161,5	65,7	147,9		198,9	62,1	193,8		763,3	71,4	680,1	
	Arbres isolés	5,0	2,0		809	9,4	2,9		1 699	9,4	0,9		1 969
	Buissons	3,4	1,4			6,1	1,9			9,3	0,9		
	Autres	0,0	0,0			2,3	0,7			3,5	0,3		
	Total AHF	245,9	100,0		7 292	320,3	100,0		16 827	1069,1	100,0		10 787
	Forêt	798,2				4 948,1				2 604,2			
	Total	1044,1				5 268,4				3 673,3			

		Ohey	Paliseul	Condé-sur-L'Escaut
Indicateurs	Taux de boisement forestier (%)	14,1 %	44,5 %	23,3 %
	Taux de boisement total (%)	18,4 %	47,3 %	32,8 %
	Proportion d'ahf (%)	23,5 %	6,1 %	29,1 %
	Densité de haie (km/km²)	2,6	1,7	6,1

Répartition entre zones du plan de secteur

Ohey

Zone autres
5,4%

Zone forestière
7,6%

Zone agricole
57,4%

Zone habitat
29,6%

Paliseul

Zone autres
6,9%

Zone agricole
44,4%

Zone forestière
24,3%

Zone habitat
24,4%
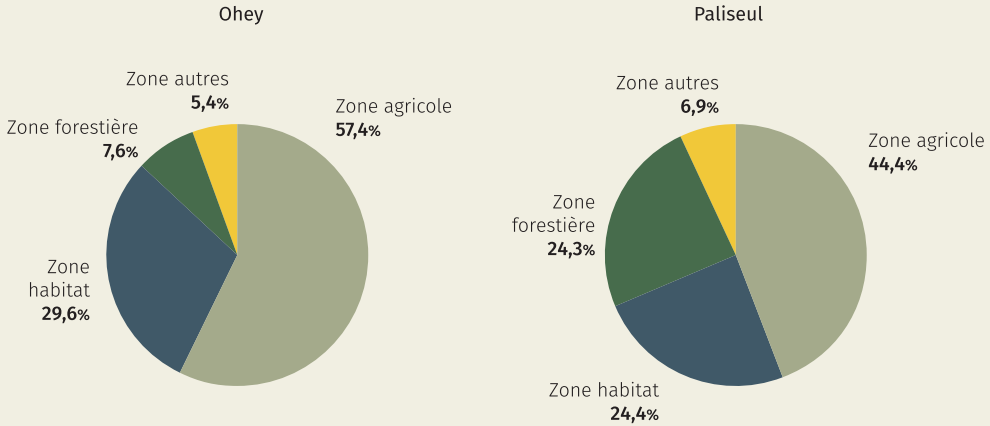
Taux de présence au sein de chacune des zones

Ohey

17,1 %

8,8 %

3,2 %

2,5 %

Zone agricole
Zone habitat
Zone forestière
Zone autres

Paliseul

12,3 %

6,6 %

3 %

1,4 %

Zone agricole
Zone habitat
Zone forestière
Zone autres
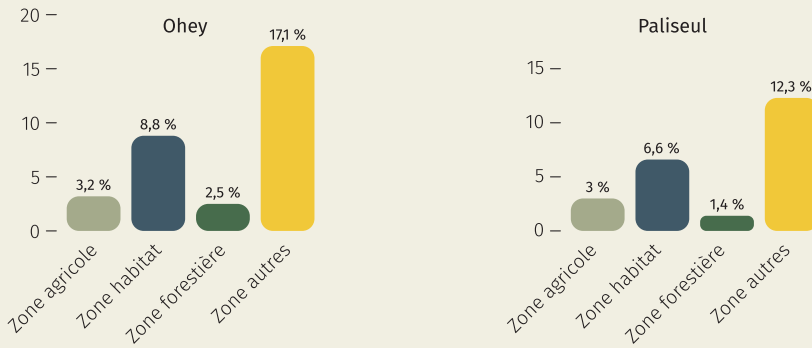
Figure 3. Répartition et taux de présence (surface d'AHF par rapport à la surface de la zone d'affectation) des AHF par classe d'affectation selon le plan de secteur.

Figure 4. Distribution par classe de hauteur des éléments ligneux hors forêt observés en 2014 et leur variation par rapport à 2019.

4-8 m
8-12 m
12-16 m
16-20 m
20 m et plus

Ohey

11,1%
5,7%
4,9%
4,1%
3,9%

Paliseul

8,9%
7,6%
7,0%
6,2%
8,2%

Éléments présents en 2014

Détection des changements entre 2014 et 2019

Nbre d'éléments présents

10 000
5000
2000
500

Orthophoto 2012 (SPW)

Hauteur : 15,7 m

Orthophoto 2019 (SPW)

Longueur : 246 m
Hauteur : 7 m

Orthophoto 2012 (SPW)

Orthophoto 2019 (SPW)
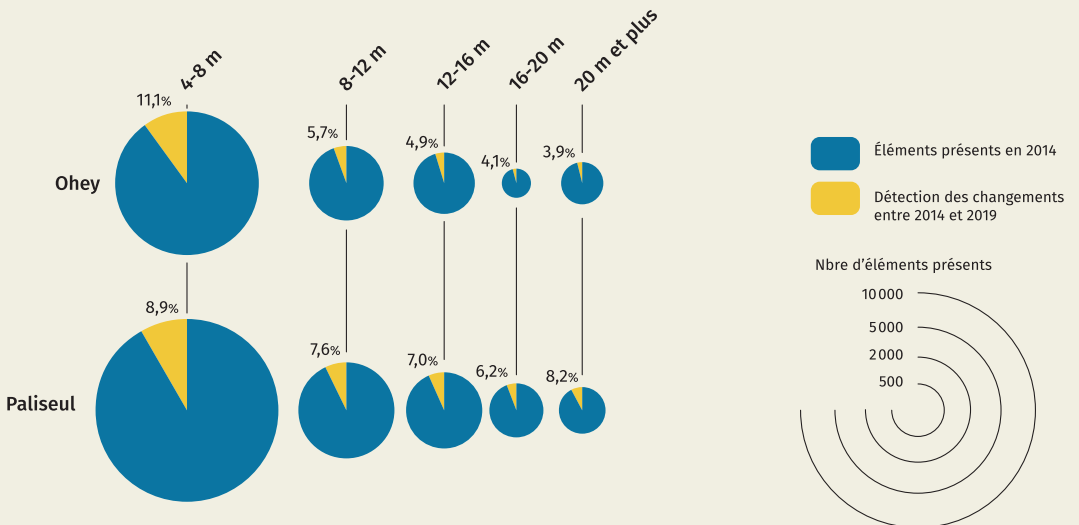
Figure 5. Exemple de détections de changement correspondant à une suppression effective de l'élément ligneux.

Figure 6. Cartographie de la connectivité des AHF pour la commune d'Ohey (à gauche) et pour la zone de Condé-sur-L'Escaut (à droite).

- 🟥 Élément non connecté
- 🟩 Élément connecté
- 🟩 Forêt

0　1　2　3 km

0　1　2　3　4 km
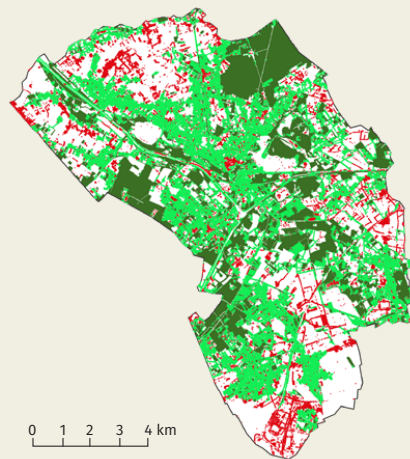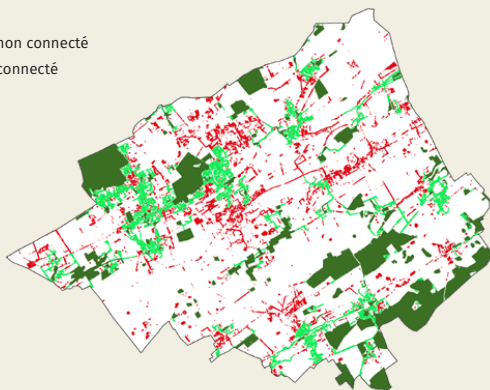
servés en 2014 et leur variation par rapport à 2019. La proportion d'éléments ligneux affectés par un changement important de hauteur est de l'ordre de 8 % pour les deux communes.

Une évaluation par photointerprétation sur un échantillon d'une centaine d'objets a montré que 85 % des détections de changement correspondaient effectivement à une suppression d'élément ligneux (figure 5). Les 15 % restant concernent des éléments de très petite taille, des entretiens de haie ou encore des artéfacts liés à l'imprécision du MNS 2019 ou à une mauvaise délimitation des éléments ligneux lors des étapes précédentes.

En ce qui concerne la connectivité des éléments ligneux, le critère de connectivité retenu correspond à une distance inter-éléments ne dépassant pas 10 mètres. L'indice qui en découle représente la proportion des AHF reliés aux surfaces forestières en respectant l'application de ce critère de distance. Pour les trois zones d'études, l'indice de connectivité ainsi estimé vaut respectivement 55 % pour Ohey, 57 % pour Paliseul et 84 % pour la zone de Condé-sur-l'Escaut (figure 6).

Conclusions

La méthode de cartographie des éléments ligneux hors forêts présentée dans cet article souligne le très haut potentiel du LiDAR aérien, pour cartographier et mesurer les éléments ligneux. La méthode est actuellement en cours d'application sur une bonne partie (12 000 km²) du territoire Wallon.

On ne peut que se réjouir que le SPW ait décidé de programmer une nouvelle campagne d'acquisition LiDAR sur l'ensemble du territoire régional, dont le produit devrait présenter une densité de points de l'ordre de 10 points/m².

La chaîne de traitement, qui a été conçue dans le cadre de cette étude, est fortement automatisée et peut être facilement adaptée pour traiter n'importe quel jeu de données LiDAR aérien. Elle pourra notamment être utilisée pour étendre la cartographie des AHF à l'ensemble du territoire wallon dès que la nouvelle couche sera disponible.

Les résultats obtenus sur les trois sites ont permis d'apprécier la richesse des informations susceptibles

POINTS-CLEFS

▶ Malgré l'évolution récente des politiques environnementales et leur intérêt pour les éléments ligneux hors forêt, ceux-ci restent peu étudiés et mal quantifiés.

▶ Le LiDAR aérien présente un très haut potentiel pour cartographier et mesurer les éléments ligneux que ce soit en forêt ou hors forêt.

▶ Une chaîne de traitement automatisée a été développée pour exploiter ces données LiDAR et générer une couche cartographique délimitant les éléments ligneux situés hors forêt et les catégorisant en cinq classes.

▶ Une telle cartographie constitue une source d'information précieuse pour asseoir la gestion des arbres hors forêt à l'échelle d'une région.

genetic resources. Food and Agriculture Organization of the United Nations, CGRFA-14/13/11, 29 p. Ⓦ

⁵ **Guillerme** S., **Alet** B., **Briane** G., **Coulon** F., **Maire** É. (2009). L'arbre hors forêt en France. Diversité, usages et perspectives. *Revue Forestière Française* 61(5) : 543-560. Ⓦ

⁶ **SPW ARNE** (2019). *Les méthodes agroenvironnementales et climatiques* (MAEC). SPW ARNE, 12 p. Ⓦ

d'être dérivées d'un tel produit cartographique, notamment en termes de dimension, de connectivité et d'évolution dans le temps.

Les pistes de recherche pour rendre cet outil plus complet portent sur la détection des AHF dans un stade précoce, sur la quantification de la biomasse présente dans les éléments ligneux cartographiés, et enfin sur l'identification de leur composition spécifique, en recourant notamment à des techniques d'intelligence artificielle.

L'outil développé dans le cadre de ce projet et les perspectives d'améliorations envisagées nous paraissent intéressants à considérer dans le contexte du programme ambitieux que s'est fixé le Gouvernement wallon en termes de plantations de haies. ■

Crédits photo. AWAF (p. 45).

Corentin Bolyn[1]
Nicolas Latte[1]
Anne Fourbisseur[2]
Vincent Colson[3]
Olivier Baudry[4]
Philippe Lejeune[1]
cbolyn@uliege.be

[1] Gembloux Agro-Bio Tech (ULiège)
 Passage des Déportés 2 | B-5030 Gembloux
[2] Carah Asbl
 Rue Paul Pastur, 11 | B-7800 Ath
[3] Cellule d'Appui à la Petite Forêt Privée (OEWB)
 Rue de la Croissance 4 | B-6900 Marche-en-Famenne
[4] AWAF asbl
 Rue de la Charmille 16 | B-4577 Strée

Bibliographie

¹ **Bolyn** C., **Lejeune** P., **Michez** A., **Latte** N. (2019). Automated classification of trees outside forest for supporting operational management in rural landscapes. *Remote Sensing* 11(10) : 1146. Ⓦ

² **Dedry** L., **De Thier** O., **Perin** J., **Bonnet** S., **Lejeune** P. (2015). ForEstimator : un nouvel outil cartographique pour mieux connaître la forêt wallonne. *Forêt Nature* 135 : 40-46. Ⓦ

³ **EURAF** (2020). 5ᵗʰ European Agroforestry Conference. Ⓦ

⁴ **FAO** (2013). *Draft strategic priorities for action for the conservation, sustainable use and development of forest*

2. A map of the main types of forest stands for Belgium and Northern France

This article presents a tree species classification method for mapping forest stands of Belgium and Northern France. It was the continuity and the improvement of the method detailed in chapter 2. Achieved results and their related conclusions lead to the development of the method detailed in chapter 3.

Bolyn, C., Latte, N., Colson, V., Fourbisseur, A., Vanderheeren, N., & Lejeune, P. (2020). Une carte des principaux types de peuplements forestiers de Belgique et du Nord de la France [Publisher: Forêt Wallonne asbl]. *Forêt.Nature*, *156*. Retrieved January 24, 2021, from https://orbi.uliege.be/handle/2268/252311

FORÊT
•NATURE

OUTILS POUR UNE GESTION RÉSILIENTE DES ESPACES NATURELS

UNE CARTE DES PRINCIPAUX TYPES DE PEUPLEMENTS FORESTIERS DE BELGIQUE ET DU NORD DE LA FRANCE

Corentin Bolyn (GxABT-ULiège), **Nicolas Latte** (GxABT-ULiège), **Vincent Colson** (CAPFP-OEWB), **Anne Fourbisseur** (Carah), **Nicolas Vanderheeren** (CRPF Grand Est), **Philippe Lejeune** (GxABT-ULiège)

foretnature.be

Une carte des principaux types de peuplements forestiers de Belgique et du Nord de la France

Corentin Bolyn[1] | Nicolas Latte[1] | Vincent Colson[2] | Anne Fourbisseur[3]
Nicolas Vanderheeren[4] | Philippe Lejeune[1]

[1] Gembloux Agro-Bio Tech (ULiège)
[2] Cellule d'Appui à la Petite Forêt Privée (OEWB)
[3] Carah Asbl
[4] Centre Régional de la Propriété Forestière Grand Est

Grâce aux nouvelles images satellitaires il est aujourd'hui possible de mieux identifier les peuplements et leur composition. Si la précision reste trop faible pour en faire un outil de gestion local, les améliorations à venir sont prometteuses pour les forestiers.

RÉSUMÉ

La connaissance de la ressource forestière à l'échelle d'une région ou d'un pays est un préalable à la mise en place d'une politique forestière réfléchie. Complémentaire aux inventaires par échantillonnage, la télédétection constitue une source alternative d'information pour la description des ressources forestières aux échelles régionales, nationales et transnationales. Avec le lancement récent des satellites Sentinel-1 et Sentinel-2 (Copernicus) en 2014-2016, l'offre en image satellitaire a connu une petite révolution. Ces nouvelles données ont agrandi le champ des possibles en termes de cartographie des forêts et de leur compo-
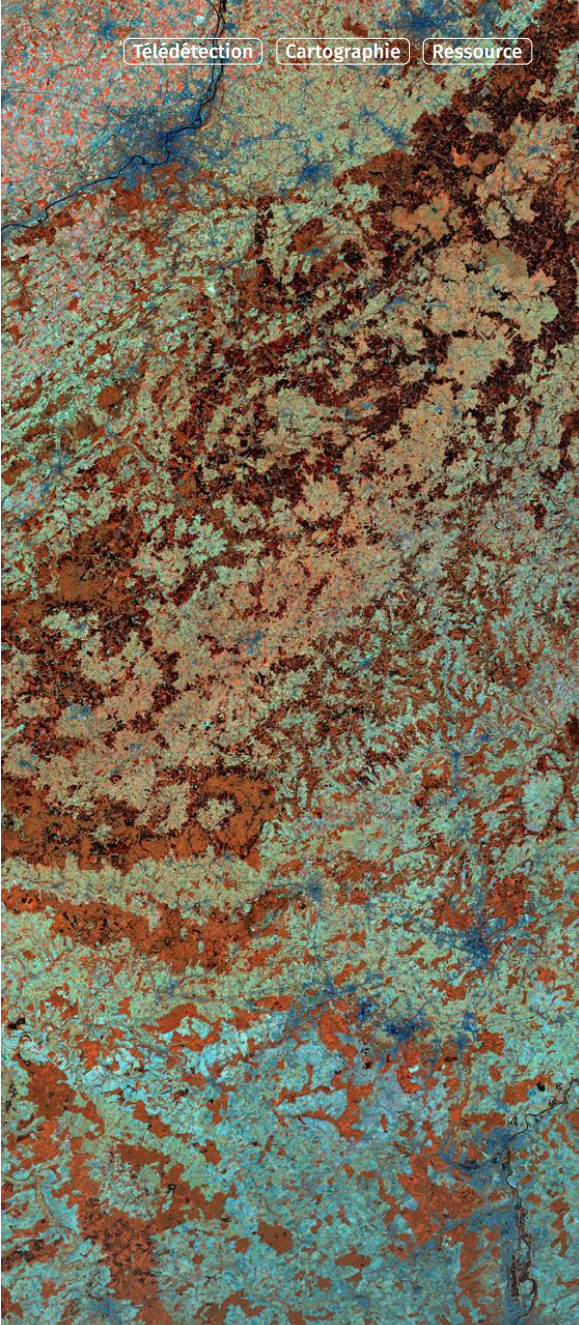
La connaissance globale de la ressource forestière à l'échelle d'une région ou d'un pays est un préalable à la mise en place d'une politique forestière réfléchie. Cette connaissance passe généralement par la mise en place d'inventaires forestiers à grande échelle réalisés par échantillonnage (placettes). Bien que de tels inventaires constituent une source précieuse de renseignements pour les acteurs de la forêt, ils présentent trois limitations importantes. Tout d'abord, le plan d'échantillonnage empêche bien souvent de fournir des résultats pertinents pour des zones de surfaces faibles. De plus, le suivi de la dynamique forestière est limité par la durée longue du cycle des inventaires régionaux et nationaux, qui peut dépasser les 10 ans. Enfin, si l'on considère la production ligneuse, les rayons d'approvisionnement de l'industrie du bois s'étendent bien au-delà des frontières administratives auxquelles se limitent les inventaires.

La télédétection constitue une source alternative d'information pour la description des ressources forestières aux échelles régionale, nationale et transnationale. Parmi ces informations, on pense, en premier lieu, à la délimitation des forêts et à leur composition spécifique. Avec le lancement du programme Copernicus et de ses satellites Sentinel-1 et Sentinel-2 en 2014-2016 (encart 1), l'offre en images satellitaires a connu une petite révolution. Le projet interreg *Forêt Pro Bos** a utilisé cette nouvelle source de données pour développer une méthode de cartographie des principaux types de peuplements de Belgique et du Nord de la France. Forêt Pro Bos ne couvrant pas l'ensemble du territoire belge, le soutien de Gembloux Agro-Bio Tech (via l'Accord-cadre de recherches et de vulgarisation forestières) et du projet Interreg *Regiowood 2*** a permis d'étendre cette étude au reste du territoire belge.

Des images satellitaires à la carte thématique

Des images sans nuages

La première difficulté qui a dû être surmontée dans cette étude réside dans la taille de la zone d'intérêt : 62 000 km². Même si les images Sentinel-2 sont livrées par tuile de 100 km de côté, la zone d'étude comprend au total quatorze tuiles. La seconde difficulté a été de générer une image synthétique sur l'ensemble de la zone, à la fois homogène radiométriquement et exempte de nuages. Pour surmonter ces deux difficultés, il a fallu combiner un grand nombre d'images (plus de cinq cents) acquises à différentes dates durant la période de végétation 2018 (du 1er mai au 30 septembre 2018).

sition spécifique. Dans ce contexte, une méthode a été développée pour cartographier les principaux types de peuplement de Belgique et du Nord de la France. Bien que la précision atteinte à ce jour reste trop faible pour en faire un outil de gestion local suffisamment fiable, les résultats ont démontré le très grand potentiel des images Sentinel pour réaliser la cartographie des essences forestière sur une échelle transfrontalière. Cette approche en développement laisse entrevoir des améliorations conséquentes à moyen termes pour soutenir les acteurs de la gestion forestière.

Encart 1. La constellation de Satellites Sentinel

L'agence spatiale européenne (ESA) a développé une série de missions satellite, appelées *Sentinels*, spécialement pour les besoins opérationnels du programme *Copernicus* de la commission européenne[2]. Ce dernier vise à fournir des données de précision, actualisées et aisément accessibles afin d'améliorer la gestion de l'environnement, de comprendre et limiter les effets du changement climatique et d'assurer la sécurité civile. Parmi celles déjà en orbite, deux constellations de deux satellites sont particulièrement intéressantes pour le suivi des forêts par télédétection : Sentinel-1 et Sentinel-2.

Sentinel-1

La mission Sentinel-1 comprend deux satellites héliosynchrones à orbite polaire. Les Satellites Sentinel-1A et 1B ont été lancé en avril 2014 et avril 2016 respectivement. Ils fournissent de tout temps, nuit et jour, des images radar de la surface terrestre. Chaque satellite a un cycle de répétition de 12 jours avec 175 orbites par cycle. La constellation offre ainsi un cycle de répétition exact de 6 jours à l'équateur[3].

Sentinel-2

Les satellites Sentinel-2A et Sentinel-2B ont été conçus pour fournir de l'imagerie optique haute résolution. Ils ont été lancés respectivement les 23 juin 2015 et 7 mars 2017. Placés sur la même orbite héliosynchrone, déphasés de 180° l'un de l'autre, ils ont une fréquence de revisite très élevée : 10 jours à l'équateur pour chaque satellite, c'est-à-dire 5 jours pour les deux satellites. En juillet 2020, environ 20 millions de produits ont été générés et mis à disposition gratuitement en téléchargement, ce qui représente un total de 10 pétaoctets (10^{15} octets).

Le capteur des satellites Sentinel-2 enregistre la lumière du soleil réfléchie par la surface terrestre en treize bandes spectrales. Parmi celles-ci, quatre bandes sont enregistrées à 10 mètres de résolution spatiale (1 pixel représente 100 m² au sol), six bandes à 20 mètres et trois bandes à 60 mètres. La haute fréquence de revisite et la qualité des données en font un outil précieux pour le monitoring de la végétation en général et des forêts en particulier[4].
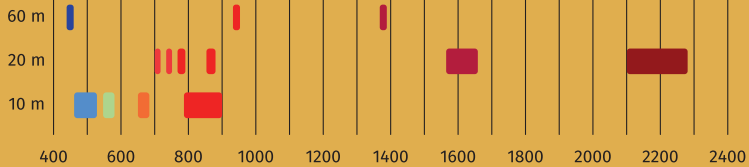
Bandes Sentinel-2 en fonction de leur résolution spatiale (source : cesbio.cnrs.fr).

Sentinel-1

Sentinel-2

© esa

© esa
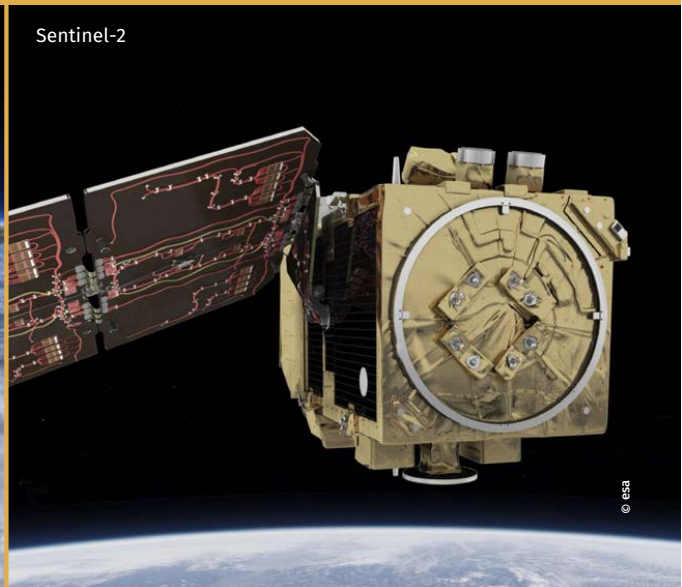
Contrairement aux images optiques Sentinel-2, les images radar Sentinel-1 sont insensibles à la couverture nuageuse mais elles sont beaucoup plus difficiles à déchiffrer en raison d'un phénomène de chatoiement important, surtout en présence de végétation. Pour contrer ce problème, les images Sentinel-1 ont été agrégées par période de 1 mois.

Pour l'année 2018, qui est l'année d'acquisition des données sources pour la méthode présentée dans cet article, nous disposons donc de plusieurs images : une image Sentinel-2 (période de végétation 2018) et douze images Sentinel-1 (une par mois de l'année 2018). Ces données sont illustrées à la figure 1.

Cartographier l'emprise forestière

Préalablement à la cartographie des principaux types de peuplements, il a été nécessaire de délimiter les zones forestières selon les critères édictés par la FAO : surface supérieure à 0,5 hectare et largeur d'au moins 20 mètres. Cette définition a en outre été restreinte aux surfaces ligneuses, c'est-à-dire, effectivement boisées. Les mises à blanc et les landes ne sont donc pas reprises dans cette cartographie. Les surfaces forestières ligneuses ont été délimitées par une méthode de classification opérée par pixel (10 mètres de côté) reposant sur les images synthétiques présentées plus haut (Sentinel-1 et 2). Le résultat de cette première étape est illustré à la figure 2.

Cartographier les principales essences forestières

La troisième étape visait à différencier les principaux types de peuplement présents au sein de ces surfaces forestières ligneuses. Les cartes de composition en essences considèrent généralement trois classes: feuillus, résineux et mixtes. Une classification plus fine a

Figure 1. Illustration des images synthétiques. **1** : Sentinel-2 en composition colorée (RGB). **2** : Sentinel-2 en fausses couleurs (Nir, Swir 1 et Swir 2). **3** : Sentinel-1 janvier 2018. **4** : Sentinel-1 août 2018. La ligne rouge délimite la zone considérée par le projet Interreg Forêt Pro Bos. La ligne noire délimite les frontières nationales.
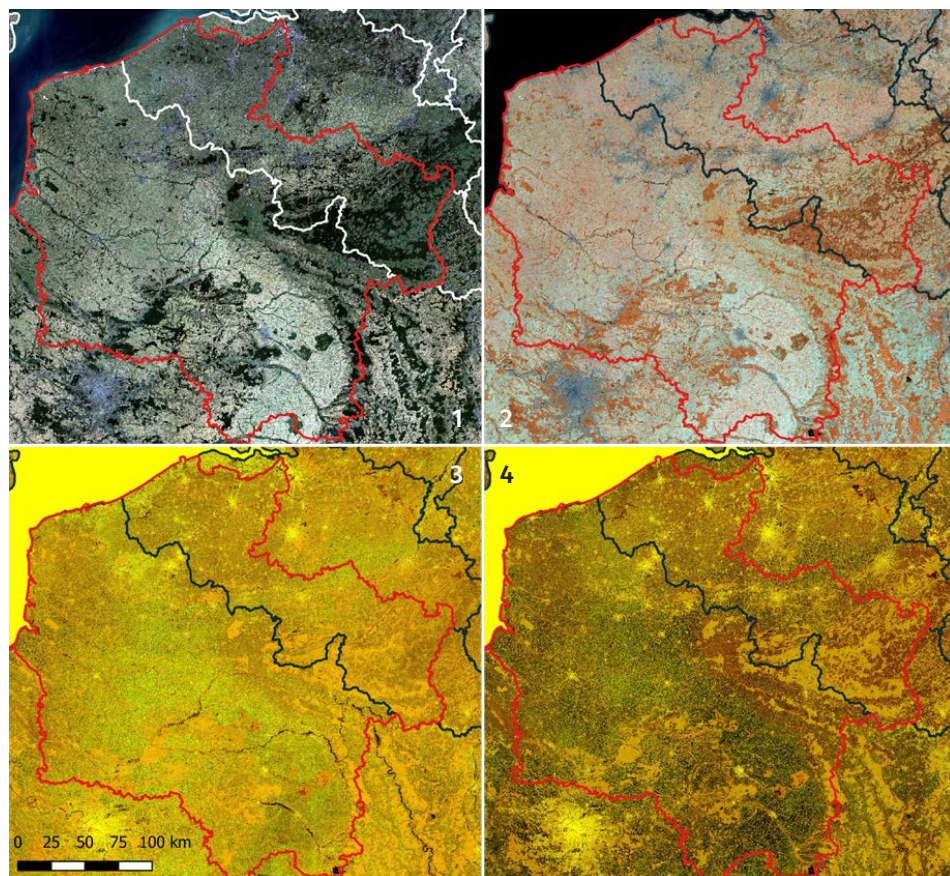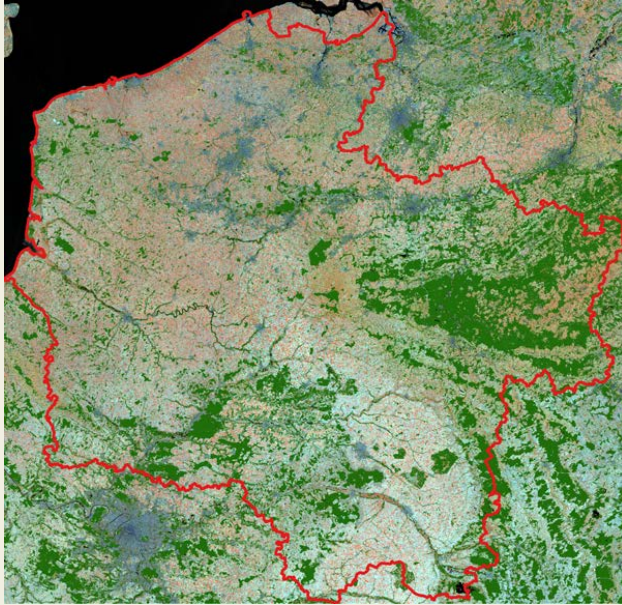
Figure 2. Surfaces forestières ligneuses de la zone du projet Interreg Forêt Pro Bos.

Figure 3. Répartition spatiale des données d'entrainement utilisées pour la confection de la carte.

- Frontière nationale
- Département français ou province belges
- Projet Interreg France-Wallonie-Vlaanderen
- Sites pilotes du projet
- Parcelle de référence
- Production participative

été réalisée en considérant les principales essences feuillues et résineuses. La légende retenue comporte cinq classes résineuses : douglas, épicéas, mélèzes, pins et autres résineux ; et quatre classes feuillues : chênes, hêtre, peupliers et autres feuillus.

Les données utilisées pour l'entrainement des modèles de classification se présentent sous la forme de polygones délimitant des portions de forêts homogènes, composées majoritairement d'une seule essence. Ces données sont issues de quatre sources :

- En Wallonie, une sélection d'îlots extraits du parcellaire des forêts publiques produit par le DNF .
- La mise à jour des parcelles de peuplier digitalisées lors d'un précédent projet Interreg « Transpop » (2000-2003).
- Des polygones digitalisés spécifiquement par l'équipe technique du projet Forêt Pro Bos (essentiellement pour le peuplier).
- Des polygones digitalisés par production participative dont nous parlerons plus loin.

La figure 3 présente la distribution spatiale du jeu de données d'entrainement utilisé pour la confection de la carte. Cette répartition est fortement déséquilibrée. Au sein de la zone d'étude, les données d'entrainement sont majoritairement situées en Wallonie ou dans de petites zones pilotes localisées dans les départements de l'Aisne, de la Marne et du Nord.

La carte des peuplements a été construite en deux temps avec une approche « pixel » (10 mètres de côté). Tout d'abord, des modèles de classification (forêts aléatoires) ont été générés au départ des données d'entrainement et des treize images synthétiques issues des données satellites. Un modèle a été généré par classe (neuf au total) permettant d'estimer la probabilité d'appartenance de chaque pixel à la classe considérée. Ensuite, la probabilité de présence de chaque classe a été estimée sur l'ensemble de la zone. Pour chaque pixel, la classe ayant la probabilité la plus élevée a finalement été retenue. La figure 4 présente le résultat final sur l'ensemble de la zone d'étude et la figure 5 pour la Wallonie. La figure 6 illustre le niveau de détail de la carte à une échelle plus fine en la comparant avec le parcellaire digitalisé du DNF.

Évaluation qualitative
La qualité de la carte a été évaluée au sein des sites pilotes du projet Forêt Pro Bos (figure 3) à l'aide d'un inventaire de terrain indépendant (c'est-à-dire, non utilisés pour la construction des modèles de classification) complété par photo-interprétation dans le cas du peuplier. L'analyse de la précision de la carte est donc trop fragmentaire pour être extrapolée à l'ensemble de la zone d'étude.
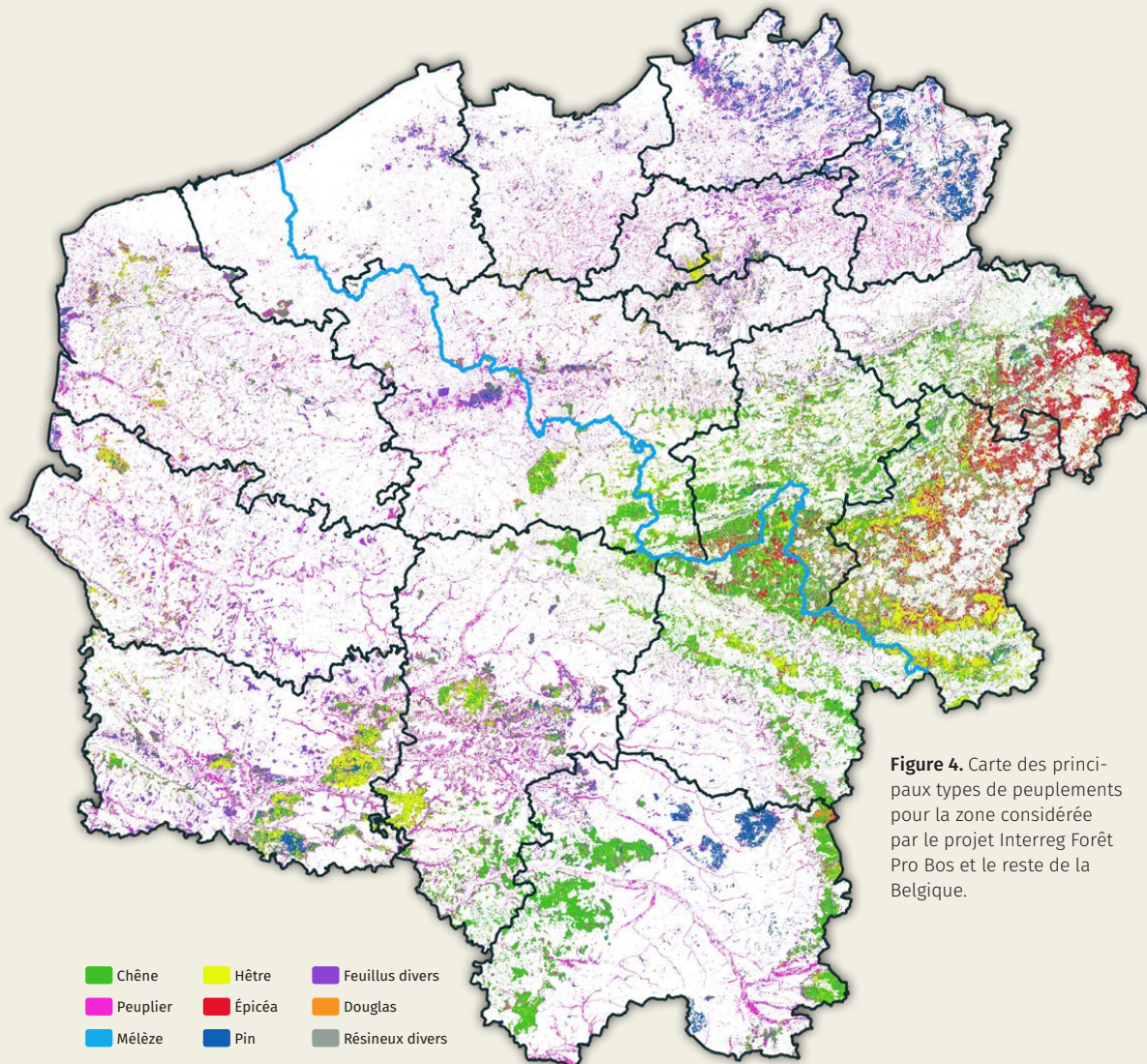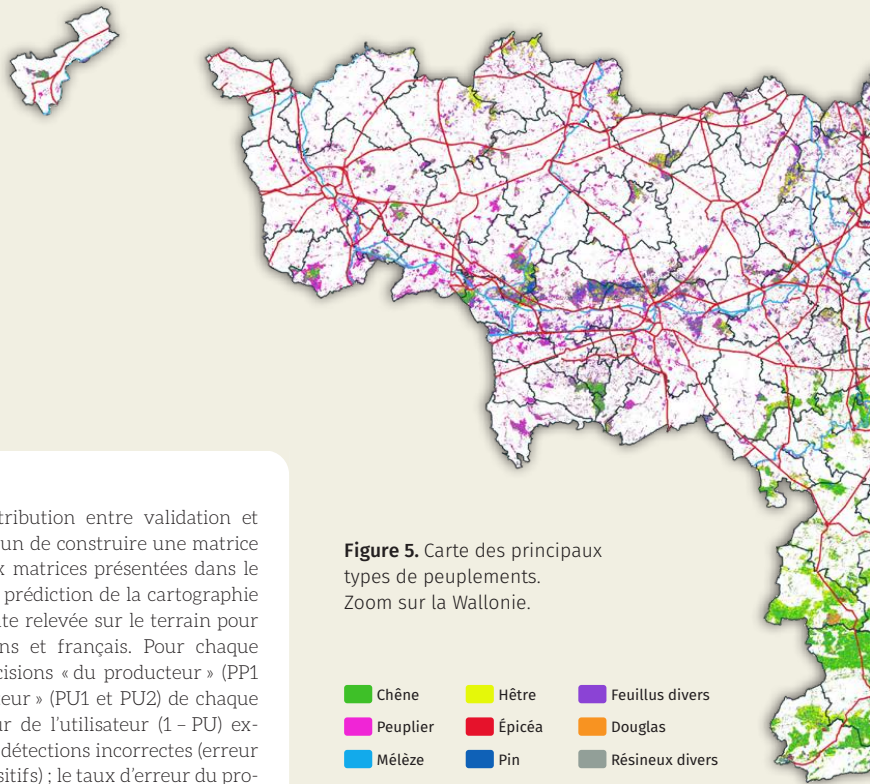
Figure 4. Carte des principaux types de peuplements pour la zone considérée par le projet Interreg Forêt Pro Bos et le reste de la Belgique.

|		
🟩 Chêne	🟨 Hêtre	🟪 Feuillus divers
🟪 Peuplier	🟥 Épicéa	🟧 Douglas
🟦 Mélèze	🟦 Pin	⬜ Résineux divers

L'évaluation de la précision repose sur 918 points de contrôle, répartis aléatoirement dans les zones forestières des sites pilotes (figure 3). Lors des visites de terrain de ces points, la surface terrière a été mesurée au relascope à encoche, et ventilée par essence. Pour chaque point de contrôle, la ou les classes inventoriées sur le terrain ont été comparées à l'essence prédite par la carte. Cette comparaison s'est faite selon deux modalités. La première, plus stricte : la classe prédite est-elle identique à la classe dominante sur le terrain ? La deuxième, plus souple : la classe prédite est-elle l'une des trois classes les plus présentes sur le terrain ? Cette deuxième modalité a été envisagée car une proportion importante des points de contrôle se situait dans des peuplements mélangés.

La répartition spatiale des données d'entrainement étant très hétérogène (figure 3), nous avons séparé les sites pilotes wallons (comprenant le site pilote à cheval sur la frontière) et les sites pilotes français pour évaluer les différences de résultats entre ces deux zones.

Figure 5. Carte des principaux types de peuplements. Zoom sur la Wallonie.

- Chêne
- Hêtre
- Feuillus divers
- Peuplier
- Épicéa
- Douglas
- Mélèze
- Pin
- Résineux divers
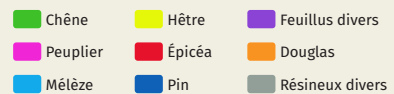
Pour visualiser la distribution entre validation et prédiction, il est commun de construire une matrice de confusion. Les deux matrices présentées dans le tableau 1 comparent la prédiction de la cartographie avec la classe dominante relevée sur le terrain pour les sites pilotes wallons et français. Pour chaque matrice, il y a les précisions « du producteur » (PP1 et PP2) et « de l'utilisateur » (PU1 et PU2) de chaque classe. Le taux d'erreur de l'utilisateur (1 – PU) exprime la proportion de détections incorrectes (erreur d'excédents ou faux positifs) ; le taux d'erreur du producteur (1 – PP) exprime la proportion non détectée d'une classe au profit d'une autre (erreur de déficits ou faux négatifs). PP1 et PU1 ont été calculés selon la modalité 1. PP2 et PU2 ont été calculés selon la modalité 2.

Les inventaires de terrain ayant été réalisés uniquement sur les sites pilotes du projet Forêt Pro Bos, il est impossible d'extrapoler les analyses de précision à l'ensemble de la zone d'étude. Néanmoins, ces chiffres permettent de tirer des conclusions sur le comportement de nos modèles dans des zones représentatives des contextes forestiers du projet. Globalement, les erreurs de prédiction de la cartographie sont liées à la confusion avec les essences trop peu représentées dans les données d'entrainement. Sans surprise, les classes « autres feuillus » et « autres résineux » sont les plus concernées. Enrichir ces données pour les rendre plus exhaustives et précises, voire récolter suffisamment d'informations pour distinguer de nouvelles classes, amélioreraient grandement la précision de la carte.

Les précisions de l'utilisateur sont encourageantes, allant jusqu'à 90 % pour l'épicéa côté wallon. Pour cette classe, ceci signifie que la grande majorité des pixels inventoriés contiennent bel et bien l'essence cartographiée. Mais au vu des différences de précision entre PU1 et PU2, l'essence la plus présente est régulièrement non

détectée, confondue avec une essence secondaire en mélange. Les essences les plus problématiques sont le mélèze, le pin et les autres résineux, présentant une trop forte proportion de faux positifs. La confusion de prédiction du pin avec les autres feuillus et des autres résineux avec l'épicéa (tableau 1A), indiquent des problèmes de quantité et de qualité des données d'entrainement utilisées pour la construction des modèles de ces classes. Dans les sites pilote français, les précisions n'ont pas été calculées pour certaines essences car elles étaient absentes ou trop peu présentes lors de l'inventaire. Les fausses détections (faux positifs) de pin persistent, confondus cette fois majoritairement avec la classe « autres résineux », et la précision de l'utilisateur chute à 57 % pour le peuplier (tableau 1B). Une partie importante des peupleraies cartographiées sont en réalité des « autres feuillus ».

Une précision de production élevée signifie que les faux négatifs sont rares sur la carte. Côté belge, deux classes ont un taux de détection plus faible : l'épicéa (52 %) et le groupe « autres feuillus » (15 %). La plupart des pixels d'épicéa non détectés ont été classés en tant
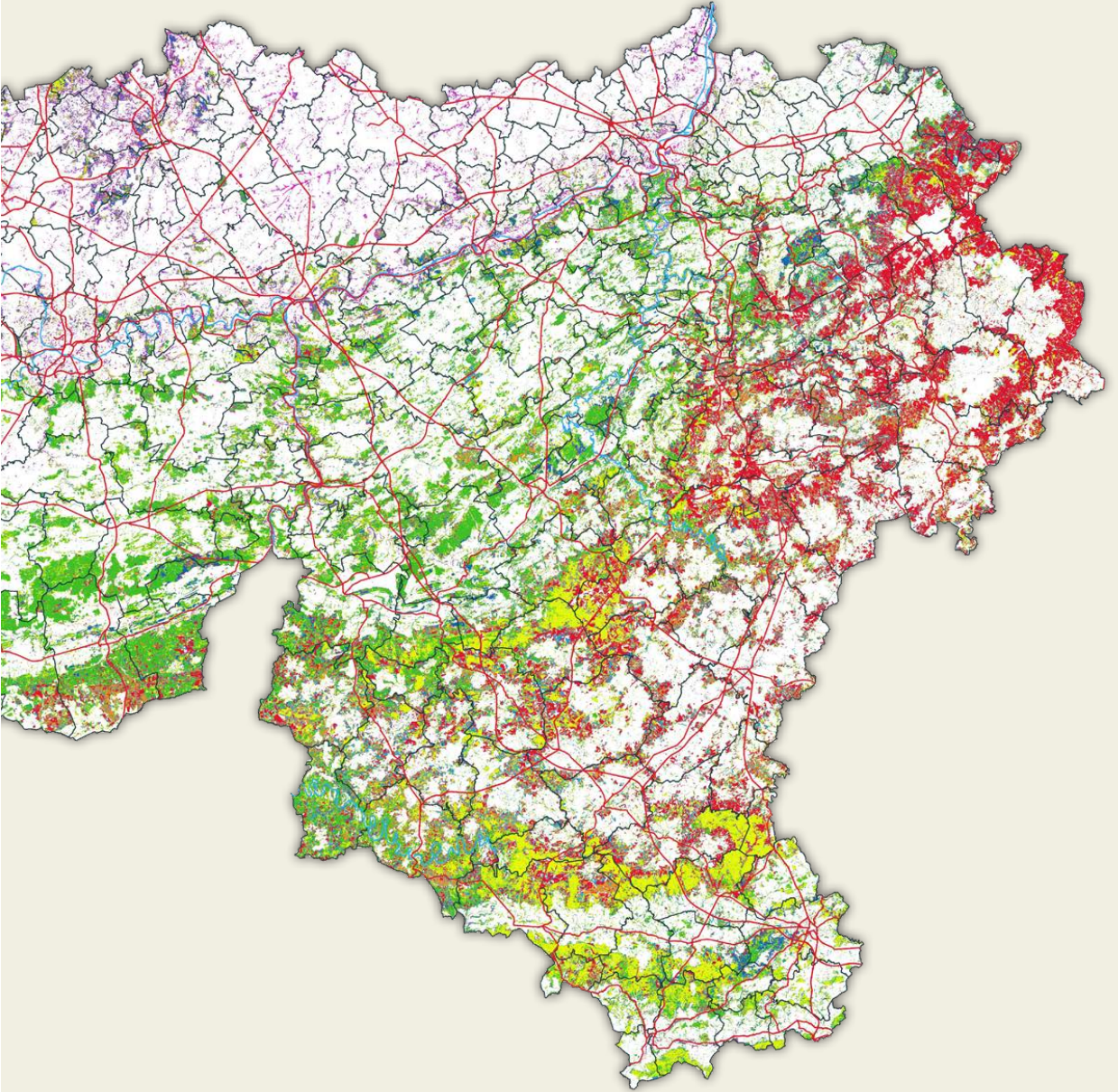
Figure 6. Comparaison de la cartographie des essences avec le parcellaire digitalisé du DNF.

A. Sites pilotes wallons

		CH	DO	EP	FE	HE	MZ	PE	PI	RE	PU1	PU2
	CH	124	0	0	67	6	2	5	1	0	60%	81%
	DO	0	32	11	0	0	0	1	0	0	73%	77%
	EP	0	5	65	0	2	0	0	0	0	90%	90%
Prédiction	FE	16	0	0	30	4	0	5	0	0	55%	76%
	HE	44	0	4	39	123	1	1	0	0	58%	74%
	MZ	9	7	5	7	3	29	2	5	0	43%	57%
	PE	2	0	1	29	1	0	97	0	0	75%	78%
	PI	5	5	6	23	5	2	4	33	0	40%	43%
	RE	4	4	34	2	1	1	0	0	7	13%	21%
	PP1	61%	60%	52%	15%	85%	83%	84%	85%	100%		
	PP2	78%	68%	58%	43%	89%	86%	84%	87%	100%		

Validation (colonnes CH à RE)

B. Sites pilotes français

		CH	DO	EP	FE	HE	MZ	PE	PI	RE	PU1	PU2
	CH	43	0	0	22	0	0	3	1	0	62%	74%
	DO	0	0	1	0	0	0	0	0	0		
	EP	0	0	0	0	0	0	0	0	0		
Prédiction	FE	52	0	1	91	0	0	15	0	0	57%	86%
	HE	12	1	0	13	2	0	2	0	0		
	MZ	0	0	0	0	0	1	0	0	0		
	PE	20	0	0	66	1	0	118	2	0	57%	57%
	PI	6	2	6	7	2	0	5	14	18	23%	55%
	RE	0	0	0	0	0	0	0	0	0	0%	0%
	PP1	32%			46%			83%	82%	0%		
	PP2	72%			53%			83%	82%	22%		

Validation (colonnes CH à RE)

Tableau 1. Matrices de confusion générées par comparaison du relevé de terrain et de la cartographie des principaux types de peuplements.

qu'« autres résineux ». La classe « autres feuillus », quant à elle, se confond avec cinq autres classes. En France, les deux classes « autres feuillus » et « autres résineux » sont mal détectées (PP2 de 53 % et 22 %, respectivement). De nouveau, on peut observer une différence nette pour certaines classes entre PP1 et PP2, ce qui confirme la difficulté des modèles à détecter l'essence la plus présente en mélange.

Des perspectives encourageantes

Cette approche de cartographie de nos forêts à large échelle est encore en développement. À ce jour, force est de reconnaître que les confusions restent trop im-

portantes pour en faire un outil de gestion suffisamment fiable. Les perspectives qu'ouvre ce travail sont néanmoins très intéressantes. En effet, il n'existe pas à l'heure actuelle de produits équivalents sur de telles surfaces et les résultats atteints sont plus qu'encourageants. Si l'on considère la zone d'étude dans son entièreté, les différences d'occupation forestière entre les régions couvertes par le projet apparaissent nettement sur la cartographie des types de peuplements (figure 4). C'est en cette variabilité que réside la difficulté de travailler à un niveau interrégional. Les développements réalisés sont novateurs et démontrent l'intérêt de la télédétection pour caractériser la ressource forestière.

Améliorer la carte : tout le monde peut y participer
Conscients que la carte produite présente des imperfections et que celles-ci sont probablement plus importantes dans les régions périphériques de la zone d'étude (Départements de l'Oise, de la Somme et du Pas-de-Calais, provinces flamandes), nous avons mis en place une démarche de science participative (aussi qualifiée de production participative). Le principe consiste à donner accès à la carte produite au sein d'une application web* dans laquelle l'utilisateur peut, de manière très simple, digitaliser de nouveaux polygones de référence et encoder la ou les essences observées. Les données ainsi récoltées devraient permettre à la fois de tester la qualité de la carte en dehors des zones pilotes du projet, mais aussi, à plus long terme, de construire une nouvelle carte plus robuste car reposant sur des données d'entrainement plus nombreuses et mieux réparties sur la zone d'étude. Au moment d'écrire ces lignes, 140 nouveaux polygones ont déjà été encodés dans le système.

Conclusions et perspectives

Les travaux menés dans le cadre du projet Forêt Pro Bos ont permis de démontrer le très grand potentiel des images Copernicus pour réaliser la cartographie des principales essences forestières sur une échelle transfrontalière (62 000 km²). Alors que les images Sentinel-1 se sont révélées particulièrement utiles pour la délimitation des surfaces forestières ligneuses, la production d'une image Sentinel-2 de synthèse sans nuage correspondant à la période de végétation est la principale source d'informations utilisée pour discriminer les groupes d'essence.

Le fait de disposer de données d'entrainement de qualité et bien réparties sur l'ensemble de la zone d'étude est un élément important pour garantir une qualité uniforme de la carte produite. À ce niveau, des progrès doivent encore être réalisés. Les données d'entrainement étaient disponibles en plus grande quantité sur le territoire wallon et non disponibles dans les départements de l'Oise, de la Somme et du Pas-

de-Calais, ainsi que dans les provinces flamandes. Le recours aux outils de sciences participatives est une piste intéressante pour combler cette lacune.

En plus de constituer un jeu de données d'entrainement exhaustif, la principale voie d'amélioration méthodologique de la carte présentée concerne la prise en compte des mélanges d'essences à l'échelle du pixel (10 x 10 mètres). À ce stade, seule l'essence considérée comme dominante au sein du pixel est renseignée.

Les recherches en cours visent à réorganiser les modèles de prédiction pour pouvoir évaluer les mélanges d'essences et leur proportion pour chaque pixel (par exemple chêne-hêtre ou épicéa-douglas). Ces nouveaux travaux s'inscrivent dans le cadre du projet *Cartofor*** et font appel à des algorithmes d'intelligence artificielle qualifiés d'apprentissage profond.

L'évolution rapide des données de télédétection disponibles et des outils de modélisation laisse entrevoir des améliorations conséquentes dans ce domaine de recherche à moyen terme. Celles-ci aboutiront à des outils de plus en plus fiables pour soutenir les acteurs de la gestion forestière. ∎

POINTS-CLEFS

▶ La connaissance de la ressource forestière à l'échelle d'une région ou d'un pays est un préalable à la mise en place d'une politique forestière réfléchie.

▶ La télédétection constitue une source alternative d'information pour la description des ressources forestières aux échelles régionales, nationales et transnationales.

▶ Le lancement de la constellation des satellites Sentinel (Copernicus) a agrandi le champ des possibles en termes de cartographie des forêts et de leur composition spécifique.

▶ Une méthode de cartographie des principaux types de peuplement de Belgique et du nord de la France a été développée.

▶ Les résultats atteints ont démontré le très grand potentiel des images Sentinel pour réaliser la cartographie des essences forestières sur une échelle transfrontalière.

Bibliographie

[1] **Alderweireld** M., **Burnay** F., **Pitchugin** M., **Lecomte** H. (2015). *Inventaire Forestier Wallon. Résultats 1994-2012.* DNF, SPW ARNE, 236 p. Ⓦ

[2] **ESA** (2020). Overview. *www.esa.int/Applications/Observing_the_Earth/Copernicus/Overview3* (consulté le 02.09.2020). Ⓦ

[3] **ESA** (2020). Sentinel-1. Missions. Sentinel Online. *sentinel.esa.int/web/sentinel/missions/sentinel-1* (consulté le 02.09.2020). Ⓦ

[4] **ESA** (2020). Sentinel-2. Missions. Sentinel Online. *sentinel.esa.int/web/sentinel/missions/sentinel-2* (consulté le 02.09.2020). Ⓦ

Corentin Bolyn[1]
Nicolas Latte[1]
Vincent Colson[2]
Anne Fourbisseur[3]
Nicolas Vanderheeren[4]
Philippe Lejeune[1]
cbolyn@uliege.be

[1] Gembloux Agro-Bio Tech (ULiège)
Passage des Déportés 2 | B-5030 Gembloux

[2] Cellule d'Appui à la Petite Forêt Privée (OEWB)
Rue de la Croissance 4 | B-6900 Marche-en-Famenne

[3] Carah Asbl
Rue Paul Pastur, 11 | B-7800 Ath

[4] Centre Régional de la Propriété Forestière Grand Est

B

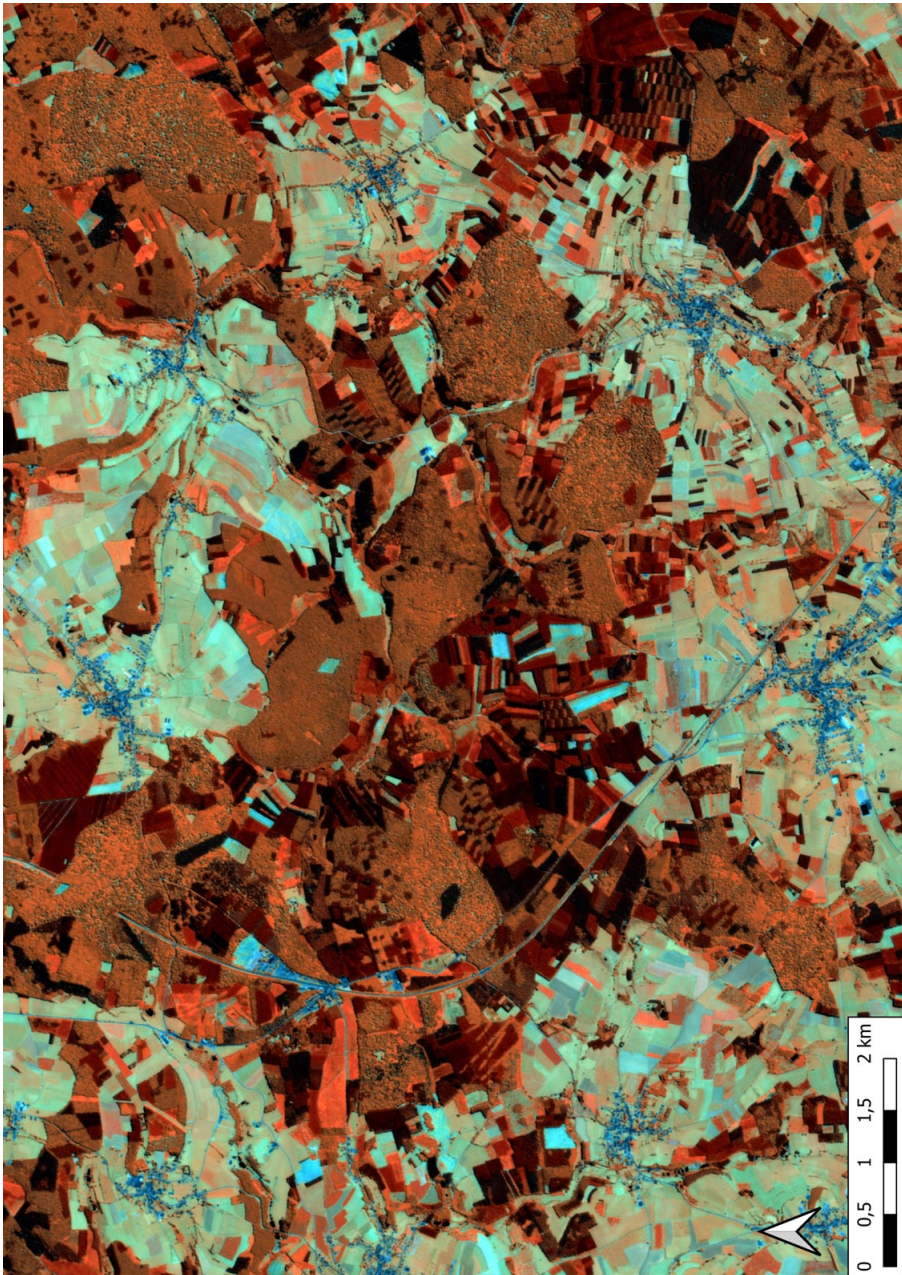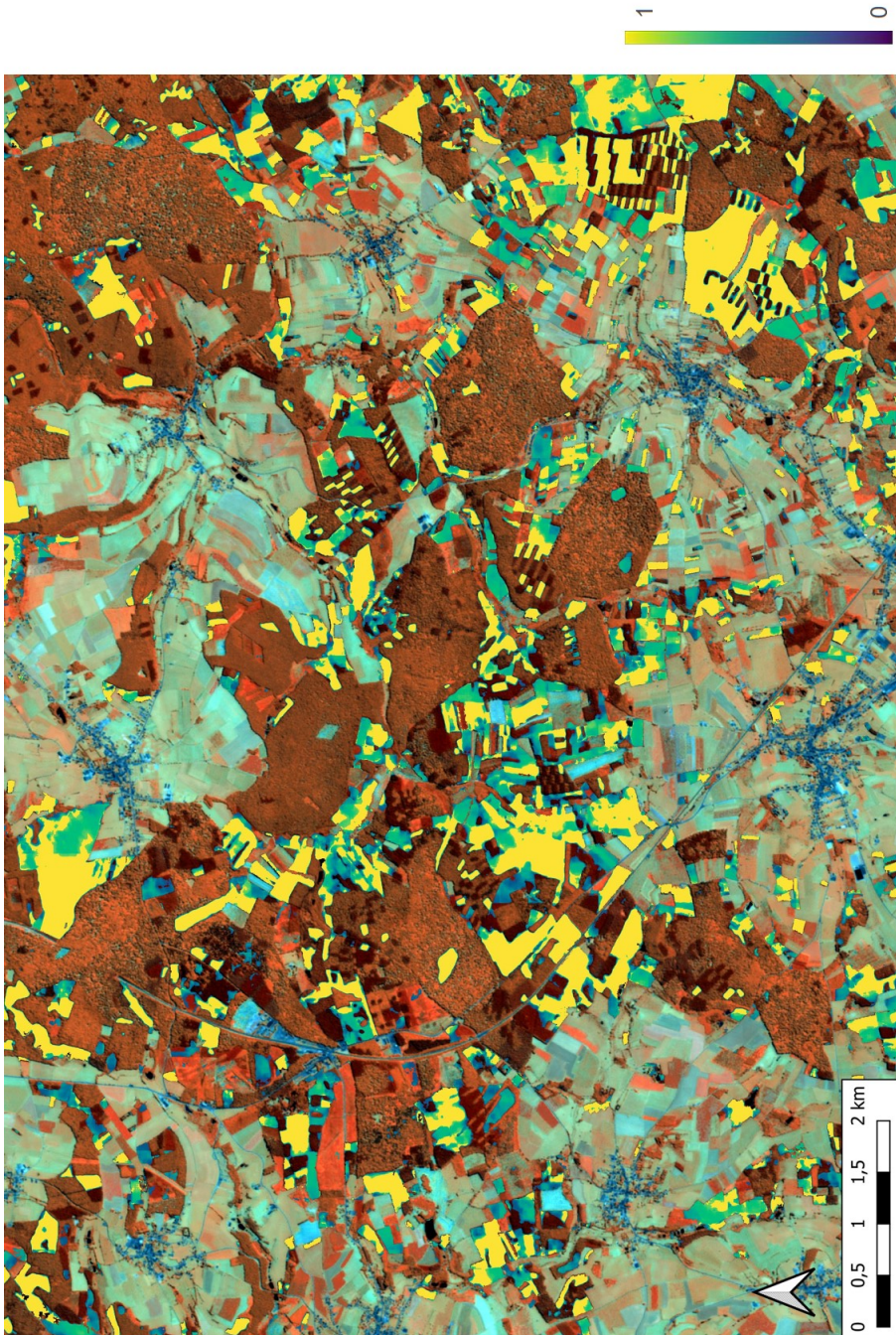## Additional illustrations

1. Tree species proportions map

Figure B.1: S2 surface reflectance syntheses (B8A, B11, B12) generated considering the vegetation period from 15 May to 15 September 2018. We super-resolved the ten S2 bands at 2.5 m as described in Latte and Lejeune (2020).
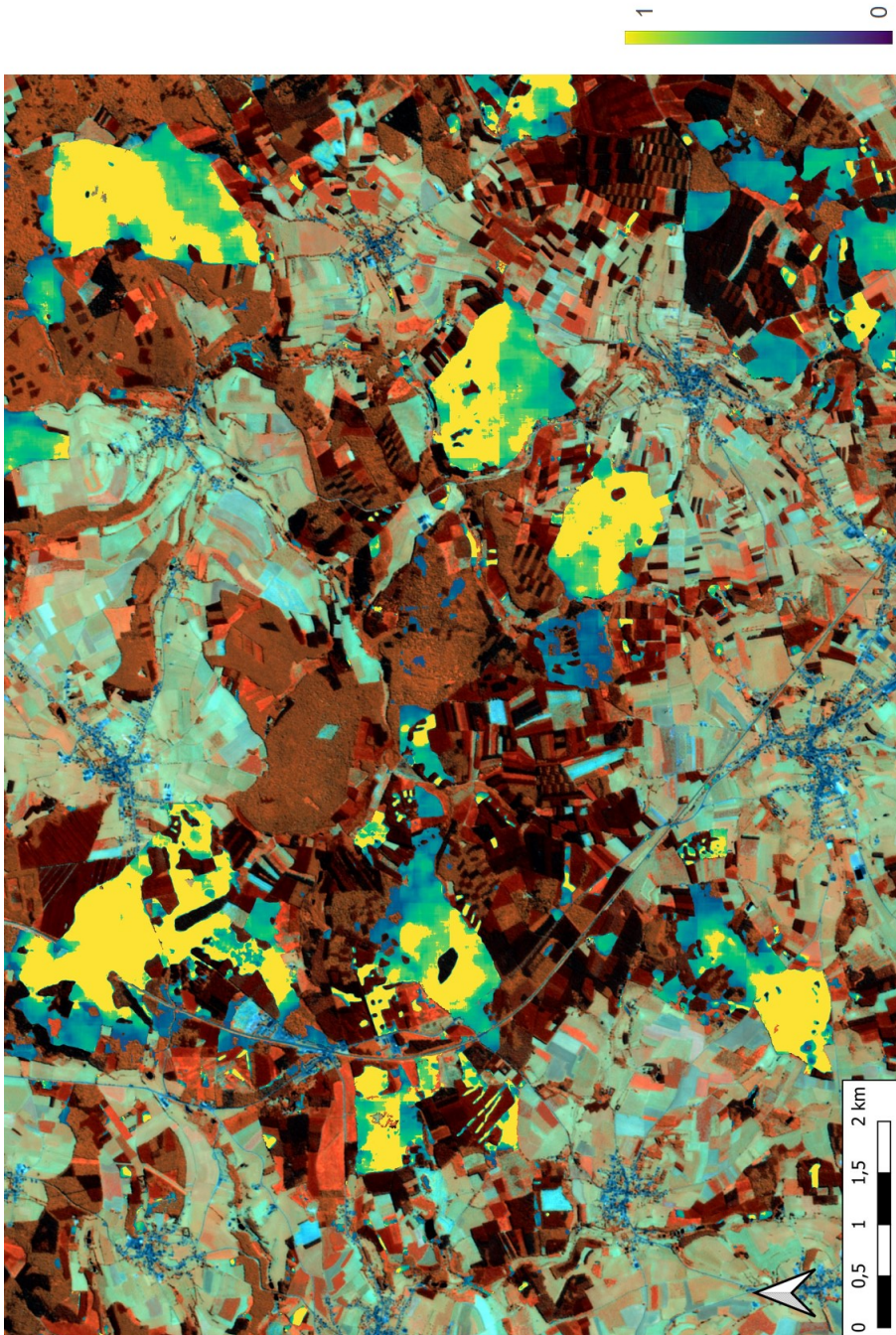
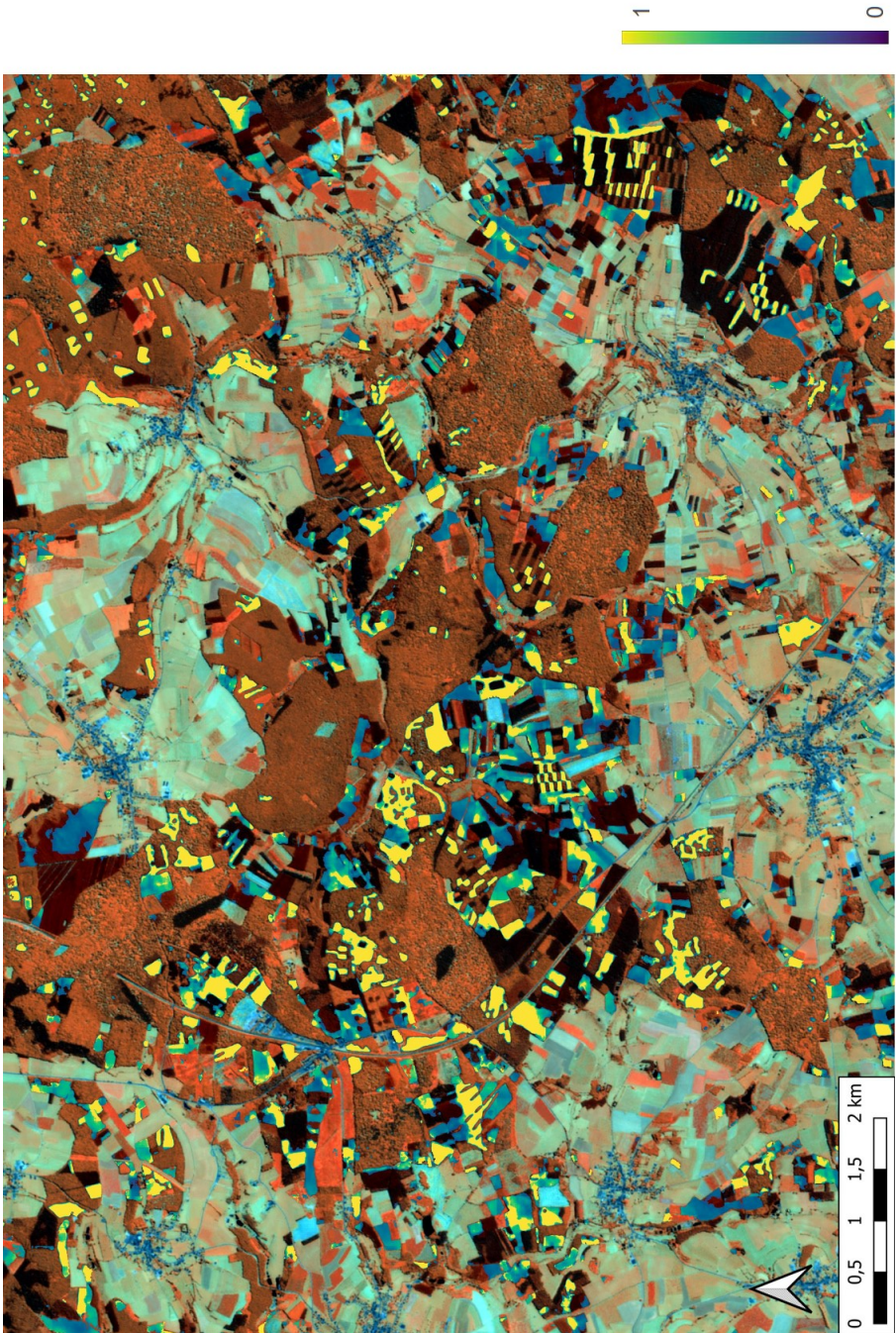**Figure B.2:** Proportion of Spruces extracted from the tree species proportions map (chapter 3).
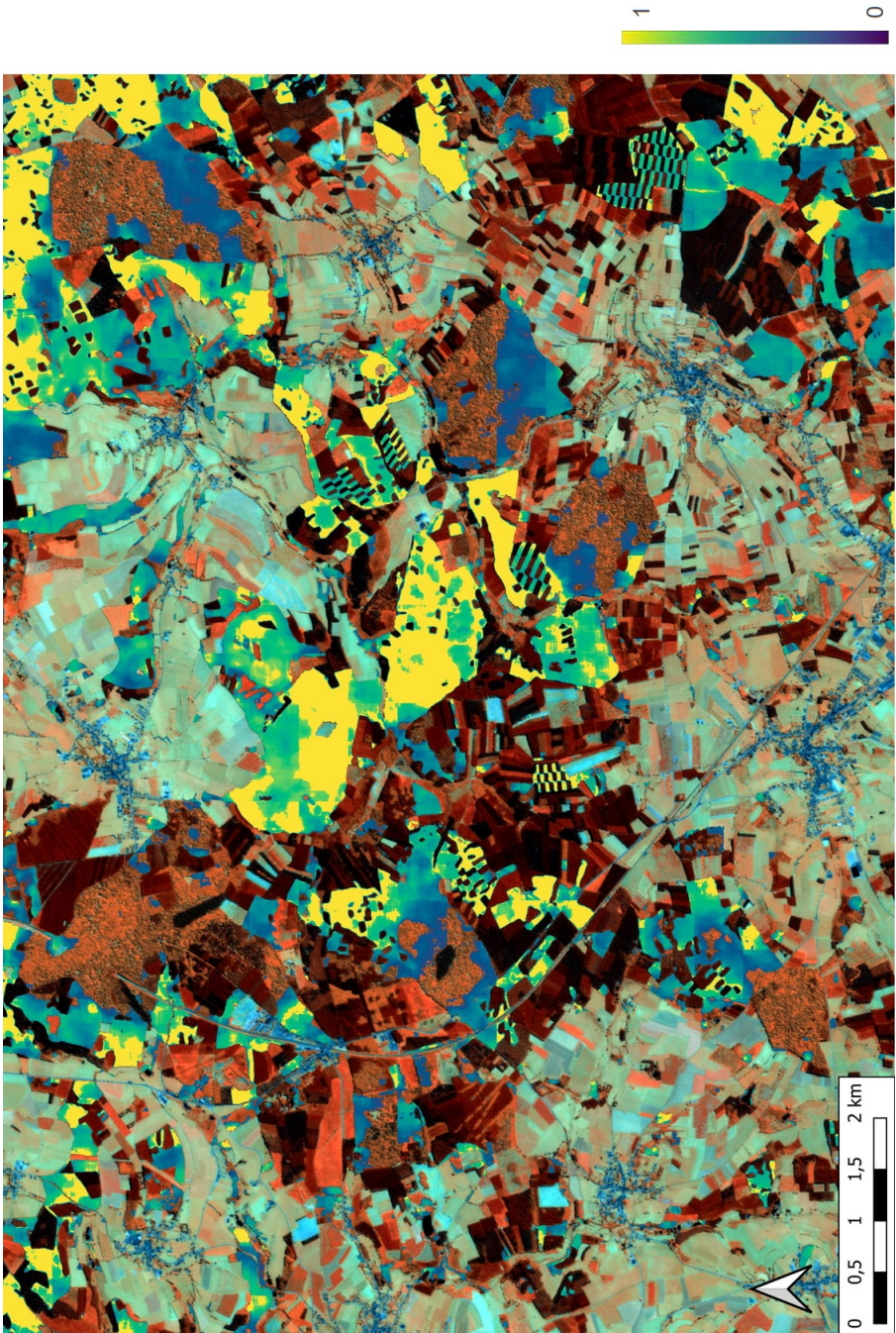
Figure B.3: Proportion of Oaks extracted from the tree species proportions map
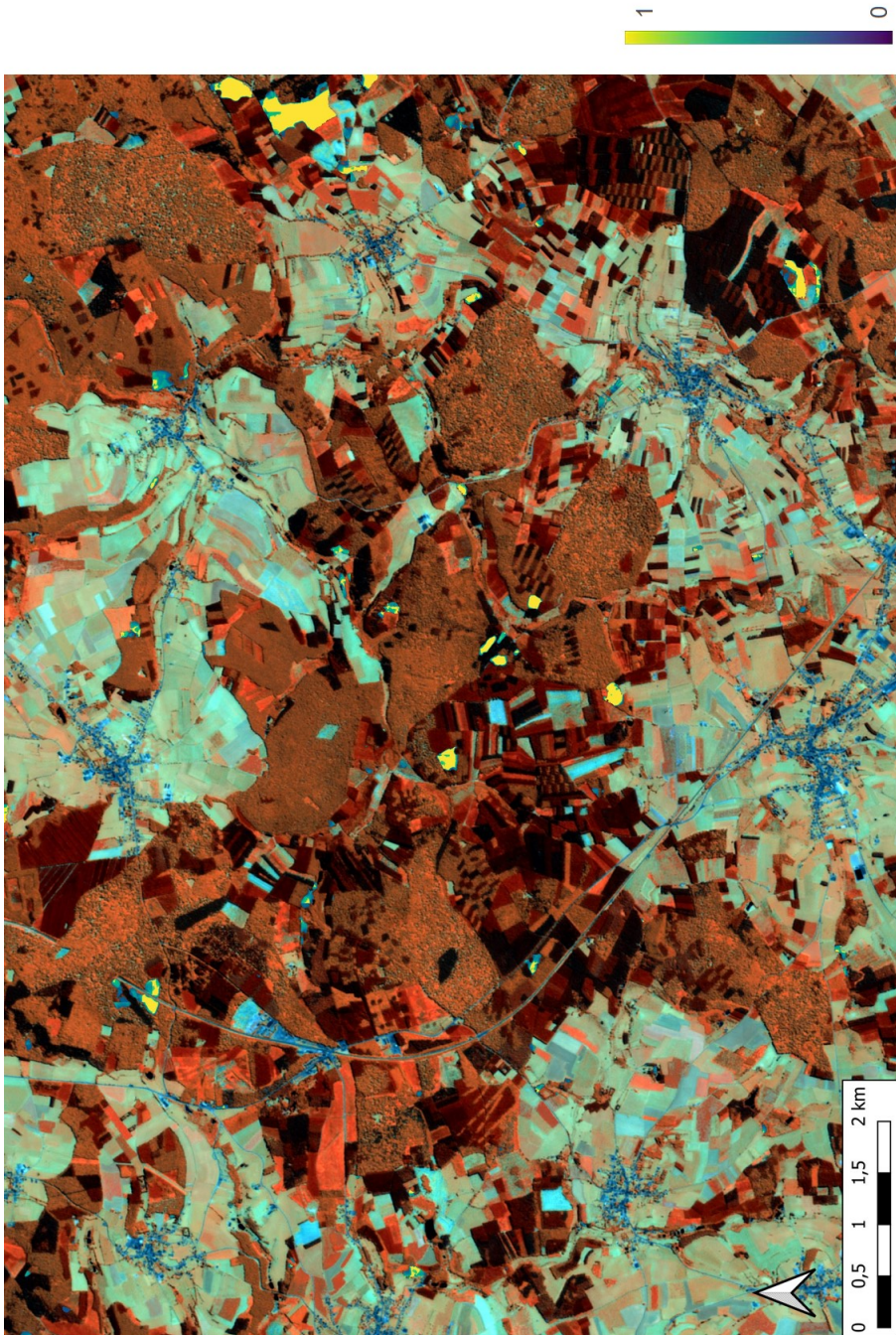(chapter 3).

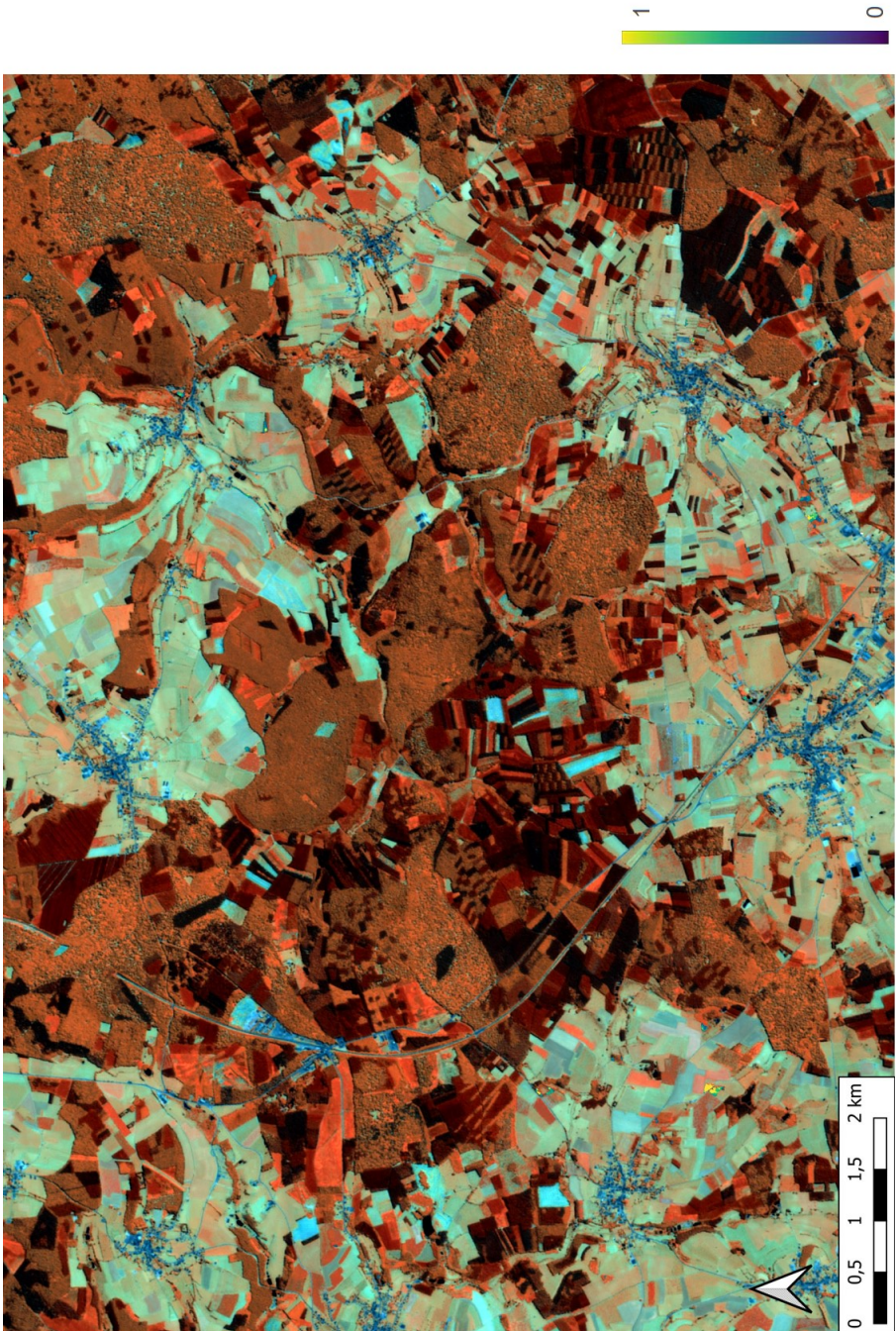**Figure B.4:** Proportion of Beech extracted from the tree species proportions map (chapter 3).

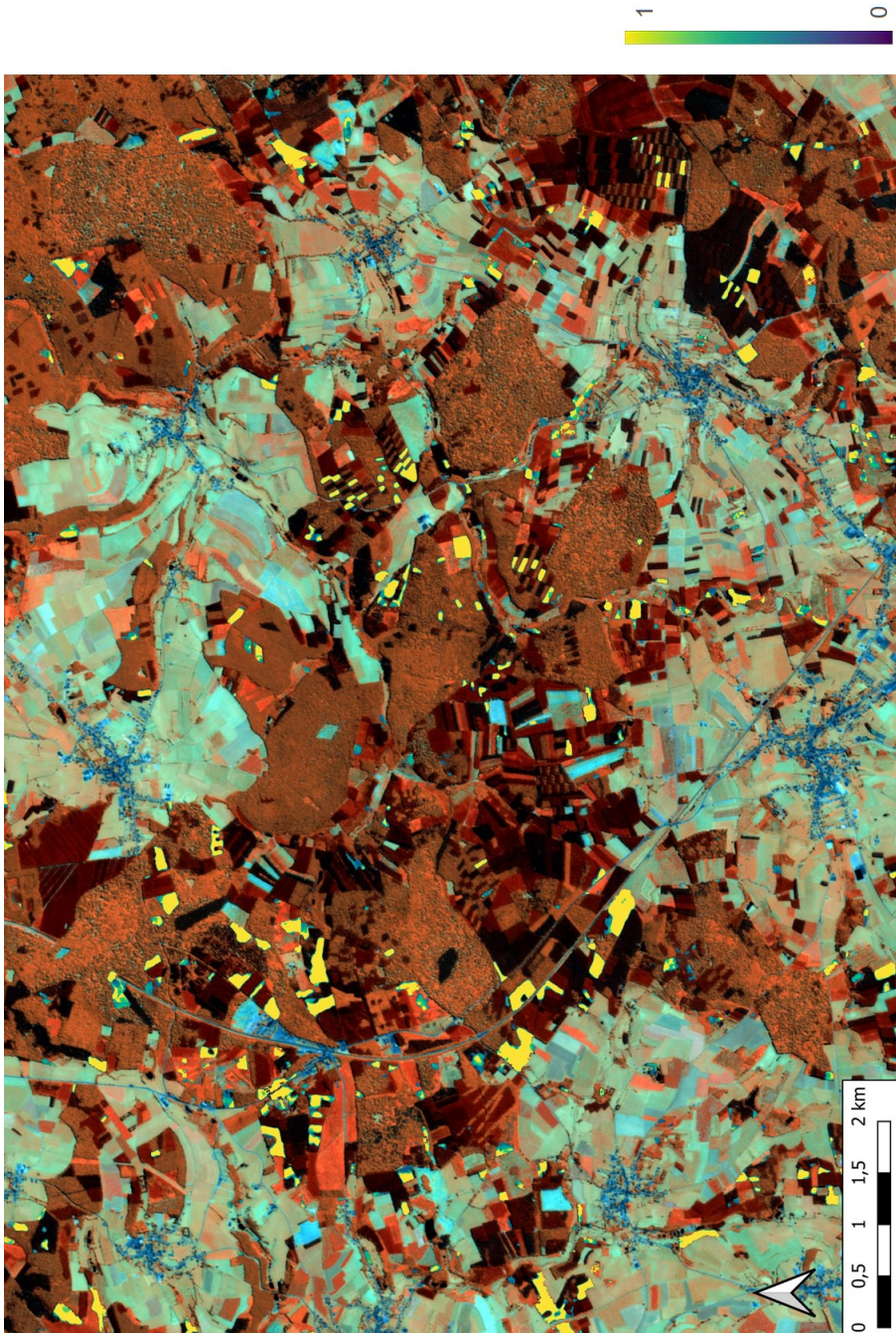**Figure B.5:** Proportion of Douglas fir extracted from the tree species proportions map (chapter 3).

Figure B.6: Proportion of Pines extracted from the tree species proportions map (chapter 3).
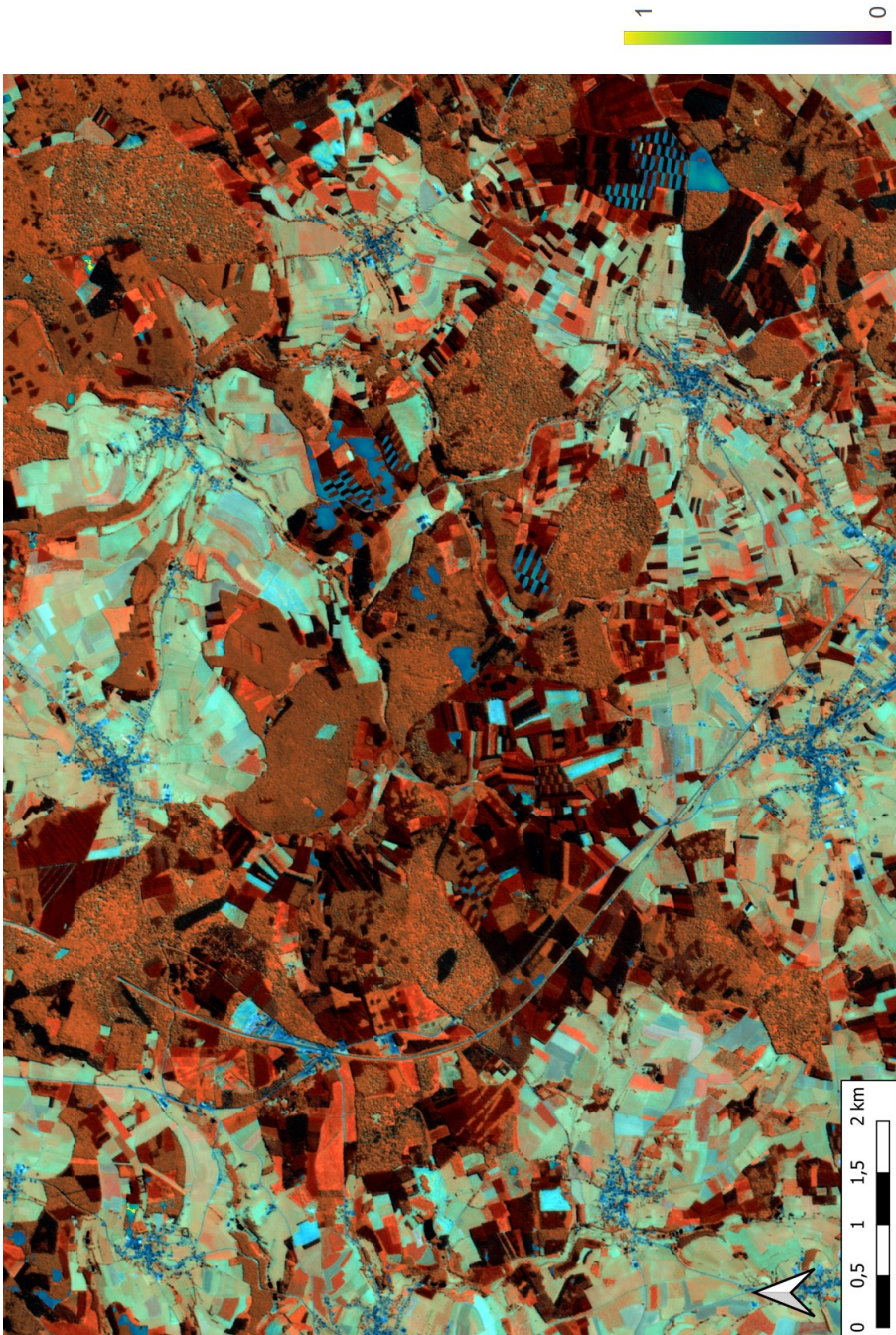
Figure B.7: Proportion of Poplars extracted from the tree species proportions map (chapter 3).
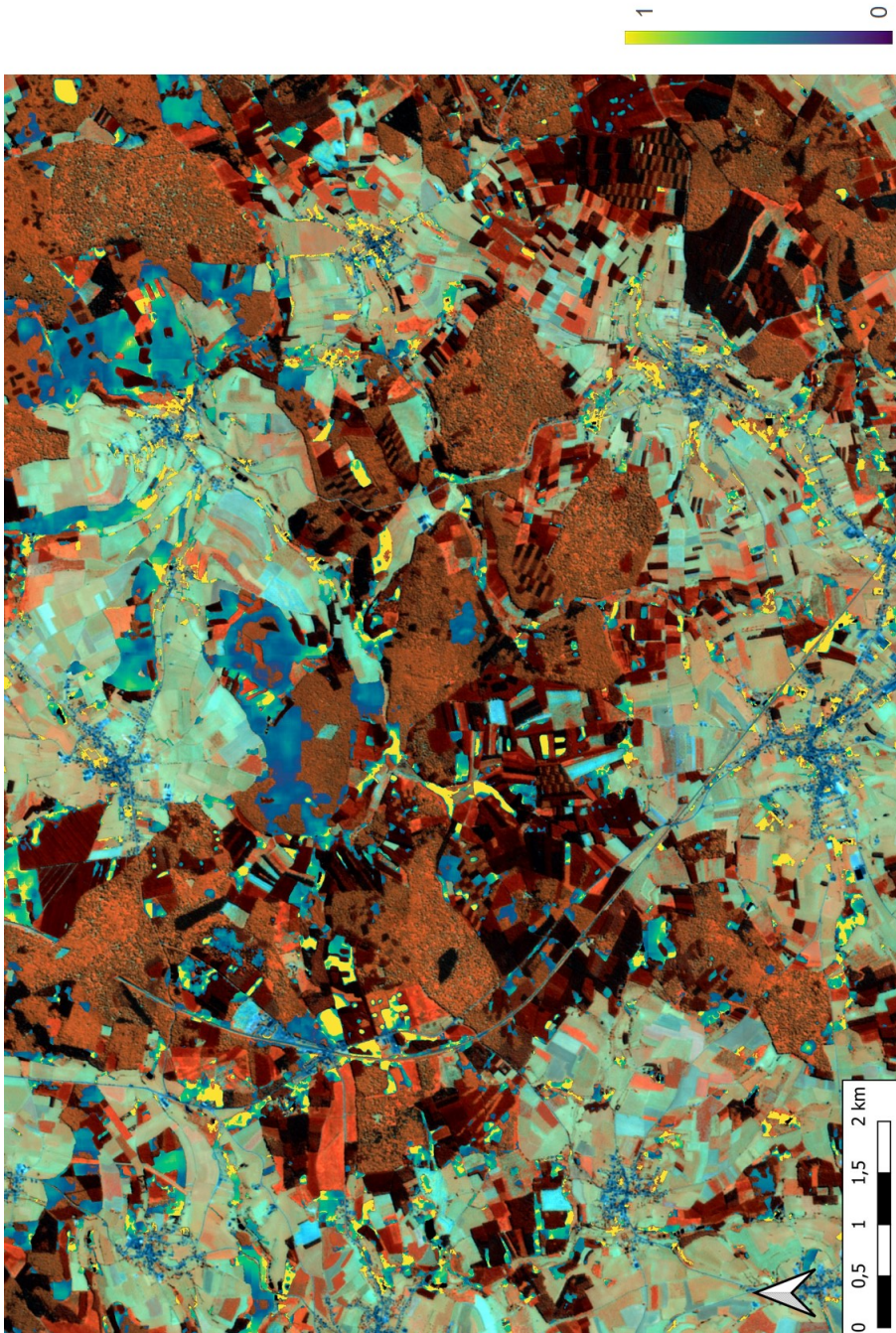
Figure B.8: Proportion of Larches extracted from the tree species proportions map (chapter 3).
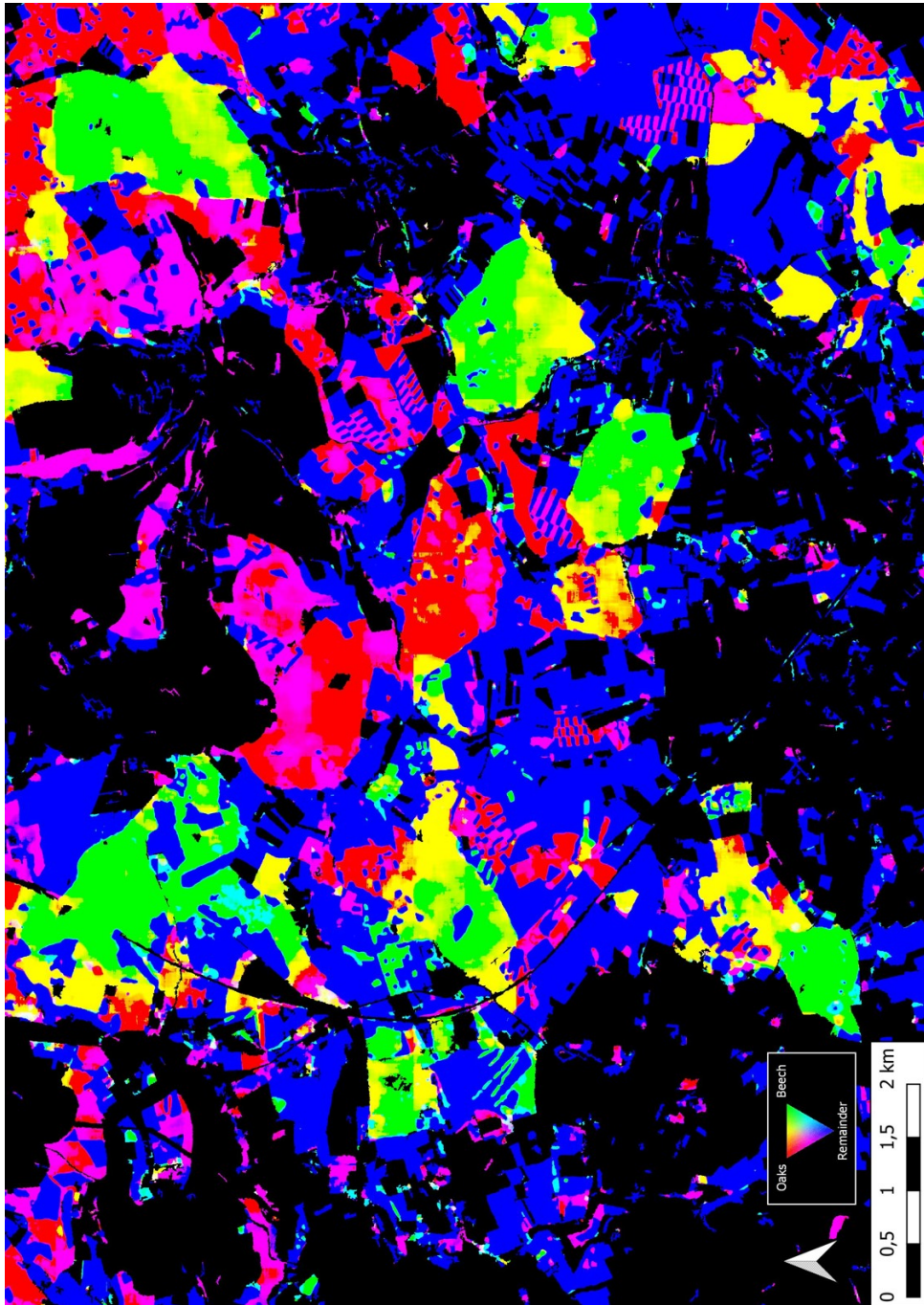
Figure B.9: Proportion of Birches extracted from the tree species proportions map (chapter 3).

Figure B.10: Proportion of Other extracted from the tree species proportions map (chapter 3).

131

Figure B.11: False colour image of the tree species proportions map (chapter 3). Red: proportion of oaks, green: proportion of Beech, blue: proportion of the remaining classes.
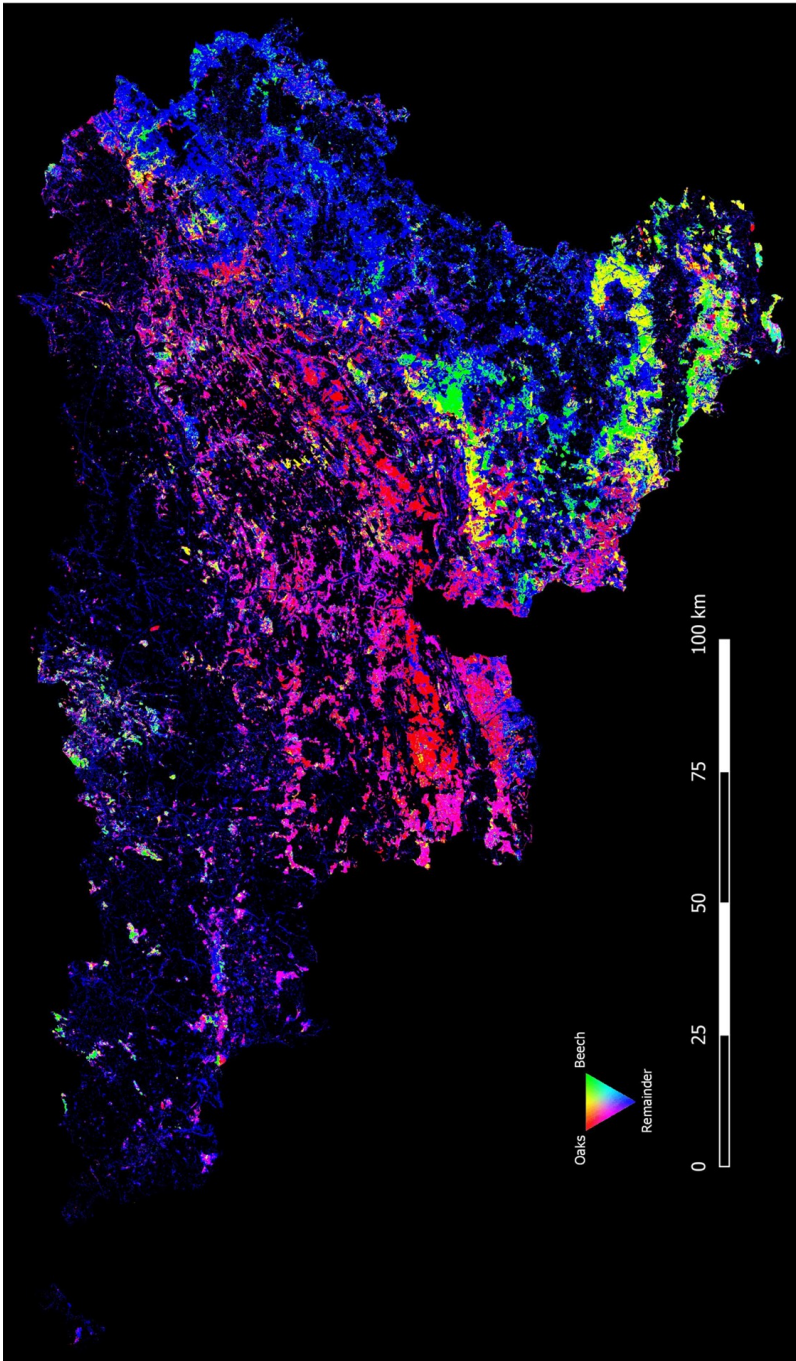
Figure B.12: False colour image of the tree species proportion map (chapter 3) for the whole study area, the Walloon Region (Southern Belgium). Red: proportion of Oaks, green: proportion of Beech, blue: proportion of the remaining classes.

Bibliography

Alderweireld, M., Burnay, F., Pitchugin, M., & Lecomte, H. (2015, April). *Inventaire Forestier Wallon - Résultats 1994 - 2012*. SPW. Retrieved April 3, 2017, from http://orbi.ulg.ac.be/handle/2268/181169

Astola, H., Häme, T., Sirro, L., Molinier, M., & Kilpi, J. (2019). Comparison of sentinel-2 and landsat 8 imagery for forest variable prediction in boreal region. *Remote Sensing of Environment*, *223*, 257–273. https://doi.org/10.1016/j.rse.2019.01.019

Axelsson, A., Lindberg, E., Reese, H., & Olsson, H. (2021). Tree species classification using sentinel-2 imagery and bayesian inference. *International Journal of Applied Earth Observation and Geoinformation*, *100*, 102318. https://doi.org/10.1016/j.jag.2021.102318

Bellefontaine, R., Petit, S., Pain Orcet, M., Deleporte, P., & Bertault, J. G. (2002). Trees outside forests: Towards better awareness. *Trees outside forests: towards better awareness.* Retrieved February 26, 2023, from https://www.cabdirect.org/cabdirect/abstract/20046798932

Bjerreskov, K. S., Nord-Larsen, T., & Fensholt, R. (2021). Classification of nemoral forests with fusion of multi-temporal sentinel-1 and 2 data. *Remote Sensing*, *13*(5), 950. https://doi.org/10.3390/rs13050950

Bolyn, C., Latte, N., Colson, V., Fourbisseur, A., Vanderheeren, N., & Lejeune, P. (2020). Une carte des principaux types de peuplements forestiers de Belgique et du Nord de la France [Publisher: Forêt Wallonne asbl]. *Forêt.Nature*, *156*. Retrieved January 24, 2021, from https://orbi.uliege.be/handle/2268/252311

Bolyn, C., Latte, N., Fourbisseur, A., Colson, V., Baudry, O., & Lejeune, P. (2020). Cartographie et caractérisation des arbres hors forêt à l'aide de la technologie LiDAR [Publisher: Forêt Wallonne asbl]. *Forêt.Nature*, *155*. Retrieved January 24, 2021, from https://orbi.uliege.be/handle/2268/250834

Bolyn, C., Lejeune, P., Michez, A., & Latte, N. (2019). Automated classification of trees outside forest for supporting operational management in rural landscapes. *Remote Sensing*, *11*(10), 1146. https://doi.org/10.3390/rs11101146

Bolyn, C., Lejeune, P., Michez, A., & Latte, N. (2022). Mapping tree species proportions from satellite imagery using spectral–spatial deep learning. *Remote Sensing of Environment*, *280*, 113205. https://doi.org/10.1016/j.rse.2022.113205

Bolyn, C., Michez, A., Gaucher, P., Lejeune, P., & Bonnet, S. (2018). Forest mapping and species composition using supervised per pixel classification of sentinel-2 imagery. *Biotechnol. Agron. Soc. Environ.*, 16.

Boyd, D. S., & Danson, F. M. (2005). Satellite remote sensing of forest resources: Three decades of research development. *Progress in Physical Geography: Earth and Environment*, *29*(1), 1–26. https://doi.org/10.1191/0309133305pp432ra

Brandt, M., Tucker, C. J., Kariryaa, A., Rasmussen, K., Abel, C., Small, J., Chave, J., Rasmussen, L. V., Hiernaux, P., Diouf, A. A., Kergoat, L., Mertz, O., Igel, C., Gieseke, F., Schöning, J., Li, S., Melocik, K., Meyer, J., Sinno, S., . . . Fensholt, R. (2020). An unexpectedly large count of trees in the west african sahara and sahel [Number: 7832 Publisher: Nature Publishing Group]. *Nature*, *587*(7832), 78–82. https://doi.org/10.1038/s41586-020-2824-5

FAO. (2013). *Forests and trees outside forests are essential for global food security and nutrition (international conference on forests for food security and nutrition)*. Food and Agriculture Organization of the United Nations (FAO).

Fassnacht, F., Latifi, H., Stereńczak, K., Lefsky, M., Straub, C., Waser, L., Ghosh, A., & Modzelewska, A. (2016). Review of studies on tree species classification from remotely sensed data. *Remote Sensing of Environment*, *184*.

Genuer, R., Poggi, J.-M., & Tuleau-Malot, C. (2016). *VSURF: Variable selection using random forests* [R package version 1.0.3]. https://CRAN.R-project.org/package=VSURF

Girard, M. C., & Girard, C. M. (2010). *Traitement des données de télédétection* [OCLC: 1091131298]. Dunod.

Grabska, E., Frantz, D., & Ostapowicz, K. (2020). Evaluation of machine learning algorithms for forest stand species mapping using sentinel-2 imagery and environmental data in the polish carpathians. *Remote Sensing of Environment*, *251*. https://doi.org/10.1016/j.rse.2020.112103

Grabska, E., Hostert, P., Pflugmacher, D., & Ostapowicz, K. (2019). Forest stand species mapping using the sentinel-2 time series. *Remote Sensing*, *11*. https://doi.org/10.3390/rs11101197

Gudex-Cross, D., Pontius, J., & Adams, A. (2017). Enhanced forest cover mapping using spectral unmixing and object-based classification of multi-temporal landsat imagery. *Remote Sensing of Environment*, *196*, 193–204. https://doi.org/10.1016/j.rse.2017.05.006

Hansen, M. C., Potapov, P. V., Moore, R., Hancher, M., Turubanova, S. A., Tyukavina, A., Thau, D., Stehman, S. V., Goetz, S. J., Loveland, T. R., Kommareddy, A., Egorov, A., Chini, L., Justice, C. O., & Townshend, J. R. G. (2013). High-resolution global maps of 21st-century forest cover change [Publisher: American Association for the Advancement of Science]. *Science*, *342*(6160), 850–853. https://doi.org/10.1126/science.1244693

Hemmerling, J., Pflugmacher, D., & Hostert, P. (2021). Mapping temperate forest tree species using dense sentinel-2 time series. *Remote Sensing of Environment*, *267*, 112743. https://doi.org/10.1016/j.rse.2021.112743

Hlásny, T., König, L., Krokene, P., Lindner, M., Montagné-Huck, C., Müller, J., Qin, H., Raffa, K. F., Schelhaas, M.-J., Svoboda, M., Viiri, H., & Seidl, R. (2021). Bark beetle outbreaks in europe: State of knowledge and ways forward for management. *Current Forestry Reports*, *7*(3), 138–165. https://doi.org/10.1007/s40725-021-00142-x

Hoscilo, A., & Lewandowska, A. (2019). Mapping forest type and tree species on a regional scale using multi-temporal sentinel-2 data. *Remote Sensing*, *11*, 929. https://doi.org/10.3390/rs11080929

Hulley, M. (2012). The urban heat island effect: Causes and potential solutions. In *Metropolitan sustainability* (pp. 79–98). Elsevier. https://doi.org/10.1533/9780857096463.1.79

Immitzer, M., Neuwirth, M., Böck, S., Brenner, H., Vuolo, F., & Atzberger, C. (2019). Optimal input features for tree species classification in central europe based on multi-temporal sentinel-2 data. *Remote Sensing*, *11*, 2599. https://doi.org/10.3390/rs11222599

Inglada, J., Arias, M., Tardy, B., Hagolle, O., Valero, S., Morin, D., Dedieu, G., Sepulcre, G., Bontemps, S., Defourny, P., & Koetz, B. (2015). Assessment of an operational system for crop type map production using high temporal and spatial resolution satellite optical imagery. *Remote Sensing*, *7*(9), 12356–12379. https://doi.org/10.3390/rs70912356

Inglada, J., Vincent, A., Arias, M., Tardy, B., Morin, D., & Rodes, I. (2017). Operational high resolution land cover map production at the country scale using satellite image time series. *Remote Sensing*, *9*(1), 95. https://doi.org/10.3390/rs9010095

Jandl, R., Spathelf, P., Bolte, A., & Prescott, C. E. (2019). Forest adaptation to climate change—is non-management an option? [Number: 2 Publisher: BioMed Central]. *Annals of Forest Science*, *76*(2), 1–13. https://doi.org/10.1007/s13595-019-0827-x

Jenkins, M., & Schaap, B. (2018). *Forest ecosystem services*. United Nations Forum of Forests.

Khosravipour, A., Skidmore, A. K., Isenburg, M., Wang, T., & Hussin, Y. A. (2014). Generating pit-free canopy height models from airborne lidar. *Photogrammetric Engineering & Remote Sensing*, *80*(9), 863–872. https://doi.org/10.14358/PERS.80.9.863

Konrad Turlej, C., Ozdogan, M., & Radeloff, V. C. (2022). Mapping forest types over large areas with landsat imagery partially affected by clouds and SLC gaps. *International Journal of Applied Earth Observation and Geoinformation*, *107*, 102689. https://doi.org/10.1016/j.jag.2022.102689

Kumar, M., Kumar, R., Bishnoi, P., Sihag, V., Bishnoi, R., Rani, S., Sindhu, P., Budhwar, S., Kumar, P., Sharma, S., Sharma, P., Sharma, R., Pandey, V., Dahiya, M., Arya, V. S., Singh, T. P., & Kumar, V. (2021). A geo-spatial approach to assess trees outside forest (ToF) in haryana state, india [_eprint: https://onlinelibrary.wiley.com/doi/pdf/10.1002/ldr.3960]. *Land Degradation & Development*, *32*(13), 3588–3597. https://doi.org/10.1002/ldr.3960

Latte, N., & Lejeune, P. (2020). PlanetScope radiometric normalization and sentinel-2 super-resolution (2.5 m): A straightforward spectral-spatial fusion of multi-satellite multi-sensor images using residual convolutional neural networks. *Remote Sensing*, *12*. https://doi.org/10.3390/rs12152366

Li, S., Brandt, M., Fensholt, R., Kariryaa, A., Igel, C., Gieseke, F., Nord-Larsen, T., Oehmcke, S., Carlsen, A. H., Junttila, S., Tong, X., d'Aspremont, A., & Ciais, P. (2023). Deep learning enables image-based tree counting, crown segmentation and height prediction at national scale. *PNAS Nexus*, pgad076. https://doi.org/10.1093/pnasnexus/pgad076

Liu, S., Brandt, M., Nord-Larsen, T., Chave, J., Reiner, F., Lang, N., Tong, X., Ciais, P., Igel, C., Pascual, A., Guerra-Hernandez, J., Li, S., Mugabowindekwe, M., Saatchi, S., Yue, Y., Chen, Z., & Fensholt, R. (2023). The overlooked contribution of trees outside forests to tree cover and woody biomass across europe. *SCIENCE ADVANCES*.

Maxwell, A., Warner, T., & Fang, F. (2018). Implementation of machine-learning classification in remote sensing: An applied review. *International Journal of Remote Sensing*, *39*, 2784–2817. https://doi.org/10.1080/01431161.2018.1433343

McCollin, D., Jackson, J., Bunce, R., Barr, C., & Stuart, R. (2000). Hedgerows as habitat for woodland plants. *Journal of Environmental Management*, *60*(1), 77–90. https://doi.org/10.1006/jema.2000.0363

Michez, A., Huylenbroeck, L., Bolyn, C., Latte, N., Bauwens, S., & Lejeune, P. (2020). Can regional aerial images from orthophoto surveys produce high quality photogrammetric canopy height model? a single tree approach in western europe. *International Journal of Applied Earth Observation and Geoinformation*, *92*, 102190. https://doi.org/10.1016/j.jag.2020.102190

Nandasena, W. D. K. V., Brabyn, L., & Serrao-Neumann, S. (2022). Using remote sensing for sustainable forest management in developing countries. In *The palgrave handbook of global sustainability* (pp. 1–22). Springer International Publishing. https://doi.org/10.1007/978-3-030-38948-2_35-1

Olofsson, P., Foody, G. M., Stehman, S. V., & Woodcock, C. E. (2013). Making better use of accuracy data in land change studies: Estimating accuracy and area and quantifying uncertainty using stratified estimation. *Remote Sensing of Environment*, *129*, 122–131. https://doi.org/10.1016/j.rse.2012.10.031

Persson, M., Lindberg, E., & Reese, H. (2018). Tree species classification with multi-temporal sentinel-2 data. *Remote Sensing*, *10*, 1794. https://doi.org/10.3390/rs10111794

Phiri, D., Simwanda, M., Salekin, S., Nyirenda, V. R., Murayama, Y., & Ranagalage, M. (2020). Sentinel-2 data for land cover/use mapping: A review [Number: 14 Publisher: Multidisciplinary Digital Publishing Institute]. *Remote Sensing*, *12*(14), 2291. https://doi.org/10.3390/rs12142291

Rawat, J. K., Fao, R., Dasgupta, S., Kumar, R., Kumar, A., Chauhan, K. V. S., European Commission, B., & EC/FAO Partnership Programme, R. (2003). *Training manual on inventory of trees outside forests (TOF)*. Bangkok (Thailand) FAO. Retrieved February 26, 2023, from http://www.fao.org/docrep/006/AC840E/AC840E00.HTM

Ronneberger, O., Fischer, P., & Brox, T. (2015, May 18). U-net: Convolutional networks for biomedical image segmentation. Retrieved September 17, 2023, from http://arxiv.org/abs/1505.04597

Rossi, J.-P., Garcia, J., Roques, A., & Rousselet, J. (2016). Trees outside forests in agricultural landscapes: Spatial distribution and impact on habitat connectivity for forest organisms. *Landscape Ecology*, *31*(2), 243–254. https://doi.org/10.1007/s10980-015-0239-8

Schnell, S., Altrell, D., Ståhl, G., & Kleinn, C. (2015). The contribution of trees outside forests to national tree biomass and carbon stocks—a comparative study across three continents. *Environmental Monitoring and Assessment*, *187*(1). https://doi.org/10.1007/s10661-014-4197-4

Schnell, S., Kleinn, C., & Ståhl, G. (2015). Monitoring trees outside forests: A review. *Environmental Monitoring and Assessment*, *187*(9). https://doi.org/10.1007/s10661-015-4817-7

Schwaiger, F., Poschenrieder, W., Biber, P., & Pretzsch, H. (2019). Ecosystem service trade-offs for adaptive forest management. *Ecosystem Services*, *39*, 100993. https://doi.org/10.1016/j.ecoser.2019.100993

See, L., Schepaschenko, D., Lesiv, M., McCallum, I., Fritz, S., Comber, A., Perger, C., Schill, C., Zhao, Y., Maus, V., Siraj, M. A., Albrecht, F., Cipriani, A., Vakolyuk, M., Garcia, A., Rabia, A. H., Singha, K., Marcarini, A. A., Kattenborn, T., ... Obersteiner, M. (2015). Building a hybrid land cover map with crowdsourcing and geographically weighted regression. *ISPRS Journal of Photogrammetry and Remote Sensing*, *103*, 48–56. https://doi.org/10.1016/j.isprsjprs.2014.06.016

Soille, P., & Vogt, P. (2022). MORPHOLOGICAL SPATIAL PATTERN ANALYSIS: OPEN SOURCE RELEASE. *The International Archives of the Photogrammetry, Remote Sensing and Spatial Information Sciences*, *XLVIII-4/W1-2022*, 427–433. https://doi.org/10.5194/isprs-archives-XLVIII-4-W1-2022-427-2022

Soille, P., & Vogt, P. (2009). Morphological segmentation of binary patterns. *Pattern Recognition Letters*, *30*(4), 456–459. https://doi.org/10.1016/j.patrec.2008.10.015

Stehman, S. V., & Foody, G. M. (2019). Key issues in rigorous accuracy assessment of land cover products. *Remote Sensing of Environment*, *231*, 111199. https://doi.org/10.1016/j.rse.2019.05.018

Strahler, A. H., Woodcock, C. E., & Smith, J. A. (1986). On the nature of models in remote sensing. *Remote Sensing of Environment*, *20*(2), 121–139. https://doi.org/10.1016/0034-4257(86)90018-0

Tomppo, E., Gschwantner, T., Lawrence, M., & McRoberts, R. E. (Eds.). (2010). *National forest inventories*. Springer Netherlands. https://doi.org/10.1007/978-90-481-3233-1

Waldner, F., & Defourny, P. (2017). Where can pixel counting area estimates meet user-defined accuracy requirements? *International Journal of Applied Earth Observation and Geoinformation*, *60*, 1–10. https://doi.org/10.1016/j.jag.2017.03.014

Welle, T., Aschenbrenner, L., Kuonath, K., Kirmaier, S., & Franke, J. (2022). Mapping dominant tree species of german forests. *Remote Sensing*, *14*(14), 3330. https://doi.org/10.3390/rs14143330

Wessel, M., Brandmeier, M., & Tiede, D. (2018). Evaluation of different machine learning algorithms for scalable classification of tree types and tree species based on sentinel-2 data. *Remote Sensing*, *10*. https://doi.org/10.3390/rs10091419

Xi, Y., Ren, C., Tian, Q., Ren, Y., Dong, X., & Zhang, Z. (2021). Exploitation of time series sentinel-2 data and different machine learning algorithms for detailed tree species classification. *IEEE Journal of Selected Topics in Applied Earth Observations and Remote Sensing*, *14*, 7589–7603. https://doi.org/10.1109/JSTARS.2021.3098817

Yuan, Q., Shen, H., Li, T., Li, Z., Li, S., Jiang, Y., Xu, H., Weiwei, T., Yang, Q., Wang, J., Gao, J., & Zhang, L. (2020). Deep learning in environmental remote sensing: Achievements and challenges. *Remote Sensing of Environment*, *241*, 111716. https://doi.org/10.1016/j.rse.2020.111716

Zagajewski, B., Kluczek, M., Raczko, E., Njegovec, A., Anca, D., & Kycko, M. (2021). Comparison of random forest, support vector machines, and neural networks for post-disaster forest species mapping of the krkonoše/karkonosze transboundary biosphere reserve. *Remote Sensing*, *13*, 2581. https://doi.org/10.3390/rs13132581

Zhou, Z., Siddiquee, M. M. R., Tajbakhsh, N., & Liang, J. (2018, July 18). UNet++: A nested u-net architecture for medical image segmentation. Retrieved September 17, 2023, from http://arxiv.org/abs/1807.10165

Zomer, R. J., Neufeldt, H., Xu, J., Ahrends, A., Bossio, D., Trabucco, A., van Noordwijk, M., & Wang, M. (2016). Global tree cover and biomass carbon on agricultural land: The contribution of agroforestry to global and national carbon budgets. *Scientific Reports*, *6*(1). https://doi.org/10.1038/srep29987

Webpages

Cambridge dictionary [Forest]. (2023, February 22). Retrieved February 25, 2023, from https://dictionary.cambridge.org/dictionary/english/forest

Elijah Koech, K. (2023). *Softmax activation function — how it actually works* [Towards data science]. Retrieved September 16, 2023, from https://towardsdatascience.com/softmax-activation-function-how-it-actually-works-d292d335bd78

Food and agriculture organisation of the united nations [Global forest resources assessment 2020, terms and definitions]. (2020). Retrieved February 25, 2023, from https://www.fao.org/3/I8661EN/i8661en.pdf

Global forest change. (2023). Retrieved March 26, 2023, from https://glad.earthengine.app/view/global-forest-change

Landsat science. (2023). Retrieved September 25, 2023, from https://landsat.gsfc.nasa.gov/

LifeWatch-WB ecotope database | lifewatch regional portal. (2023). Retrieved September 24, 2023, from https://www.lifewatch.be/en/lifewatch-wb-ecotope-database

NASA. (2019, August 23). *What is remote sensing?* [Earthdata] [Publisher: Earth Science Data Systems, NASA]. Retrieved March 18, 2023, from https://www.earthdata.nasa.gov/learn/backgrounders/remote-sensing

Small woody features — copernicus land monitoring service. (2015). Retrieved March 26, 2023, from https://land.copernicus.eu/pan-european/high-resolution-layers/small-woody-features

USGS EROS archive. (2023). Retrieved September 25, 2023, from https://www.usgs.gov/centers/eros/science/usgs-eros-archive-sentinel-2-comparison-sentinel-2-and-landsat

Wallonie. (2019, September 9). *Déclaration de politique régionale du Gouvernement wallon 2019-2024* [Wallonie]. Retrieved March 18, 2023, from https://www.wallonie.be/fr/actualites/declaration-de-politique-regionale-du-gouvernement-wallon-2019-2024

Wikipedia. (2023). *Softmax function*. Retrieved September 16, 2023, from https://en.wikipedia.
    org/wiki/Softmax_function